A protease and a lipoprotein jointly modulate the conserved ExoR-ExoS-ChvI signaling pathway critical in *Sinorhizobium meliloti* for symbiosis with legume hosts

Julian A. Bustamante [1¶], Josue S. Ceron [1¶], Ivan Thomas Gao [1¶], Hector A. Ramirez [1¶], Milo V. Aviles [1], Demsin Bet Adam [1], Jason R. Brice [1], Rodrigo Cuellar [1], Eva Dockery [1], Miguel Karlo Jabagat [1], Donna Grace Karp [1], Joseph Kin-On Lau [1], Suling Li [1], Raymondo Lopez-Magaña [1], Rebecca R. Moore [1], Bethany Kristi R. Morin [1], Juliana Nzongo [1], Yasha Rezaeihaghighi [1], Joseph Sapienza-Martinez [1], Tuyet Thi Kim Tran [1], Zhenzhong Huang [1], Aaron J. Duthoy [2], Melanie J. Barnett [2], Sharon Long [2], and Joseph C. Chen [1*]

[1] Department of Biology, San Francisco State University, San Francisco, California, United States of America

[2] Department of Biology, Stanford University, Stanford, California, United States of America

* Corresponding author

E-mail: chenj@sfsu.edu (JCC)

¶ Julian A. Bustamante, Josue S. Ceron, Ivan Thomas Gao, Hector A. Ramirez contributed equally to this work. Author order was determined alphabetically.

Running title: proteolytic regulation of ExoR

Abstract word count: 221

Abstract

Sinorhizobium meliloti is a model alpha-proteobacterium for investigating microbe-host interactions, in particular nitrogen-fixing rhizobium-legume symbioses. Successful infection requires complex coordination between compatible host and endosymbiont, including bacterial production of succinoglycan, also known as exopolysaccharide-I (EPS-I). In *S. meliloti* EPS-I production is controlled by the conserved ExoS-ChvI two-component system. Periplasmic ExoR associates with the ExoS histidine kinase and negatively regulates ChvI-dependent expression of *exo* genes, necessary for EPS-I synthesis. We show that two extracytoplasmic proteins, LppA (a lipoprotein) and JspA (a metalloprotease), jointly influence EPS-I synthesis by modulating the ExoR-ExoS-ChvI pathway and expression of genes in the ChvI regulon. Deletions of *jspA* and *lppA* led to lower EPS-I production and competitive disadvantage during host colonization, for both *S. meliloti* with *Medicago sativa* and *S. medicae* with *M. truncatula*. Overexpression of *jspA* reduced steady-state levels of ExoR, suggesting that the JspA protease participates in ExoR degradation. This reduction in ExoR levels is dependent on LppA and can be replicated with ExoR, JspA, and LppA expressed exogenously in *Caulobacter crescentus* and *Escherichia coli*. Akin to signaling pathways that sense extracytoplasmic stress in other bacteria, JspA and LppA may monitor periplasmic conditions during interaction with the plant host to adjust accordingly expression of genes that contribute to efficient symbiosis. The molecular mechanisms underlying host colonization in our model system may have parallels in related alpha-proteobacteria.

Author summary

Symbiotic bacteria that live in the roots of legume plants produce biologically accessible nitrogen compounds, offering a more sustainable and environmentally sound alternative to industrial fertilizers generated from fossil fuels. Understanding the multitude of factors that contribute to successful interaction between such bacteria and their plant hosts can help refine strategies for improving agricultural output. In addition, because disease-causing microbes share many genes with these beneficial bacteria, unraveling the cellular mechanisms that facilitate host invasion can reveal ways to prevent and treat infectious diseases. In this report we show that two genes in the model bacterium *Sinorhizobium meliloti* contribute to effective symbiosis by helping the cells adapt to living in host plants. This finding furthers knowledge about genetics factors that regulate interactions between microbes and their hosts.

Introduction

Rhizobia-legume symbioses account for a substantial proportion of terrestrial nitrogen fixation, converting molecular dinitrogen to a reduced, more bioavailable form such as ammonia (Herridge *et al.*, 2008). Optimization of such biological nitrogen fixation in agriculture may reduce reliance on industrial fertilizers and their negative environmental impacts, including fossil fuel consumption, release of greenhouse gas, and eutrophication (Ferguson *et al.*, 2010; Graham & Vance, 2003; Olivares *et al.*, 2013). The mutualistic relationship requires complex communication and coordination between specific rhizobia and compatible legume plants (Long, 2016; Masson-Boivin & Sachs, 2018), as well as bacterial adaptation to the “stresses” of the host plant environment (Hawkins & Oresnik, 2021; Ledermann *et al.*, 2021). Flavonoids released by the host plant induce bacterial production of essential signaling molecules called Nod factors, lipochitooligosaccharides that elicit root hair curling, plant cell division, and nodule development (Gibson *et al.*, 2008). Colonization of nodules typically begins with bacterial cells invading the root hair via plant cell wall-derived tunnels called infection threads, followed by release into the nodule primordium and engulfment into symbiosomes, membrane-bound organelles in the plant cytoplasm, in which the rhizobia differentiate into bacteroids capable of fixing nitrogen in exchange for carbon compounds from the host (Barnett & Fisher, 2006; Poole *et al.*, 2018). The root nodules can be determinate or indeterminate, depending on the host: one major distinction is that determinate nodules lack a persistent meristem and contain cells at similar stages of development, whereas indeterminate nodules exhibit a sequential gradient of development, with dividing cells in the meristem at one end, next to progressive zones of invasion, nitrogen fixation, and senescence (Ferguson *et al.*, 2010).

The alphaproteobacterium *Sinorhizobium meliloti* and its compatible hosts, including *Medicago sativa* (alfalfa) and *M. truncatula* (barrel medic), emerged as models for indeterminate nodulation (Jones *et al.*, 2007). Alfalfa is a major feed crop, its annual production valued at over $11 billion in the U.S. alone (USDA Crop Values 2022 Summary), while *M. truncatula* serves as a genetically tractable reference species (Burks *et al.*, 2018). Factors found to be critical for *S. meliloti* to form mutualistic symbiosis have been shown to play similar roles during host infection in related pathogens, such as *Brucella* spp., suggesting mechanistic parallels between mutualism and pathogenesis (Jones *et al.*, 2007). One such shared mechanism is the ExoS-ChvI two-component phosphorelay pathway, conserved across related alpha-proteobacteria,

93 particularly within the Rhizobiales group (Greenwich *et al.*, 2023; Heavner *et al.*, 2015). ExoS is
94 a membrane-bound histidine kinase with a periplasmic sensor domain, while ChvI is its cognate
95 response regulator (Cheng & Walker, 1998b). Mutations in ExoS and ChvI as well as their
96 orthologs in other endosymbionts, including BvrS-BvrR in the mammalian pathogen *Brucella*
97 *abortus* and ChvG-ChvI in the plant pathogen *Agrobacterium tumefaciens*, impair host
98 colonization (Alakavuklar *et al.*, 2023; Bélanger *et al.*, 2009; Charles & Nester, 1993; Chen *et*
99 *al.*, 2008; Mantis & Winans, 1993; Sola-Landa *et al.*, 1998; Vanderlinde & Yost, 2012; Wang *et*
100 *al.*, 2010a; Wells *et al.*, 2007). A third component of the signaling system, ExoR, acts as a
101 periplasmic repressor of ExoS via physical association (Chen *et al.*, 2008; Wells *et al.*, 2007).
102 ExoR is regulated by proteolysis (Lu *et al.*, 2012; Wiech *et al.*, 2015; Wu *et al.*, 2012), and
103 binding to ExoS protects it from degradation (Chen *et al.*, 2008). Mutations in *S. meliloti* ExoR
104 also disrupt symbiosis (Chen *et al.*, 2008; Doherty *et al.*, 1988; Ozga *et al.*, 1994; Wells *et al.*,
105 2007; Yao *et al.*, 2004), but the ExoR ortholog in *B. abortus* seems dispensable for virulence
106 (Castillo-Zeledón *et al.*, 2021), and mutation in *A. tumefaciens exoR* interferes with binding to
107 plant root surfaces while permitting disease progression (Tomlinson *et al.*, 2010). These
108 observations may reflect a more nuanced role of ExoR during host invasion.
109
110 Cues that suggest transition into the host environment appear to stimulate the ExoR-ExoS-ChvI
111 signaling cascade to promote a developmental shift from free-living to symbiotic (Greenwich *et*
112 *al.*, 2023). Acidic pH that mimics the rhizosphere leads to degradation of ExoR and induction of
113 the ChvG-ChvI pathway in *A. tumefaciens* (Heckel *et al.*, 2014; Li *et al.*, 2002; Wu *et al.*, 2012;
114 Yuan *et al.*, 2008). In *B. abortus*, a combination of acidic pH and nutrient limitation, conditions
115 similar to those found during passage through autophagosome-like compartments, activates
116 BvrS-BvrR signaling (Altamirano-Silva *et al.*, 2021; Altamirano-Silva *et al.*, 2018; Rivas-Solano
117 *et al.*, 2022). However, conditions that specifically trigger the ExoR-ExoS-ChvI pathway in *S.*
118 *meliloti* remain elusive (Bélanger *et al.*, 2009; Keating, 2007; Ratib *et al.*, 2018), and different
119 cues for divergent species are possible. Furthermore, some cues may directly activate the
120 ExoS sensor kinase and bypass ExoR: recent studies indicate that peptidoglycan stress induces
121 the *A. tumefaciens* ChvG-ChvI system independently of ExoR (Williams *et al.*, 2022), and that in
122 *S. meliloti*, membrane disruption due to a phosphatidylcholine deficiency activates ExoS without
123 a concomitant decrease in steady-state levels of ExoR (Geiger *et al.*, 2021). In the free-living
124 alphaproteobacterium *Caulobacter crescentus*, which lacks an ExoR ortholog, the ChvG-ChvI
125 system was shown to be stimulated by various stresses, including DNA damage, acidic pH,

126 osmotic upshift, and inhibition of cell wall synthesis (Frohlich *et al.*, 2018; Quintero-Yanes *et al.*,
127 2022; Stein *et al.*, 2021).
128
129 Irrespective of the specific triggers, the ExoR-ExoS-ChvI system influences a multitude of
130 physiological activities, including exopolysaccharide (EPS) production, motility, biofilm
131 formation, cell envelope maintenance, and nutrient utilization, befitting its pivotal regulation of
132 symbiotic development (Bélanger *et al.*, 2009; Wang *et al.*, 2010a; Wells *et al.*, 2007; Yao *et al.*,
133 2004). Similarly, orthologs in *A. tumefaciens* and *Bartonella henselae* control parallel processes
134 crucial for pathogenesis (Alakavuklar *et al.*, 2021; Heckel *et al.*, 2014; Quebatte *et al.*, 2010). In
135 *B. abortus*, BvrS and BvrR also coordinate diverse functions and upon activation directly target
136 genes involved in metabolite deployment, cell envelope modulation, cell division, and virulence
137 (Guzman-Verri *et al.*, 2002; Lamontagne *et al.*, 2007; Manterola *et al.*, 2007; Manterola *et al.*,
138 2005; Martinez-Nunez *et al.*, 2010; Rivas-Solano *et al.*, 2022; Viadas *et al.*, 2010). Initial
139 transcriptome profiles of *S. meliloti exoS*::Tn*5* and *exoR*::Tn*5* mutants revealed altered
140 expression of hundreds of genes (Wells *et al.*, 2007; Yao *et al.*, 2004), but subsequent
141 interrogation that included identification of genomic regions bound by ChvI winnowed the direct
142 targets of the response regulator down to 64, many known to participate in physiological
143 activities described above (Chen *et al.*, 2009; Ratib *et al.*, 2018). Perhaps illustrating the
144 complex interaction of regulatory pathways and the difficulty of signal deconvolution, a
145 significant fraction of ChvI targets also changed expression with other published perturbations
146 (Ratib *et al.*, 2018), including acid stress (de Lucena *et al.*, 2010; Draghi *et al.*, 2016; Hellweg *et*
147 *al.*, 2009), antimicrobial peptide treatment (Penterman *et al.*, 2014), phosphate starvation (Krol
148 & Becker, 2004), cyclic nucleotide accumulation (Krol *et al.*, 2016), overexpression of SyrA
149 (Barnett & Long, 2015), and mutations in *podJ*, *cbrA*, *ntrY*, and *emrR* (Calatrava-Morales *et al.*,
150 2017; Fields *et al.*, 2012; Gibson *et al.*, 2007; Santos *et al.*, 2014).
151
152 One key subset of the regulon induced upon ExoS-ChvI activation is the *exo* genes, responsible
153 for synthesis of succinoglycan, or EPS-I, originally characterized in *S. meliloti* strain Rm1021 as
154 the only symbiotically active EPS (Becker *et al.*, 2002; Long *et al.*, 1988; Pellock *et al.*, 2000;
155 Reuber & Walker, 1993). An increase in EPS-I production, usually concomitant with a decrease
156 in flagellar motility (Alakavuklar *et al.*, 2021; Ratib *et al.*, 2018), represents a physiological
157 transition from saprophytic to endosymbiotic, as EPS-I contributes to successful interaction
158 between compatible symbiotic partners. Mutants that lack EPS-I or synthesize variants with
159 altered structures (for example, absence of succinylation) exhibit defects in the initiation or

160 elongation of infection threads, while changes in EPS-I levels can influence symbiotic efficiency
161 (Barnett & Long, 2018; Cheng & Walker, 1998a; Geddes *et al.*, 2014; Jones, 2012; Mendis *et*
162 *al.*, 2016); thus, both the quality and quantity of EPS-I matter during infection. EPS-I may serve
163 as a recognition signal, particularly for suppressing host defenses (Jones *et al.*, 2008). When
164 *Mesorhizobium loti* invades *Lotus japonicus*, a legume host that develops determinate nodules,
165 recognition of bacterial EPS by a plant receptor-like kinase facilitates symbiosis, as mutants that
166 do not produce EPS can still form symbiosis, whereas those that synthesize inappropriate,
167 truncated forms of EPS cannot, and the plant receptor is required to restrain infection by
168 bacteria with inappropriate EPS (Kawaharada *et al.*, 2015; Kawaharada *et al.*, 2017; Kelly *et al.*,
169 2013). While no corresponding plant receptor for *S. meliloti* EPS-I has been identified so far
170 (Maillet *et al.*, 2020), EPS-I does enhance tolerance of various environmental assaults (Miller-
171 Williams *et al.*, 2006; Vriezen *et al.*, 2007), including those encountered during host
172 colonization, such as acidity, oxidative stress, and antimicrobial peptides (Arnold *et al.*, 2018;
173 Arnold *et al.*, 2017; Davies & Walker, 2007; Hawkins *et al.*, 2017; Lehman & Long, 2013).
174
175 In particular, EPS-I confers resistance to the antimicrobial activity of NCR247 (Arnold *et al.*,
176 2018; Arnold *et al.*, 2017), which belongs to a diverse family of small, nodule-specific cysteine-
177 rich (NCR) peptides encoded by legumes in the inverted-repeat-lacking clade (IRLC), where
178 plants with indeterminate nodules typically reside (Mergaert *et al.*, 2003; Poole *et al.*, 2018; Van
179 de Velde *et al.*, 2010). Structurally similar to characterized defensins (Maroti *et al.*, 2015),
180 different NCR peptides regulate bacterial load *in planta* and influence distinct aspects of
181 terminal bacteroid differentiation, including maintaining survival and preventing premature
182 senescence (Cao *et al.*, 2017; Farkas *et al.*, 2014; Horváth *et al.*, 2015; Kim *et al.*, 2015;
183 Sankari *et al.*, 2022; Wang *et al.*, 2010b). In addition to EPS-I, other bacterial factors can
184 modulate the effects of NCR peptides (Arnold *et al.*, 2017; Benedict *et al.*, 2021). For example,
185 BacA, long recognized as critical in both *S. meliloti* and *B. abortus* for host colonization (LeVier
186 *et al.*, 2000), reduces membrane permeabilization and cell death induced by NCR247 *ex planta*
187 (Haag *et al.*, 2011). Some *S. meliloti* strains produce HrrP, a peptidase capable of degrading
188 NCR peptides, attenuating their antimicrobial effects and altering the host ranges of the bacteria
189 (Price *et al.*, 2015). These molecular arsenals for exerting control evoke the Red Queen
190 hypothesis, which proposes that coevolving partners engage in a continual arms race to
191 maintain the relationship (Brockhurst, 2011; Van Valen, 1973): “it takes all the running you can
192 do, to keep in the same place” (Carroll, 1900 [1872]).
193

194 One of the genes previously identified in a transposon-based screen as necessary for *S. meliloti*
195 resistance against NCR247 *ex planta* is SMc03872, which encodes a periplasmic protease
196 conserved in alpha-proteobacteria and confers a competitive advantage during symbiosis with
197 alfalfa (Arnold *et al.*, 2017). SMc03872 was also identified in a genetic selection for
198 suppressors that ameliorated the osmosensitivity of a *podJ* null mutant (Fields *et al.*, 2012).
199 That work demonstrated that PodJ is a conserved polarity factor that contributes to cell
200 envelope integrity and EPS-I production in *S. meliloti*, and that deletion of SMc03872 or
201 SMc00067, encoding a lipoprotein, reduced EPS-I levels. Here we show that SMc03872 and
202 SMc00067 jointly influence EPS-I production by lowering the steady-state levels of periplasmic
203 ExoR and thus activating the ExoS-ChvI signal transduction pathway. This regulation
204 contributes to competitive fitness during host colonization, suggesting that SMc03872 and
205 SMc00067 facilitate transition to a gene expression pattern more suitable for the host
206 environment.
207
208
209

210 # Results

211

212 **LppA and JspA jointly contribute to EPS-I biosynthesis and symbiotic competitiveness**

213 In a previous suppressor analysis to identify mutants that alleviated the cell envelope defects of
214 the *podJ1* deletion strain, we found two genes (SMc00067 and SMc03872) whose interruption
215 or deletion led to consistent and significant reduction in EPS-I production (Fields *et al.*, 2012).
216 SMc00067 (annotated as *lppA*) encodes a 148-amino acid lipoprotein, while SMc03872 (here
217 named *jspA*, for *podJ* suppressor protease A) encodes a 497-amino acid metalloprotease that
218 contains an M48 peptidase domain, with a conserved HEXXH active site, and a LysM domain,
219 commonly associated with peptidoglycan binding (Fig. 1) (Arnold *et al.*, 2017; Becker *et al.*,
220 2009; Galibert *et al.*, 2001). BLAST searches against representative bacterial species indicated
221 that both genes are highly conserved within the Rhizobiales group of alphaproteobacteria,
222 based on shared synteny and protein sequences (Boratyn *et al.*, 2013). Outside of the
223 Rhizobiales group, orthologs of LppA were rare or difficult to identify, while the sequence
224 similarities of JspA homologs were generally lower than those found within Rhizobiales (Table
225 S1). Both LppA and JspA contain lipoprotein signal peptides at their N-termini, each with a
226 stretch of hydrophobic amino acids followed by an invariant Cys within the lipobox motif (Fig.
227 1B) (Juncker *et al.*, 2003). In the original annotation for LppA, the protein starts seven codons
228 upstream of the LAGC lipobox, with VVASGVA, but N-terminal extension of 12 codons adds
229 more hydrophobic amino acids, allowing a more optimal signal sequence; thus, we have
230 numbered the amino acid sequence accordingly. The lipoprotein signals suggest that each
231 protein is exported out of the cytoplasm and attached to the inner or outer membrane (Kovacs-
232 Simon *et al.*, 2011).

233

234 To verify that LppA and JspA contribute to EPS-I production, we performed complementation
235 analysis by introducing plasmids carrying *lppA* or *jspA* under the control of a taurine-inducible
236 promoter (P_{tau}) (Mostafavi *et al.*, 2014) into wild-type or deletion strains. Serial dilutions of
237 strains were spotted onto plates containing calcofluor, which fluoresces when bound to EPS-I
238 (Finan *et al.*, 1985). Consistent with previously published results (Fields *et al.*, 2012), *lppA* or
239 *jspA* deletion strain carrying the empty vector exhibited lower levels of EPS-I production, with
240 60-70% of calcofluor fluorescence compared to wild-type strains carrying the vector, in the
241 absence or presence of taurine (Fig. 2A and 2B). Wild-type and deletion strains with plasmids
242 carrying *lppA* or *jspA* showed similar fluorescence levels as their counterparts with the vector in

243 the absence of taurine and elevated fluorescence levels in the presence of taurine. Similar
244 results were obtained with the closely related *S. medicae* strain WSM419: deletion of the *lppA*
245 or *jspA* ortholog in that strain reduced fluorescence on plates containing calcofluor (Fig. S1A),
246 and complementation with the heterologous *S. meliloti* gene rescued the defect (Fig. S1B,
247 strains JOE5290 and JOE5264). At higher taurine concentrations (5 and 10 mM), induction of
248 *jspA* expression in *S. meliloti* Rm1021 inhibited colony formation (Fig. 2C), but this effect was
249 not observed with *lppA* expression, even with the highest possible concentration of taurine (100
250 mM) (Fig. 2A). While induction of *lppA* or *jspA* expression promoted EPS-I production in wild
251 type or corresponding deletion strains, *lppA* expression in the *jspA* mutant (Fig. 2A, bottom
252 image) and *jspA* expression in the *lppA* mutant (Fig. 2B, bottom image) failed to increase
253 calcofluor fluorescence. Furthermore, *jspA* overexpression did not cause growth arrest in the
254 *lppA* mutant (Fig. 2D). These results suggest that LppA and JspA act in concert to stimulate
255 EPS-I production.
256
257 Since EPS-I is critical for infection thread formation during host colonization, we asked if
258 deletion of *lppA* or *jspA* leads to a symbiosis defect. *M. sativa* seedlings were inoculated with
259 wild-type Rm1021 or Δ*lppA* or Δ*jspA* derivatives, and *M. truncatula* seedlings were inoculated
260 with wild-type WSM419 or its Δ*lppA* or Δ*jspA* derivatives because WSM419 forms more efficient
261 symbiosis with *M. truncatula* than *S. meliloti* strains (Ghosh *et al.*, 2021; Larrainzar *et al.*, 2014;
262 Terpolilli *et al.*, 2008). We did not observe obvious differences in plant growth and the
263 development of root nodules on nitrogen-free medium over the course of four weeks: the
264 average numbers of pink, nitrogen-fixing nodules per plant were similar 21 and 28 days after
265 inoculation with different bacterial strains (Table S2), suggesting that the two genes are not
266 required for symbiosis. To examine more closely if LppA and JspA contribute to efficient host
267 colonization, we conducted competitive infection assays in which seedlings were inoculated with
268 mixtures containing equal numbers of two strains, and bacteria were recovered from root
269 nodules 28 days post-inoculation to determine occupancy rates (Materials and methods). One
270 or both strains were marked with distinct antibiotic resistance to facilitate identification via
271 plating after extraction from nodules. *M. sativa* plants were inoculated with mixtures of Rm1021
272 derivatives (Fig. 3A), while *M. truncatula* plants were inoculated with mixtures of WSM419
273 derivatives (Fig. 3B). Consistent with previous reports (Fields *et al.*, 2012; Gage, 2002), we
274 found that a small percentage of the nodules contained mixed populations of bacteria, while the
275 majority of nodules were dominated by one strain. Discounting those nodules containing mixed
276 populations, roughly equal numbers of nodules (45 – 55%) were occupied by each strain when

277 the inoculum contained two wild-type strains (marked or unmarked). In contrast, *lppA* or *jspA*
278 mutants were recovered from significantly fewer nodules (6 – 26% of the nodules) when
279 competed against wild-type strains (Fig. 3 and Table S3). These results align with previous
280 demonstration that JspA is important for protection against the NCR247 antimicrobial peptide
281 and for competitiveness during symbiosis between *S. meliloti* and *M. sativa* (Arnold *et al.*, 2017).
282 Furthermore, our results show that both JspA and LppA contribute to competitiveness, in two
283 different model symbiotic interactions.
284
285 **JspA and LppA affect expression of EPS-I and flagellar genes**
286 Next, we investigated how JspA and LppA may influence EPS-I production by determining if
287 they affect gene expression in *S. meliloti*. First, we used a transcriptional fusion to the β-
288 glucuronidase (GUS) reporter gene (Chen *et al.*, 2009) to measure expression of *exoY*,
289 encoding a galactosyltransferase required for EPS-I biosynthesis (Reuber & Walker, 1993).
290 Expression levels were examined in both PYE and LB rich media because our past experiences
291 indicated that differences between strains could be more apparent in one particular medium
292 (Fields *et al.*, 2012). Consistent with EPS-I levels monitored via calcofluor fluorescence (Fig. 2),
293 deletion of *jspA* or *lppA* reduced *exoY* expression to 55 - 72% of wild-type levels, in both LB and
294 PYE media (Table 1). Second, we examined reporter fusions to *flaC* and *mcpU* (Gibson *et al.*,
295 2007), respectively encoding a flagellin and a chemoreceptor (Hoang *et al.*, 2008; Scharf &
296 Schmitt, 2002), as expression of genes involved in flagellar motility and chemotaxis often
297 change in opposition to those involved in EPS-I production (Bahlawane *et al.*, 2008; Barnett *et*
298 *al.*, 2004; Fields *et al.*, 2012). Deletion of *jspA* or *lppA* increased expression of these two genes
299 significantly in LB medium (to 134 - 159% of wild type), but less clearly in PYE medium (to 114 -
300 129% of wild type) (Table 1). Finally, expression levels of *exoY*, *flaC*, and *mcpU* in the Δ*jspA*
301 Δ*lppA* double mutant were similar to those in the single mutants (Table 1), again suggesting that
302 JspA and LppA function in the same genetic pathway.
303
304 We also used the transcriptional fusions to *exoY* and *flaC* to assess the effects of constitutive
305 *jspA* or *lppA* expression from a plasmid-borne, taurine-inducible promoter (with the same P_{tau}-
306 regulated constructs as those in Fig. 2) (Table 2). Induction of *jspA* expression with 10 mM
307 taurine in PYE for three hours was sufficient to significantly alter expression of both *exoY* and
308 *flaC* in the wild-type background. Such induction also complemented the drop in *exoY*
309 expression seen in the Δ*jspA* mutant. In contrast, induction of *lppA* expression did not affect
310 *flaC* or *exoY* significantly under various conditions tested (Table 2). We only found a modest

311 increase in *exoY* transcription in the wild-type background when *lppA* expression was induced
312 for six hours with 100 mM taurine in LB medium. Such induction also sufficed to complement
313 the drop in *exoY* expression in the Δ*lppA* mutant. Notably, overexpression of *jspA* could not
314 reverse the decrease in *exoY* expression in the Δ*lppA* mutant, and overexpression of *lppA* could
315 not reverse the same effect in the Δ*jspA* mutant. Overall, expression analysis with
316 transcriptional reporters reflected the results obtained with calcofluor fluorescence (Fig. 2): *lppA*
317 appears to require higher concentrations of the taurine inducer compared to *jspA* to cause
318 detectable physiological changes, and both genes need each other to function.
319
320 To determine if LppA acts as a lipoprotein and JspA acts as a protease, we mutated the lipobox
321 motif of LppA and the peptidase domain of JspA (Fig. 1B) and assessed the mutant derivatives'
322 effects on EPS-I synthesis and gene expression. For LppA, we mutated Cys_{23} of the lipobox
323 motif to Ser and tagged both the wild-type and mutant versions at the C-terminus with an HA
324 epitope. While constructing the *lppA-HA* allele, we serendipitously obtained alleles with
325 conversion of Gly_{96} to Trp and Ala_{78} to Ser and decided to analyze each of the corresponding
326 two mutants as well. Due to the relatively minor changes in reporter gene expression when
327 *lppA* was overexpressed in the wild-type background (Table 2), we mainly examined the
328 functionality of various *lppA* alleles in the Δ*lppA* background. Overexpression of these various
329 derivatives ($LppA_{C23S}$, LppA-HA, $LppA_{C23S}$-HA, $LppA_{G96W}$-HA, $LppA_{A78S}$-HA) in the Δ*lppA* mutant
330 from the plasmid-borne P_{tau} promoter did not increase the fluorescence levels of colonies on
331 calcofluor plates compared to the vector-only control, whereas overexpression of LppA did (Fig.
332 4A). Induction of LppA or LppA-HA significantly elevated expression of the *exoY* fusion reporter
333 to similar levels (180 – 195% of that in the Δ*lppA* mutant with the vector), while $LppA_{C23S}$ and
334 $LppA_{C23S}$-HA did not (Table 3). The other two variants, $LppA_{G96W}$-HA and $LppA_{A78S}$-HA,
335 increased *exoY* expression modestly but significantly (123 – 130%) (Table 3). Immunoblot
336 analysis using antibodies against the HA epitope indicated that the steady-state levels of all HA-
337 tagged derivatives of LppA, when constitutively expressed from plasmids, are relatively similar
338 in wild-type, Δ*lppA*, and Δ*jspA* backgrounds, except for $LppA_{C23S}$-HA, which appears to be
339 expressed at very low levels in all backgrounds (Fig. 4B). These results suggest that acylation
340 at the lipobox Cys allows LppA to anchor to the membrane and mature into a stable lipoprotein.
341 Addition of an HA epitope at the C-terminus appears to reduce the functionality of LppA, while
342 the G96W and A78S mutations further diminish protein activity without affecting its stability
343 detectably.
344

345 For JspA, we mutated residues within the HEMAH active site, His147 to Ala, or Glu148 to Ala or
346 Asp (Fujimura-Kamada *et al.*, 1997), and tagged wild-type and mutant versions at the C-
347 terminus with the HA epitope. When constitutively expressed from the plasmid-borne P_{tau}
348 promoter in the wild-type background with 5 mM taurine, both JspA and JspA-HA elevated the
349 fluorescence of colonies on calcofluor plates, but only JspA inhibited colony formation (Fig. 4C).
350 None of the three active site mutants (H147A, E148A, E148D), untagged or tagged, enhanced
351 fluorescence or affected growth. In addition, we expressed *S. meliloti* JspA and its derivatives
352 in three related alphaproteobacteria -- *S. medicae* WSM419, *S. fredii* NGR234, and *C.*
353 *crescentus* NA1000 -- to assess if JspA activity is conserved (Fig. S1B, S2). In WSM419,
354 expression of JspA complemented the EPS-I production defect of the Δ*jspA* mutant, whereas
355 expression of $JspA_{E148A}$ did not (Fig. S1B). In both WSM419 and NGR234, overexpression of
356 JspA inhibited colony formation, while overexpression of $JspA_{E148A}$-HA did not (Fig. S2).
357 Overexpression of $JspA_{E148A}$ and JspA-HA inhibited growth to different extents in these two
358 species (Fig. S2), suggesting that JspA variants have different activities in distinct genetic
359 backgrounds: overproduction of a proteolytically inactive JspA seems more deleterious in
360 NGR234 than in *S. meliloti* Rm1021 or *S. medicae* WSM419. In contrast, expression of JspA
361 and its derivatives in the more distantly related NA1000 did not inhibit growth until higher levels
362 of induction (10 mM taurine), possibly due to the general stress of protein overproduction
363 because similar levels of inhibition were observed for all alleles.
364
365 Results similar to those seen with calcofluor plates were obtained when analyzing JspA
366 derivatives with transcriptional fusion of the GUS reporter to *exoY* in *S. meliloti*: overexpression
367 of JspA-HA significantly increased *exoY* transcription, but to a lesser extent compared to
368 untagged JspA (Table 3). As with JspA, JspA-HA also increased *exoY* expression in the Δ*jspA*
369 mutant but not in the Δ*lppA* mutant, again indicating that JspA needs LppA for activity. The
370 E148A and E148D variants, untagged or tagged, both failed to elevate *exoY* expression to
371 levels achieved by JspA and JspA-HA, indicating that the active site of the protease is
372 necessary for function. Immunoblotting indicated that HA-tagged versions of JspA appear to
373 reach similar steady-state levels in wild-type, Δ*lppA*, and Δ*jspA* backgrounds (Fig. 4D, 4E),
374 demonstrating that variations in activity are not likely due to differences in protein stability in
375 different genetic backgrounds. Together, these results suggest that the active site of JspA is
376 critical for its proteolytic activity, but other domains contribute to function and may interfere with
377 cellular processes when overexpressed, consistent with previous demonstration by Arnold *et al.*

378 (2017) that the peptidase active site, the lipobox motif, and the LysM domain are all necessary
379 for protection against the antimicrobial activity of NCR247.
380
381 **LppA and JspA participate in the ExoR-ExoS-ChvI signaling pathway**
382 Considering that LppA and JspA are likely extracytoplasmic, we wondered how they influence
383 transcription of EPS-I and flagellar genes. To uncover their mechanism of action, we performed
384 whole-genome expression analysis using Affymetrix GeneChips (Barnett *et al.*, 2004). Having
385 generated mutant alleles and determined growth conditions and strain backgrounds with which
386 significant changes in gene expression could be observed, we decided to examine the
387 transcriptomes of Rm1021 carrying an empty vector or overexpressing wild-type JspA or loss-
388 of-function $JspA_{E148A}$ from a plasmid. As expected, overexpression of JspA caused changes in
389 a substantial set of genes, whereas $JspA_{E148A}$ did not: pairwise comparisons for changes greater
390 than 1.5-fold revealed 198 genes with significantly different expression between strains
391 overexpressing JspA and carrying the vector, 155 genes between JspA and $JspA_{E148A}$, and only
392 5 genes between $JspA_{E148A}$ and the vector (Fig. 5A, Table S4). 141 gene expression changes
393 were shared between the JspA versus vector and JspA versus $JspA_{E148A}$ comparisons, and
394 consequently these genes were deemed strong candidates for the JspA transcriptome: 80
395 increased expression and 61 decreased expression during JspA overexpression. Consistent
396 with measurements of *exoY* and *flaC* reporter fusions (Tables 2 and 3), a sizable portion of up-
397 regulated genes are associated with exopolysaccharide biosynthesis, while the majority of
398 down-regulated genes are associated with flagellar motility and chemotaxis. One up-regulated
399 target that stood out is *chvI*, encoding a conserved response regulator critical for viability and
400 symbiosis (Cheng & Walker, 1998b; Ratib *et al.*, 2018). To verify the results of the
401 transcriptome analysis, we constructed transcriptional fusions of the GUS reporter to *chvI* and
402 select candidates of the JspA transcriptome. Measurements of GUS activity showed expected
403 increase (for SMc01580, *pckA*, and *chvI*) or decrease (for *mcpU*) when *jspA* expression is
404 induced with taurine from the plasmid-borne P_{tau} promoter, compared to the same wild type
405 carrying the vector; in contrast, overexpression of the mutant $jspA_{E148A}$ allele did not elicit
406 significant changes (Table 4). We also evaluated expression of the *chvI* reporter when JspA
407 and variants were expressed from a plasmid-borne, IPTG-inducible promoter, P_{lac} (Khan *et al.*,
408 2008) to ensure that the observed changes could be replicated with another inducer.
409 Overexpression of JspA and JspA-HA both increased *chvI* transcription, whereas $JspA_{E148A}$,
410 untagged or tagged, did not cause similar effects (Table 4). These reporter activities support
411 the validity of the transcriptome analysis.

412

413 Knowing that the ExoR-ExoS-ChvI signaling system can control its own expression (Lu &
414 Cheng, 2010; Ratib *et al.*, 2018), we asked if JspA participates in that regulatory pathway. We
415 compared the JspA transcriptome against the published transcriptomes of ExoR/ExoS and ChvI
416 (Chen *et al.*, 2009; Ratib *et al.*, 2018; Wells *et al.*, 2007) (see Materials and methods for details)
417 and saw substantial overlap among the three sets of genes (Fig. 5B). In contrast, the JspA
418 transcriptome had minimal overlap with the published transcriptome of RpoH1, a heat shock
419 sigma factor (Fig. 5C) (Barnett *et al.*, 2012), chosen for comparison because it represented a
420 stress response distinct from that of the ExoR-ExoS-ChvI system. Hypergeometric probability
421 tests (Lund *et al.*, 2002) indicated that overlap among the JspA, ExoR/ExoS, and ChvI
422 transcriptomes are highly significant, whereas each of the three sets overlapped poorly with the
423 RpoH1 transcriptome (Table S5). As noted previously (Ratib *et al.*, 2018), there are significant
424 overlaps between the ChvI regulon and the groups of genes affected by the *podJ1* mutation
425 (Fields *et al.*, 2012) or by NCR247-treatment (Penterman *et al.*, 2014). To be expected for one
426 sharing the same genetic pathway as ChvI, JspA's transcriptome also intersects significantly
427 with the *podJ1* and NCR247 sets (Table S6). These similarities suggest that JspA contributes
428 to a regulatory pathway, likely the ExoR-ExoS-ChvI system, for responding to specific stress
429 conditions, such as those caused by the *podJ1* mutation or exposure to NCR247.
430

431 To determine if JspA and LppA influence the ExoR-ExoS-ChvI signaling pathway, we conducted
432 epistasis analysis, first using Tn5 insertions in *exoR* and *exoS* that lead to overproduction of
433 EPS-I (Doherty *et al.*, 1988). Strains carrying the *exoS96*::Tn*5* insertion produce an N-
434 terminally truncated ExoS that behaves like a constitutively active kinase (Cheng & Walker,
435 1998b), while strains carrying the *exoR95*::Tn*5* insertion produce a C-terminally altered ExoR
436 that has lost function (Lu *et al.*, 2012). Loss of *lppA* or *jspA* in these backgrounds did not
437 reduce EPS-I synthesis, suggesting that *exoR* and *exoS* are epistatic to *lppA* and *jspA* (Fig. 6A).
438 Considering that, like ExoR, mature JspA and LppA are predicted to reside in the periplasm,
439 and ExoR inhibits ExoS-ChvI signaling, we hypothesized that JspA and LppA together
440 negatively regulate ExoR activity (Fig. 6B). This model is consistent with JspA and LppA being
441 unable to reduce EPS-I production if ExoR is inoperative or if ExoS is constitutively active. To
442 test this idea further, we constructed a ChvI depletion strain, in which the only copy of *chvI* is
443 under the control of P_{lac} on a pBBR1-derived plasmid (Khan *et al.*, 2008). As ChvI is essential
444 for growth on rich medium, the ChvI depletion strain grew poorly in the absence of the IPTG
445 inducer and normally in its presence, similar to a *chvI*$^+$ strain carrying the same plasmid grown

446 in the absence or presence of IPTG (Fig. S3). We then monitored expression of the *exoY*
447 reporter when ChvI is replete or depleted and when wild-type or mutant JspA is overexpressed
448 from the P_{tau} promoter on a compatible RK2-derived plasmid (Mostafavi *et al.*, 2014) (Fig. 6C).
449 In a *chvI*$^{+}$ strain carrying the P_{lac} vector or the P_{lac}-*chvI* plasmid, constitutive expression of JspA
450 from P_{tau} increased *exoY* expression compared to the same strain carrying the P_{tau} vector (Fig.
451 6C, first four strains on the left), consistent with previous measurements (Tables 2 and 3). In
452 the ChvI depletion strain carrying the P_{tau} vector, shutting off *chvI* expression by removing IPTG
453 for six hours reduced *exoY* expression (Fig. 6C, fifth strain from left). When JspA was
454 overexpressed in the ChvI depletion strain, *exoY* expression was high when ChvI was replete in
455 the presence of IPTG (Fig. 6C, sixth strain from left, + IPTG), comparable to that seen in *chvI*$^{+}$
456 strains when JspA was overexpressed. However, depletion of ChvI in the absence of IPTG
457 prevented *exoY* expression from becoming elevated by JspA (Fig. 6C, sixth strain from left, -
458 IPTG). A ChvI depletion strain overexpressing $JspA_{E148A}$ (Fig. 6C, rightmost strain) yielded
459 similar *exoY* expression patterns as the depletion strain carrying the P_{tau} vector (Fig. 6C, fifth
460 strain from left). These results support the model that JspA functions upstream of ChvI:
461 increasing JspA levels relieves the inhibitory activity of ExoR, in turn activating the ExoS sensor
462 kinase and ChvI response regulator and promoting expression of EPS-I genes and thus EPS-I
463 production. In the absence of ChvI, JspA is unable to stimulate expression of EPS-I genes,
464 such as *exoY*.
465
466 The rhizobial ExoR-ExoS-ChvI system effects changes in gene expression in response to
467 environmental conditions, including acid stress (Altamirano-Silva *et al.*, 2018; Heckel *et al.*,
468 2014; Yuan *et al.*, 2008). Since JspA and LppA appear to act upstream of the system, we
469 investigated if they mediate transmission of environmental signals. We compared the JspA
470 transcriptome and ChvI regulon against sets of genes that changed expression upon acid
471 stress, identified in three different studies (de Lucena *et al.*, 2010; Draghi *et al.*, 2016; Hellweg
472 *et al.*, 2009). Hypergeometric probability tests indicate that the overlaps between the JspA
473 transcriptome or ChvI regulon and each of the three sets of acid response genes are significant
474 but not as strong as that between JspA and ChvI: the most significant overlaps with the JspA
475 transcriptome and ChvI regulon belong to the set identified by Hellweg, Pühler, and Weidner
476 (2009) (Table S7). However, the overlaps between the JspA transcriptome or ChvI regulon with
477 each of the three sets of acid response genes are comparable to, if not better than, overlaps
478 among the three. Thus, we chose four representative genes (SMb21188, SMc01580, *exoY*,
479 and *chvI*) from the JspA transcriptome and ChvI regulon that also appeared in one or more of

480 the acid responses and examined their expression via reporter fusions in acidic, neutral, or
481 basic pH. All four reporter fusions increased expression when wild-type Rm1021 was grown at
482 pH 6 compared to pH 7; only *exoY* showed significant increase at pH 8.5 as well (Fig. 7).
483 Deletion of *jspA* or *lppA* appeared to curtail this increase in response to acid stress, more
484 obviously for SMb21188 and SMc01580 (Fig. 7A and 7B, pink bars). For *exoY* and *chvI*, the
485 deletions reduced reporter expression compared to wild type at neutral pH (Fig. 7C and 7D,
486 yellow bars), and the fold-change between pH 6 and pH 7 in the deletion strains approximated
487 that seen in wild type (Fig. 7C and 7D, red percentages). Nevertheless, in the deletion mutants,
488 the increase in *exoY* expression due to growth at pH 6 was impacted more severely than the
489 increase due to growth at pH 8.5 (Fig. 7C). Our results suggest that, while factors other than
490 ChvI may help regulate *exoY* and *chvI* expression upon acid stress, JspA and LppA facilitate
491 ChvI's response to acid stress.
492
493 **JspA and LppA enhance ExoR degradation**
494 Because JspA is predicted to be a periplasmic protease, and JspA and LppA appear to promote
495 ExoS/ChvI activity, in opposition to ExoR, which can be regulated via proteolysis (Lu *et al.*,
496 2012; Wu *et al.*, 2012), we assessed whether JspA reduces ExoR levels. We introduced a
497 plasmid expressing *jspA* or *jspA*$_{E148A}$ from P_{lac} into a strain with *exoR-V5* allele instead of *exoR*
498 at the native locus. Induction of *jspA* expression with 1 mM IPTG in rich media inhibited growth,
499 starting 3 – 4 hours after induction (Fig. 8A and Fig. S4). Overexpression of *jspA*$_{E148A}$ did not
500 retard growth compared to a strain carrying the P_{lac} vector when cultures were grown in flasks
501 (Fig. S4B and S4C) but did modestly slow growth in 48-well plates (Fig. 8A and S4A). We
502 monitored steady-state levels of ExoR-V5 by immunoblotting with antibodies against the V5
503 epitope, at 0, 3, and 6 hours after induction. ExoR-V5 level was detectably lower in the strain
504 overexpressing JspA compared to strains carrying the vector or expressing mutant JspA$_{E148A}$,
505 six hours after induction (Fig. 8B). Our transcriptomic analysis indicated that *exoR* expression is
506 slightly elevated (1.3x) (Table S4) when *jspA* is constitutively induced. This increase in *exoR*
507 expression was verified using transcriptional fusion to the GUS reporter (Fig. 8C). Thus, the
508 decrease in ExoR level is not attributable to a drop in *exoR* expression. Instead, JspA appears
509 to negatively regulate ExoR at the protein level. The reduction in ExoR likely stimulates the
510 ExoS-ChvI pathway, resulting in feedback that elevates *exoR* transcription, as previously
511 described (Lu & Cheng, 2010).
512

513 To eliminate changes in ExoR levels due to transcriptional regulation, we placed a FLAG-tagged
514 version of *exoR* under the control of the P_{lac} promoter on a plasmid and induced expression with
515 0.5 mM IPTG in rich medium. Immunoblotting with anti-FLAG antibodies revealed a band for
516 the mature ExoR-FLAG protein at ~29 kDa, as well as a band with slightly larger molecular
517 mass, indicative of the pre-processed form (computed to be 32 kDa with the signal peptide)
518 (Fig. 9A, lane 2). We also observed additional bands with smaller molecular masses, likely
519 representing degradation products (Lu *et al.*, 2012). In the *jspA*$^+$ background, overexpression of
520 JspA-HA reduced the steady-state level of ExoR-FLAG, compared to when the strain carried the
521 vector or expressed mutant $JspA_{E148A}$-HA (Fig. 9A, lanes 2 – 4; 9B). In the Δ*jspA* background,
522 ExoR-FLAG levels were elevated compared to wild type, and overexpression of JspA-HA
523 reduced that elevation, while $JspA_{E148A}$-HA did not (Fig. 9A, lanes 6 – 8). Probing with
524 antibodies against the HA epitope indicated that steady-state levels of JspA-HA and $JspA_{E148A}$-
525 HA were comparable. Expression of untagged versions of JspA and JspAE148A in both the
526 Δ*jspA* and *jspA*$^+$ backgrounds (Fig. 9A, lanes 10 – 13) led to similar effects as the
527 corresponding HA-tagged variants on ExoR-FLAG, indicating that the tagged and untagged
528 versions of JspA behaved similarly in this assay. Next, we examined steady-state levels of
529 ExoR-FLAG when LppA is present or absent. Again, overexpression of JspA-HA reduced
530 ExoR-FLAG levels in both *jspA*$^+$ and Δ*jspA* strains (Fig. 9B, lanes 1 and 3), compared to the
531 same strains expressing mutant $JspA_{E148A}$-HA (Fig. 9B, lanes 2 and 4). However, in the Δ*lppA*
532 background, overexpression of JspA-HA did not reduce ExoR-FLAG levels compared to
533 overexpression of $JspA_{E148A}$-HA (Fig. 9B, lanes 5 and 6). These results reinforce that JspA and
534 LppA concertedly regulate the ExoR-ExoS-ChvI pathway by reducing ExoR protein levels.
535
536 To demonstrate further that JspA and LppA participate in ExoR proteolysis, we expressed the
537 three proteins in two heterologous systems, *C. crescentus* NA1000 and *E. coli* DH10B, both of
538 which lack clear *lppA* and *exoR* orthologs and contain weak *jspA* orthologs (Table S1). In
539 NA1000, ExoR-FLAG was expressed from a P_{lac} promoter on a pBBR1-based plasmid, while
540 different combinations of JspA variants and LppA were co-transcriptionally expressed from a
541 P_{tau} promoter on a compatible RK2-derived plasmid. When ExoR-FLAG was expressed in the
542 absence of JspA or LppA, we detected both the mature and pre-processed forms of the protein,
543 as well as various degradation products, by immunoblotting with anti-FLAG antibodies (Fig.
544 10A, lane 2). Expression of JspA, but not mutant $JspA_{E148A}$, reduced the steady-state level of
545 mature ExoR-FLAG but did not affect the pre-processed form (Fig. 10A, lanes 3 and 4). Levels
546 of mature ExoR-FLAG dropped further when LppA was expressed along with JspA or JspA-HA

547 (Fig. 10A, lanes 5 and 7); this reduction did not happen when LppA was expressed with
548 untagged or tagged versions of $JspA_{E148A}$ (Fig. 10A, lanes 6 and 8). Intriguingly, one of the
549 ExoR-FLAG degradation products, approximately 20-kDa in size, became more prominent when
550 only JspA, untagged or HA-tagged, was expressed (Fig. 10A, lane 3; Fig. S5A, lanes 5 and 9),
551 but lost this prominence when LppA was co-expressed with JspA (Fig. 10A, lanes 5 and 7; Fig.
552 S5A, lanes 7 and 11). Similar results were observed in *E. coli* DH10B, in which ExoR-FLAG
553 was again expressed from the same P_{lac} promoter on a pBBR1-based plasmid, while expression
554 of wild-type or mutant JspA-HA and varying levels of LppA-HA was achieved by placing different
555 constructs under the control of a weakened P_{trc} promoter on a pBR322-based plasmid (Weiss *et*
556 *al.*, 1999) (see Materials and methods) (Fig. S5B, File S1). In DH10B, expression of JspA-HA
557 alone did not reduce the steady-state level of ExoR-FLAG (lane 2 in both Fig. 10B and S5B,
558 lane 2), but co-expression of JspA-HA and LppA-HA did (lanes 4 and 6 in both Fig. 10B and
559 S5B). Furthermore, the extent of reduction in ExoR-FLAG levels depended on the level of
560 LppA-HA expression, such that mature ExoR-FLAG became undetectable when LppA-HA was
561 highly overexpressed (Fig. S5B, lane 8). This decrease in ExoR-FLAG levels failed to occur in
562 the presence of mutant $JspA_{E148A}$-HA (for example, lane 7 in both Fig. 10B and S5B). These
563 degradation patterns in *C. crescentus* and *E. coli* suggest that LppA assists JspA to proteolyze
564 ExoR.
565
566
567

Discussion

In this report, we demonstrated that two lipoproteins, JspA and LppA, jointly contribute to the production of EPS-I by regulating expression of relevant biosynthesis genes. Each also contributes to competitiveness in nodule colonization during symbiosis with *Medicago* hosts. Site-directed mutagenesis indicated that the lipobox motif of LppA and active site residues of the JspA protease are critical for their functions, consistent with annotations of predicted domains. Transcriptome, epistasis, and Western blot analyses further revealed that the two lipoproteins influence signaling through the conserved ExoS-ChvI two-component pathway and modulate the steady-state levels of ExoR, a periplasmic inhibitor of ExoS. Exposure to acidic pH is a potential cue for activating the signaling pathway.

These results suggest a model in which JspA and LppA, in response to cell envelope stress such as acid shock, facilitate the degradation of ExoR, thus enhancing phosphorelay in the ExoS-ChvI system, which generates physiological changes to counter the stress (Fig. 6B). This regulation via proteolysis appears analogous to how *E. coli* and other Gram-negative bacteria respond to envelope stress with the Cpx and sigma(E) pathways (Mitchell & Silhavy, 2019; Raivio, 2005). For the Cpx response, accumulation of misfolded proteins in the periplasm can cause DegP to degrade CpxP, a periplasmic inhibitor of the CpxAR two-component system (Isaac *et al.*, 2005). For the sigma(E) response, unfolded outer membrane proteins activate a proteolytic cascade involving DegS and RseP to degrade RseA, an inner membrane anti-sigma factor that inhibits sigma(E) (Alba *et al.*, 2002; Walsh *et al.*, 2003). While the exact molecular signal that induces degradation of ExoR is unknown, our results (Fig. 7) and evidence from other rhizobia (Altamirano-Silva *et al.*, 2018; Heckel *et al.*, 2014) indicate that acidic pH can activate the ExoS-ChvI pathway, possibly by causing protein misfolding in the cell envelope. Most likely, various other cell envelope perturbations can also potentiate the signal: for example, cell wall stress resulting from inhibition of the essential penicillin-binding protein PBP1a has recently been shown to activate the ExoS-ChvI pathway (Williams *et al.*, 2022), and JspA's LysM domain, predicted to bind peptidoglycans, was shown to be critical for protection against the antimicrobial peptide NCR247 (Arnold *et al.*, 2017). This model can accommodate a number of scenarios for how JspA and LppA jointly respond to envelope stress: for instance, LppA may enable the proper folding or positioning of JspA in the membrane, or misfolding of LppA may directly induce JspA's proteolytic activity. In particular, the complex physical

601 properties of the outer membrane (Cao & Wall, 2020; Sun *et al.*, 2022) necessitate multiple
602 regulatory checkpoints, and LppA may sense its integrity, analogous to the *E. coli* RcsF
603 lipoprotein (Tata *et al.*, 2021), and transmit disturbances to JspA. Alternatively, LppA may
604 monitor or participate in the crosslink between the outer membrane and the cell wall (Godessart
605 *et al.*, 2021), and disruptions in the process are relayed to JspA. Other envelope proteins that
606 influence ExoS-ChvI signaling, such as SyrA (Barnett & Long, 2015), may also participate in the
607 activation. Further investigation to elucidate the precise mechanisms involved would advance
608 understanding of stress response in rhizobia.
609
610 Notably, the *jspA* and *lppA* genes were originally identified in a suppressor analysis of a *podJ1*
611 mutant, which exhibits pleiotropic defects in the cell envelope (Fields *et al.*, 2012): while the
612 *podJ1* mutant grew poorly on LB medium with low salt concentrations, null mutations in *jspA* or
613 *lppA* alleviated the growth defect. A subdued envelope stress response when JspA or LppA is
614 absent may allow better growth of the *podJ1* mutant under specific conditions, as too much
615 activation can be deleterious. This interpretation is consistent with the suggestion that stress
616 response requires careful management to avoid toxicity (Mitchell & Silhavy, 2019). For
617 example, deletion of *rseA* in *E. coli* causes constitutive activation of the sigma(E) system,
618 resulting in membrane defects associated with lethality in stationary phase (Nicoloff *et al.*,
619 2017). Similarly, loss of *exoR* in *S. meliloti* led to lethality, or at least severely thwarted growth
620 (Arnold *et al.*, 2017; diCenzo *et al.*, 2018; Flores-Tinoco *et al.*, 2020; Price *et al.*, 2018), just as
621 overexpression of *jspA* did in the present study, presumably due to hyperactivation of the ExoS-
622 ChvI pathway. Deletion of *exoR* does not appear to retard growth as strongly in related rhizobia
623 such as *B. abortus* and *A. tumefaciens* (Castillo-Zeledón *et al.*, 2021; Heckel *et al.*, 2014),
624 consistent with ExoS and ChvI being critical for growth in *S. meliloti* (Bélanger *et al.*, 2009;
625 Wang *et al.*, 2010a) but not in these two other genetic models (Charles & Nester, 1993; Sola-
626 Landa *et al.*, 1998). Whether *exoR*, *exoS*, and *chvI* orthologs are required for viability appears
627 to vary in other rhizobia as well (Baraquet *et al.*, 2021; Lai *et al.*, 2016; Perry *et al.*, 2016). This
628 variability in the impact of conserved signaling pathways is not unprecedented. For example,
629 sigma(E) is essential in *E. coli* (De Las Peñas *et al.*, 1997) but not in *S. typhimurium*
630 (Humphreys *et al.*, 1999; Testerman *et al.*, 2002).
631
632 Effective management of envelope perturbations allows adaptation to environmental changes,
633 including those encountered during symbiosis (from mutualistic to pathogenic) (Hawkins &
634 Oresnik, 2021; Hews *et al.*, 2019). As impairment of ExoS and ChvI disrupts symbiosis (Barnett

635 & Long, 2015; Bélanger *et al.*, 2009; Wang *et al.*, 2010a; Wells *et al.*, 2007; Yao *et al.*, 2004),
636 and their orthologs are required for virulence in *A. tumefaciens* and *B. abortus* (Charles &
637 Nester, 1993; Sola-Landa *et al.*, 1998), *S. meliloti* likely modulates ExoS-ChvI signaling to
638 promote gene expression patterns conducive to invasion and persistence within a eukaryotic
639 host (Ratib *et al.*, 2018; Wells *et al.*, 2007), akin to pathogenic Gram-negative bacteria that use
640 the Cpx and sigma(E) pathways to express virulence factors to ensure survival during infection
641 (Fang *et al.*, 2016; Hews *et al.*, 2019; Raivio, 2005; Taylor *et al.*, 2014). For instance, JspA and
642 LppA may contribute to competitiveness by ensuring an appropriate degree of EPS-I production,
643 as the level of symbiotic EPS can optimize interaction with plant hosts (Jones, 2012). Other
644 genes regulated by JspA probably also contribute to efficient symbiosis. For example, JspA
645 inhibits expression of the transcription regulator LdtR, which plays a role in osmotic stress
646 tolerance, motility, and likely cell wall remodeling (Barnett *et al.*, 2019; Pagliai *et al.*, 2014).
647 JspA increases expression of *lsrB*, which encodes a LysR-family transcription factor required for
648 effective nodulation (Luo *et al.*, 2005) and involved in the differential expression of over 200
649 genes, including many that regulate redox homeostasis (An *et al.*, 2021). Deletion of *lsrB*
650 resulted in poor growth and increased sensitivity to the detergent deoxycholate (Barnett *et al.*,
651 2019), and *lsrB* orthologs in *B. abortus* and *A. tumefaciens* contribute to pathogenesis (Budnick
652 *et al.*, 2020; Eisfeld *et al.*, 2021; Sheehan *et al.*, 2015; Tang *et al.*, 2018). In addition, a
653 significant fraction of the JspA transcriptome consists of genes of unknown function, and
654 changes in their expression may promote fitness during host colonization as well. Many
655 uncharacterized genes in the ExoS-ChvI regulon, and by extension the JspA transcriptome, are
656 predicted to be translocated out of the cytoplasm and envelope-associated, making them more
657 likely to interact with the host environment and to maintain barrier integrity (Ratib *et al.*, 2018).
658 In particular, *jspA* was shown to confer resistance to the nodule-specific antimicrobial peptide
659 NCR247 (Arnold *et al.*, 2017). One possible explanation is that JspA changes gene expression
660 patterns via ExoS-ChvI to counter such host defenses. Nevertheless, other possible
661 explanations, not mutually exclusive, can also account for JspA's involvement in resistance
662 against cell envelope assaults: for example, JspA may degrade other substrates or signaling
663 pathways under specific conditions, or JspA and LppA may assist in the proper construction of
664 the cell envelope by ensuring proper maturation of other lipoproteins. Furthermore, a number of
665 other signaling systems, such as ActK-ActJ, CenK-CenR, CpxA-CpxR, EmmB-EmmC, FeuQ-
666 FeuP, and NtrX-NtrY, contribute to the maintenance of cell envelope integrity in rhizobia
667 (Albicoro *et al.*, 2021; Albicoro *et al.*, 2023; Barnett & Long, 2018; Bensig *et al.*, 2022;
668 Calatrava-Morales *et al.*, 2017; Griffitts *et al.*, 2008; Lakey *et al.*, 2022; Morris & Gonzalez,

669 2009; Santos *et al.*, 2010; VanYperen *et al.*, 2015; Wang *et al.*, 2013; Xing *et al.*, 2022), and
670 how these different systems cooperate with ExoS-ChvI to ensure successful symbiosis remains
671 ripe for further investigation.
672
673
674

675 # Materials and methods

676

677 **Bacterial strains, growth conditions, and genetic manipulations**

678 Strains derived from *Sinorhizobium meliloti* Rm1021 (Meade *et al.*, 1982) and *S. medicae*
679 WSM419 (Reeve *et al.*, 2010) used for this study are listed in Table S8. Other
680 alphaproteobacterial strains used were *S. fredii* NGR234 (Stanley & Cervantes, 1991; Trinick,
681 1980) and *C. crescentus* NA1000 (Evinger & Agabian, 1977). *E. coli* strains DH5α and DH10B
682 strains (both from Invitrogen) were used for molecular cloning, gene expression, and
683 maintenance of plasmids, which are listed in Table S9. *Sinorhizobium* strains were cultured at
684 30°C in LB, TY, or PYE media; *C. crescentus* was cultured at 30°C in PYE; and *E. coli* strains
685 were cultured at 30 or 37°C in LB (Fields *et al.*, 2012). When appropriate, antibiotics, agar,
686 sucrose, and/or calcofluor were added at previously published concentrations (Barnett *et al.*,
687 2000; Fields *et al.*, 2012). IPTG and taurine were added as inducers (Mostafavi *et al.*, 2014) at
688 concentrations described in the text. For pH shifts, LB medium was buffered with 20 mM 2-(*N*-
689 morpholino)ethanesulfonic acid (MES), 3-(*N*-morpholino)propanesulfonic acid (MOPS), or Tris,
690 and adjusted to pH 6, 7, or 8.5, respectively, with HCl or NaOH. Growth of cultures was
691 monitored by measuring absorbance at 600 nm (A_{600}), with aliquots from tubes or flasks or with
692 a BioTek Synergy H1m plate reader if grown in 48-well plates. Mobilization of plasmids from *E.*
693 *coli* to *Sinorhizobium* or *Caulobacter* strains via triparental mating, N3-mediated generalized
694 transduction, and two-step allelic replacement by homologous recombination were all performed
695 as previously described (Fields *et al.*, 2012; Finan *et al.*, 1986; Griffitts & Long, 2008; House *et*
696 *al.*, 2004; Martin & Long, 1984; Quandt & Hynes, 1993). Standard techniques were used for
697 manipulation and analysis of DNA, including PCR amplification, restriction digests, agarose gel
698 electrophoresis, ligation, and transformation (Ausubel *et al.*, 1998; Sambrook *et al.*, 1989).
699 Plasmids and DNA fragments were purified using commercial kits (Qiagen). Elim
700 Biopharmaceuticals synthesized custom oligonucleotides and provided Sanger DNA
701 sequencing services.

702

703 **Expression in *E. coli***

704 ExoR-FLAG was expressed in *E. coli* from an IPTG-inducible P_{lac} promoter on pMB859, derived
705 from the pSRKKm vector (Khan *et al.*, 2008). To co-express JspA-HA, $JspA_{E148A}$-HA, and LppA-
706 HA, we constructed plasmids derived from pDSW204, which is compatible with pSRKKm and
707 also allows IPTG induction with a weakened P_{trc} promoter (Weiss *et al.*, 1999): pJC720,

708 pJC730, pJC731, pJC733, pJC734, pJC735, pJC736, and pJC737 (Fig. S5, File S1). Plasmids
709 pJC720 and pJC733 carry wild-type *jspA-HA* and mutant *jspA*$_{E148A}$*-HA*, respectively, including
710 18 nucleotides upstream of *jspA*'s annotated start codon. We added *lppA-HA* to these plasmids
711 in three different configurations and assessed their expression empirically. For pJC730 and
712 pJC735, the ribosome binding site (RBS) of *E. coli araB* (Guzman *et al.*, 1995) was appended
713 upstream of *lppA-HA* and inserted after *jspA-HA* or *jspA*$_{E148A}$*-HA*. For pJC731 and pJC736,
714 *lppA-HA*, along with 54 nucleotides upstream of its originally annotated start codon (18
715 nucleotides upstream of the new start codon suggested in this report), was inserted after wild-
716 type or mutant *jspA-HA*. For pJC734 and pJC737, *lppA-HA* and its upstream sequence were
717 inserted in front of wild-type or mutant *jspA-HA*. We intended the RBS of *araB* to enhance
718 expression of *lppA-HA* in *E. coli*, but that configuration (pJC730 and pJC735) yielded the lowest
719 levels of expression (Fig. 10). Because *lppA-HA* is in-frame with wild-type or mutant *jspA-HA*
720 on pJC731, pJC734, pJC736, and pJC737, read-through translation (Ryoji *et al.*, 1983)
721 appeared to produce low levels of fusion proteins that were sometimes detectable on Western
722 blots (Fig. 10 and S5).
723
724 **Homology and domain analysis**
725 Orthologs in representative genomes and their sequence similarities to the query were
726 determined via BLAST (Boratyn *et al.*, 2013). Genomic contexts are presented as annotated in
727 the National Center for Biotechnology Information (NCBI) database (Sayers *et al.*, 2022).
728 Protein domains were predicted using InterPro (Blum *et al.*, 2021), Pfam (Mistry *et al.*, 2021),
729 and LipoP (Juncker *et al.*, 2003).
730
731 **Calcofluor assays**
732 EPS-I production was assess as previously described (Fields *et al.*, 2012), with LB plates
733 containing 0.02% calcofluor white M2R (MP Biomedicals). Liquid cultures were calibrated to the
734 same optical density (A_{600} of 0.2 – 0.5) and serially diluted ten-fold in water, and four or five µL
735 of the 10^{-2} to 10^{-6} dilutions were each spotted onto calcofluor plates containing appropriate
736 additives, such as taurine for induction and oxytetracycline for plasmid selection. Dilutions were
737 at times spotted onto PYE plates as well for comparison. Plates were examined and
738 photographed after 3-4 days of incubation with a Kodak 4000MM Pro Image Station, with its
739 associated Carestream MI software and filters (430 nm excitation and 535 nm emission). The
740 fluorescence intensity of each spot was standardized relative to the corresponding wild-type

741 control on the same plate, and the average values of the 10^{-2} to 10^{-4} spots from at least three
742 independent plates were compared.
743
744 **β-glucuronidase (GUS) assays**
745 Transcriptional fusions for β-glucuronidase (GUS) assays were constructed, and GUS activities
746 in different strains under various growth conditions were determined, as previously described
747 (Fields *et al.*, 2012; Swanson *et al.*, 1993). Fusions to *uidA* were introduced into the genome
748 using nonreplicating plasmids, and the wild-type function of the corresponding gene was
749 preserved (Table S9, File S1). Cells were lysed after measuring the optical density of the
750 culture (A_{600}), and PNPG (*p*-nitrophenyl-β-D-glucuronide) was incubated with the lysed cells
751 until the mixture turned light yellow, when A_{415} was measured. GUS activity was derived
752 according to the formula: A_{415} x 1000 / [(incubation time in minutes) x (culture volume in mL) x
753 A_{600}]. *p* values and statistical significance were determined using t-test (two-tailed, unequal
754 variance).
755
756 **Symbiosis assays**
757 Symbiotic association between *Sinorhizobium* strains and *Medicago* plants was assessed as
758 previously described (Fields *et al.*, 2012; Griffitts *et al.*, 2008; Li, 2018; Oke & Long, 1999).
759 Alfalfa (*M. sativa* GT13Rplus) and barrel medic (*M. truncatula* cultivar Jemalong A17) were
760 cultivated individually in 18x150-mm glass tubes on agar slants made with standard nodulation
761 medium [as described in (Crook *et al.*, 2012), except with 2 mM KH_2PO_4 and 0.5 mM MES, pH
762 6.3] and 11.5 g/L Phyto agar (PlantMedia); seeds were surface-sterilized with 70% ethanol and
763 50% bleach, rinsed with water, germinated in inverted 100x25-mm Petri dishes, placed on agar
764 slants, and allowed to grow for three days at 22°C under fluorescent lamps (16-h day length)
765 before inoculation. *M. sativa* was inoculated with *S. meliloti* Rm1021 strains, while *M. truncatula*
766 was inoculated with *S. medicae* WSM419 strains because WSM419 is a better symbiotic
767 partner for *M. truncatula* compared to *S. meliloti* strains, including Rm1021 (Ghosh *et al.*, 2021;
768 Larrainzar *et al.*, 2014; Terpolilli *et al.*, 2008). Bacterial cells grown to mid-logarithmic phase
769 were suspended in water to an A_{600} of 0.1, and each seedling was inoculated with 0.1 mL of the
770 suspension [approximately 10^7 colony-forming units (CFU)]. The numbers of white and pink
771 nodules that developed on plant roots were recorded at 14, 21, and 28 days post inoculation
772 (dpi). Initially white nodules turn pink due to production of leghemoglobin, indicative of nitrogen
773 fixation (Jones *et al.*, 2007). For competitive colonization assays, equal volumes of two cell
774 suspensions (with A_{600} of 0.1) were mixed and then diluted ten-fold, and each seedling was

775 inoculated with 0.1 mL of the diluted mixture (approximately 10^6 CFU). (For three of the 12
776 competitive assays with WSM419 strains, trials D1, D3, and E1, the inoculating mixtures were
777 not diluted, and each seedling received 10^7 CFU). The CFU and ratios of strains in the
778 inoculating mixtures were determined by plating serial dilutions on PYE containing streptomycin,
779 nalidixic acid, neomycin, or spectinomycin. Symbiosis competitiveness was assessed 28 dpi by
780 harvesting nodules, surface-sterilizing them individually with 10% bleach, crushing each in PYE
781 medium, and plating serial dilutions of the extracts: 10 µL each of 10^{-1} to 10^{-4} dilutions were
782 dripped to form lines on plates, and colonies were counted after three to four days of incubation
783 at 30°C. A nodule was considered to be dominated by a particular strain if more than 80% of
784 the CFU from the extract can be attributed to that strain. Consistent with previous reports
785 (Fields *et al.*, 2012; Gage, 2002), the majority of nodules were dominated by a single strain (Fig.
786 3, Table S3). For some nodules not dominated by a single strain, colonies recovered on
787 permissive plates (containing streptomycin for Rm1021 and its derivatives, or nalidixic acid for
788 WSM419 and its derivatives) were re-streaked to verify the ratios of strains (Table S3, "patch"
789 columns). In those cases, the nodule was assigned as mixed occupancy if neither strain gave
790 rise to at least 90% of the colonies tested. In some instances, two or more adjacent nodules
791 were harvested together and crushed in the same tube. If such a sample was dominated by a
792 single strain, then it counted as a single nodule for that strain. On the other hand, if the sample
793 yielded a mixture of two strains, then it was excluded from the final tally of that particular
794 competition trial [Table S3, "Mixed (Multi. Nodules)"]. In Fig. 3, *p*-values were calculated using
795 the Mann-Whitney-Wilcoxon test (two-tailed) for the *M. sativa* competitions and the t-test (two-
796 tailed, unequal variances) for the *M. truncatula* competitions. The Mann-Whitney-Wilcoxon test
797 is nonparametric but has less power for smaller sample sizes (and is ineffective for a total
798 sample size less than eight) (Motulsky, 2023); thus, the t-test was more suitable for analyzing
799 the *M. truncatula* competitions, which had fewer trials per category compared to the *M. sativa*
800 competitions. Table S3 provides the t-test *p*-values for competitions in both host plants.
801
802 **Transcriptome analysis**
803 Microarray analysis of RNA transcripts using custom Affymetrix GeneChips was conducted as
804 previously described (Barnett & Long, 2015; Barnett *et al.*, 2004). RNA purification, cDNA
805 preparation, chip hybridization, fluidics, scanning, and data analysis were performed accordingly
806 (Barnett *et al.*, 2004). Strains JOE3200 (carrying pCM130 vector), JOE4140 (expressing wild-
807 type *jspA*), and JOE4400 (expressing mutant $jspA_{E148A}$) were grown in PYE supplemented with
808 0.5 µg/mL oxytetracycline and 10 mM taurine for 4.5 hours to mid-logarithmic phase, when cells

809 were harvested for RNA extraction. Three biological replicates were used for each strain
810 analyzed. Nine pairwise comparisons were made between two strains: a change in signal was
811 considered significant if $p \leq 0.05$. As with other gene array platforms, our DNA chip measures
812 mRNA abundance, which is influenced by both transcription and mRNA decay; we use the term
813 "expression" to include the sum of all factors affecting mRNA abundance. Raw microarray data
814 have been deposited in the NCBI Gene Expression Omnibus (Barrett *et al.*, 2013) under
815 Accession GSE155833. The significance of overlap between transcriptomes or sets of genes
816 was determined using hypergeometric probability test, as previously described (Lund *et al.*,
817 2002; Ratib *et al.*, 2018). Genes in the ExoR/ExoS transcriptome were deduced from
818 interrogation of *exoR95*::Tn*5* and *exoS96*::Tn*5* mutants that have hyperactive ChvI activity
819 (Wells *et al.*, 2007); thus, many of the changes in gene expression may be indirect or
820 independent of the ExoS-ChvI pathway. In addition, two biological replicates for each strain
821 were used in that experiments (instead of the three used in the current analysis for JspA
822 transcriptome), and that could have contributed to the relatively large number of genes in the
823 ExoR/ExoS transcriptome. The ChvI regulon contains a combination of nonredundant genes
824 from two publications: (1) those that decreased expression in the ChvI(K214T) partial-loss-of-
825 function strain and increased expression in the ChvI(D52E) gain-of-function strain compared to
826 wild type (Chen *et al.*, 2009), and (2) group 1 and group 2 direct targets of ChvI (Ratib *et al.*,
827 2018).
828
829 **Western blotting**
830 Immunoblotting was performed using standard procedures (Ausubel *et al.*, 1998; Sambrook *et*
831 *al.*, 1989): 1.5 mL of culture samples were collected, resuspended in SDS sample buffer (at 150
832 μL for culture A_{600} of 1), boiled for 5 min, resolved by SDS-PAGE, and transferred to PVDF
833 membrane for detection by chemiluminescence (SuperSignal West Pico). Monoclonal anti-V5
834 (Invitrogen R960-25; AB_2556564) was used at 1:2500 dilution, anti-HA [clone 2-2.2.14]
835 (Thermo 26183; AB_10978021) used at 1:1000 to 1:5000 dilution, and antibody to *E. coli*
836 ATPase B [7E3F2] (Abcam ab110280) used at 1 ng/mL. Peroxidase-conjugated monoclonal
837 anti-FLAG M2 antibodies (Sigma A8592) were used at 1:2000 to 1:5000 dilution. Peroxidase-
838 conjugated donkey anti-mouse IgG antibodies (715-035-150) were from Jackson
839 ImmunoResearch Lab and used at 1:25,000 dilution. To examine blots containing both HA and
840 FLAG epitopes, we probed the blots first with anti-FLAG antibodies, detected them with
841 chemiluminescent substrates, washed the blots with Tris-buffered saline (Sambrook *et al.*,
842 1989) containing 0.05% Tween 20 (TBST), then probed with anti-HA primary antibodies and

843 peroxidase-conjugated secondary antibodies, and imaged again with chemiluminescence.
844 Similarly, to detect both V5 epitope and the beta subunit of ATP synthase, we probed blots first
845 with anti-V5 antibodies, imaged with chemiluminescence, washed the blots with TBST, then
846 probed with antibodies against ATPase B, and treated with chemiluminescence reagents.
847 Images captured in the second detection showed both target epitopes. Each blot image shown
848 is representative of at least two biological replicates.
849
850 **Data availability**
851 Microarray data have been deposited in the Gene Expression Omnibus (GEO) under accession
852 GSE155833. All plasmid sequences are provided as supporting information (File S1).
853
854
855

Acknowledgements

We thank Esther Chen, Mike Kahn, and Bob Fisher for discussion, support, and carrot cake. Esther Chen also provided critical feedback on the manuscript. We are grateful to past and current laboratory members for their assistance in various aspects of this project, particularly Reyna Benitez, Tanisha Saini, and Noel Lejat for performing GUS assays.

Funding

Research reported in this publication was supported by the National Institute of General Medical Sciences of the National Institutes of Health (NIH) under Award Number SC3-GM096943 to J.C.C. and National Science Foundation (NSF), Division of Integrative Organismal Systems, under Rules of Life Award Number 2015870 to S.R.L. NIH Award Number T34-GM008574 (MARC) provided support for J.A.B., J.S.C., R.C., R.L.-M., and J.N.; R25-GM048972 (Bridge to the Doctorate) supported H.A.R.; R25-GM059298 (MBRS-RISE) supported J.S.-M.; R25-GM050078 (Bridges to the Baccalaureate) supported J.S.C. and R.C.; T34-GM145400 (U-RISE) supported R.C.; and UL1-GM118985, TL4-GM118986, RL5-GM118984 (SF BUILD) supported B.K.R.M. NSF REU DBI Award Number 1156452 provided summer funding for R.L.-M. and R.B., and NSF DBI Award Number 1548297 provided summer funding for H.A.R. R.R.M. was supported by the Beckman Scholars Program. The content is solely the responsibility of the authors and does not necessarily represent the official views of the funding agencies.

881 # Figure legends

882

883 FIGURE 1. Schematics of the genomic regions around *lppA* and *jspA* and of their protein
884 products. (A) *S. meilioti lppA* (SMc00067) and *jspA* (SMc03872) share synteny with their
885 respective orthologs in closely related alphaproteobacteria, such as *B. abortus* and *A.*
886 *tumefaciens*. Gene and ORF names are shown as annotated, with pentagonal arrows
887 indicating directionality. Arrows with the same colors in different species represent probable
888 homologs, with red arrows indicating *lppA* or *jspA* orthologs; genes without annotated functions
889 or obvious orthologs in corresponding regions are depicted with shades of grey. RR and HK
890 signify response regulators and histidine kinases. The drawing is to scale; bar indicates 1 kb.
891 (B) *lppA* encodes a 148-aa lipoprotein, while *jspA* encodes a 497-aa metalloprotease. Both
892 LppA and JspA contain lipoprotein signal peptides at their N-termini; the sequences of these
893 leader peptides are shown, with red arrows indicating cleavage sites before the invariant
894 cysteine of the lipobox motifs, underlined. The N-terminus of LppA was originally annotated as
895 the 13th amino acid (V_{13}) shown here, but extension of 12 amino acids provides a better signal
896 sequence. JspA also contains M48 peptidase and LysM domains; key amino acids of the
897 peptidase domain are displayed. Grey numbers indicate residues that border the predicted
898 protein domains.

899

900

901 FIGURE 2. Calcofluor fluorescence, indicating EPS-I production, of strains expressing *lppA* or
902 *jspA*. Ten-fold serial dilutions (10^{-2} to 10^{-5}) of logarithmic-phase cultures were spotted onto LB
903 plates containing calcofluor and allowed to grow for three days prior to fluorescence imaging.
904 Darker spots on representative images indicate brighter fluorescence. Fluorescence levels
905 were measured relative to the *S. meliloti* Rm1021 wild-type (WT) strain carrying an empty vector
906 on each plate. Averages and standard deviations were calculated from measurements on at
907 least three independent days, with duplicate plates each time. (A) WT, Δ*lppA*, or Δ*jspA* strains
908 carrying the vector (pCM130 or pJC478) or a plasmid with *lppA* under the control of a taurine-
909 inducible promoter (pJC532) were grown on plates containing 0 or 100 mM taurine. (B) WT,
910 Δ*jspA*, or Δ*lppA* strains carrying the vector or a plasmid with *jspA* under the control of a taurine-
911 inducible promoter (pJC535) were grown on plates containing 0 or 2.5 mM taurine. Green bars
912 indicate comparisons when *lppA* is expressed, and those with blue borders indicate
913 comparisons with the Δ*jspA* background. Blue bars indicate comparisons when *jspA* is

914 expressed, and those with green borders indicate comparisons with the Δ*lppA* background. (C)
915 WT or Δ*jspA* strains carrying the vector or expressing *jspA* were grown on plates containing 5 or
916 10 mM taurine. (D) WT or Δ*lppA* strains carrying the vector or expressing *jspA* were grown on
917 plates containing 5 mM taurine. Relative fluorescence was not calculated for 5 or 10 mM
918 taurine due to growth inhibition of select strains.
919
920
921 FIGURE 3. Proportions of root nodules colonized by each bacterial strain after seedlings were
922 inoculated with equal mixtures of two strains. (A) *S. meliloti* Rm1021 and its derivatives were
923 used to infect *M. sativa*, while (B) *S. medicae* WSM419 and its derivatives were used to infect
924 *M. truncatula*. Rm1021 (Ω) is a derivative of Rm1021 marked with resistance to spectinomycin,
925 while WSM419^{R} are derivatives of WSM419 marked with resistance to spectinomycin or
926 neomycin. Mutations in *jspA* or *lppA* in Rm1021 were deletions or transposon insertions, while
927 those in WSM419 were all deletions. Percentages (± standard deviations) below each
928 competition indicate the mean proportions of nodules containing the mutant, wild type (WT), or a
929 mixture of the two, while the graphs depict relative abundance when mixed nodules are
930 excluded. Dark grey circles indicate the percentage of nodules occupied by WT for individual
931 competition trials. Error bars represent standard deviations. *, $p < 0.05$; **, $p < 0.01$. Bottom
932 row of each table [Trials (nodules)] indicates the number of trials (and total number of nodules
933 assessed) per competition. Detailed results from the competitive symbiosis assays are
934 available in Table S3.
935
936
937 FIGURE 4. Expression of mutant *lppA* and *jspA* alleles in *S. meliloti*. (A) Calcofluor
938 fluorescence was used to assess EPS-I production in Δ*lppA* strains expressing different alleles
939 of *lppA* from a taurine-inducible promoter. (B) Immunoblots show steady-state levels of different
940 versions of HA epitope-tagged LppA in wild-type (WT), Δ*lppA*, and Δ*jspA* backgrounds. C23S-
941 HA, G96W-HA, and A78S-HA stand for mutant versions of LppA-HA, encoded by $lppA_{C23S}$-*HA*,
942 $lppA_{G96W}$-*HA*, and $lppA_{A78S}$-*HA*, respectively. Samples were harvested from cultures grown in
943 LB with 100 mM taurine for 6 hours. (C) Wild-type Rm1021 expressing different *jspA* alleles
944 from a taurine-inducible promoter exhibit varying levels of fluorescence on calcofluor plates. (D,
945 E) Immunoblots show steady-state levels of different versions of JspA-HA. E148A-HA, E148D-
946 HA, and H147A-HA stand for mutant versions of JspA-HA, encoded by $jspA_{E148A}$-*HA*, $jspA_{E148D}$-
947 *HA*, and $jspA_{H147A}$-*HA*, respectively. Samples were harvested from (D) wild-type strains grown

948 in LB without or with 10 mM taurine for 3 hours or (E) wild-type, Δ*lppA*, or Δ*jspA* strains grown in
949 PYE with 10 mM taurine for 4.5 hours. Presence or absence of taurine in the growth medium (+
950 or -) or chromosomal *jspA* and *lppA* (+ or Δ) are indicated above each lane. Numbers to the
951 right of immunoblots (B, D) indicate approximate molecular mass standards, in kDa. Plasmids
952 pJC532, pJC605, pJC606, pJC607, pJC608, and pJC609 were used for expressing *lppA*,
953 $lppA_{C23S}$, *lppA-HA*, $lppA_{C23S}$-*HA*, $lppA_{G96W}$-*HA*, and $lppA_{A78S}$-*HA*, while pJC535, pJC555, pJC556,
954 pJC557, pJC558, pJC559, pJC560, pJC561 were used for *jspA*, $jspA_{E148A}$, $jspA_{E148D}$, $jspA_{H147A}$,
955 *jspA-HA*, $jspA_{E148A}$-*HA*, $jspA_{E148D}$-*HA*, and $jspA_{H147A}$-*HA*, respectively. Vectors used were
956 pCM130 (A, D, E) or pJC478 (C). For assessing calcofluor fluorescence (A, C), ten-fold serial
957 dilutions (10^{-2} to 10^{-5}) of logarithmic-phase cultures were spotted onto LB plates without or with
958 taurine, and allowed to grow for three days prior to fluorescence imaging. Darker spots on
959 representative images indicate brighter fluorescence.
960
961
962 FIGURE 5. Venn diagrams depicting overlaps of gene sets. (A) Circles of the Venn diagram
963 represent the numbers of genes whose expression changed >1.5-fold in three pairwise
964 comparisons: between strains that overexpress wild-type JspA or mutant $JspA_{E148A}$ (JspA vs.
965 $JspA_{E148A}$), between strains that overexpress JspA or carry the vector pCM130 (JspA vs.
966 vector), or between strains that overexpress mutant JpsA or carry the vector ($JspA_{E148A}$ vs.
967 vector). The 141 genes that appeared in both the JspA vs. vector and JspA vs. $JspA_{E148A}$
968 comparisons were grouped according to their functions, as listed on the right. ChvI belongs to
969 the group of regulators whose gene expression increased when JspA was overexpressed. (B,
970 C) The bottom Venn diagrams represent the overlaps of (B) genes that belong to the JspA or
971 ExoR/ExoS transcriptome or ChvI regulon and (C) those that belong to the RpoH1 or JspA
972 transcriptome. Gene sets and analyses of their overlaps are provided in Tables S4 and S5.
973 See Materials and methods for details about assignment of genes to the ChvI regulon and
974 ExoR/ExoS transcriptome.
975
976
977 FIGURE 6. Epistatic interaction between *jspA* and *lppA* and the *exoR-exoS-chvI* pathway. (A)
978 Calcofluor fluorescence of wild-type and mutant strains were assessed by spotting ten-fold
979 serial dilutions of cultures onto LB plates. Strain genotypes are shown to the left of the
980 fluorescence images, while percentages on the right indicate averages (± standard deviations)
981 of fluorescence levels relative to the Rm1021 wild type, set as 100% on each plate.

982 Representative images are shown, and at least two replicates were included for each
983 comparison. (B) Results from epistasis analysis, along with the predicted extracytoplasmic
984 locations of JspA and LppA, suggest that they act upstream of the ExoR-ExoS-ChvI signaling
985 pathway, as depicted by the schematic diagram. As a typical histidine kinase and response
986 regulator, ExoS and ChvI are presumed to function as homodimers (Cheng & Walker, 1998b;
987 Ratib *et al.*, 2018); for simplicity, the diagram does not show that. (C) Expression of the *exoY-*
988 *uidA* reporter was monitored in strains replete with or depleted of ChvI, while *jspA* or $jspA_{E184A}$
989 was ectopically expressed. Relevant alleles on the chromosome and on plasmids are indicated
990 below the plot: first row indicates the presence or absence of chromosomal *chvI* (+ or Δ),
991 second row indicates presence of empty vector or a plasmid that expresses *chvI* (vector or +),
992 and the third row indicates presence of vector or a plasmid that expresses wild-type or mutant
993 *jspA* (vector, +, or E148A, respectively). Δ*chvI* strains (rightmost three strains) carried a
994 complementing plasmid (pAD101) with *chvI* under the control of the P_{lac} promoter (P_{lac}-*chvI*):
995 growth in the presence of absence of IPTG resulted in expression or depletion of ChvI. For
996 comparison, $chvI^+$ strains carried the P_{lac}-*chvI* plasmid or the corresponding parent vector
997 (pSRKKm). The strains also bore a compatible vector (pCM130) or its derivatives with taurine-
998 regulated *jspA* or $jspA_{E184A}$ (pJC535 or pJC555). Strains were grown in LB with 10 mM taurine
999 for 6 hours, while expressing or depleting ChvI, prior to measurement of GUS activities.
1000 Averages and standard deviations (error bars) were calculated with measurements from at least
1001 five different days. **, $p < 0.01$ between specified measurements.
1002
1003
1004 FIGURE 7. Effects of *jspA* and *lppA* on transcriptional responses to pH shift. Changes in gene
1005 expression were determined using fusions of *uidA* (encoding the GUS reporter) to (A)
1006 SMb21188, (B) SMc01580, (C) SMb20946 (*exoY*), and (D) SMc02560 (*chvI*) at their native loci,
1007 generated in such a way as to preserve the function of the gene being examined. GUS
1008 activities in Rm1021 wild-type, Δ*jspA*, and Δ*lppA* strains were measured 4.5 hours after cultures
1009 were shifted from pH 7 to pH 6 (pink bars), 7 (yellow bars), or 8.5 (blue bars) in LB medium.
1010 Activity at pH 6 relative to pH 7 for each genotype is shown as the red percentage above each
1011 pink bar. Maroon * or ** within a bar for one of the mutants represents significant difference ($p <$
1012 0.05 or $p < 0.01$, respectively) when compared to the same condition in wild type. Analogously,
1013 black * or ** indicates significant difference when activity at pH 6 or 8.5 is compared to that at
1014 pH 7 for the same genotype. Averages and standard deviations (error bars) were calculated
1015 from three to six independent measurements.

1016

1017

1018 FIGURE 8. Effects of JspA on ExoR levels. (A) Plot depicts growth of *exoR-V5* strains carrying
1019 the pSRKGm vector or derivatives (pJC652 or pJC653) with *jspA* or *jspA*$_{E184A}$ (noted as E148A)
1020 under control of the P_{lac} promoter. Strains JOE5242, JOE5244, and JOE5246 were grown in
1021 48-well plates, with 0.4 mL PYE plus 1 mM IPTG per well. Absorbance at 600 nm (A600) was
1022 measured every 30 minutes. Average readings for three different days are depicted, with
1023 surrounding shadings indicating standard deviations. In the absence of IPTG, all strains
1024 exhibited growth patterns similar to that of the vector-carrying strain in the presence of IPTG
1025 (see Fig. S4A). (B) Immunoblot shows steady-state levels of ExoR-V5 and the beta subunit of
1026 ATP synthase at 0, 3, and 6 hours after inducing expression of *jspA* or *jspA*$_{E184A}$, compared
1027 against levels in the vector-carrying strain. Approximate molecular mass, in kDa, are shown to
1028 the left of the blot, while lane numbers are shown below. Growth conditions were similar to that
1029 in (A), except that strains were cultured in flasks. (C) Expression of the *uidA* reporter fusion to
1030 *exoR* from its native locus was assessed in strains carrying the vector (pCM130) or
1031 overproducing JspA or JspA$_{E148A}$ (with pJC535 or pJC555). Strains were grown with 10 mM
1032 taurine for 4.5 hours prior to measurement of GUS activities. Averages and standard deviations
1033 were calculated from at least four measurements. *, $p < 0.05$ when compared against the
1034 vector-carrying strain.

1035

1036

1037 FIGURE 9. Steady-state levels of ExoR-FLAG when *jspA* or *lppA* differentially expressed. (A)
1038 Levels of ExoR-FLAG in the presence of different versions of JspA were assessed by
1039 immunoblotting with anti-FLAG antibodies (bottom blot), while expression of JspA-HA was
1040 verified with anti-HA antibodies (top blot). ExoR-FLAG expression is indicated above the blots:
1041 + signifies that expression of ExoR-FLAG from pMB859 was induced with 0.5 mM IPTG in TY
1042 medium for 4.5 hours, while - signifies that the strain carried the empty vector pSRKKm under
1043 the same conditions. Presence (+) or deletion (Δ) of the native *jspA* in the chromosome is also
1044 indicated. Different versions of JspA were induced with 10 mM taurine as follows: wild-type
1045 JspA from pJC614 (black +), mutant JspA$_{E148A}$ from pJC615 (black *), wild-type JspA-HA from
1046 pJC616 (red +), mutant JspA$_{E148A}$-HA from pJC617 (red *), and no expression from the vector
1047 pJC473 (-). (B) Immunoblots show steady-state levels of ExoR-FLAG and JspA-HA in the
1048 presence or absence of chromosomal *lppA*. The presence (+) or deletion (Δ) of native *jspA* or
1049 *lppA* on the chromosome is shown above the blots. Expression of JspA-HA, wid-type (+) or

1050 mutant (*), is indicated above the blots as in (A) (JspA-HA row). All strains in (B) expressed
1051 ExoR-FLAG from pMB859, induced with 0.5 mM IPTG. Approximate molecular mass, in kDa,
1052 are shown to the left of the blots, while lane numbers are shown below. Positions of bands
1053 representing JspA-HA and ExoR-FLAG are indicated to the right of the blots. Both sets of blots
1054 were first probed with anti-FLAG antibodies and then anti-HA antibodies (see Materials and
1055 methods). The bottom images were captured first, while the top images were acquired from the
1056 same respective blots after the second probing.
1057
1058
1059 FIGURE 10. Steady-state levels of ExoR-FLAG when co-expressed with JspA and LppA in *C.*
1060 *crescentus* NA1000 or *E. coli* DH10B. (A) Levels of ExoR-FLAG and JspA-HA were assessed
1061 in NA1000 by immunoblotting with anti-FLAG and anti-HA antibodies. ExoR-FLAG expression
1062 is indicated above the blot: + signifies that expression of ExoR-FLAG from pMB859 was
1063 induced with 0.1 mM IPTG in PYE medium for 4 hours, while - signifies that the strain carried
1064 the empty vector pSRKKm under the same conditions. Expression of LppA and different
1065 versions of JspA were induced with 10 mM taurine from the following plasmids: lanes 1 and 2,
1066 pJC473 vector when neither expressed (- for both LppA and JspA); lane 3, pJC614 for JspA
1067 (black +); lane 4, pJC615 for $JspA_{E148A}$ (black *); lane 5, pJC702 for both LppA and JspA; lane 6,
1068 pJC706 for LppA and $JspA_{E148A}$; lane 7, pJC707 for LppA and JspA-HA (red +); and lane 8,
1069 pJC708 for LppA and $JspA_{E148A}$-HA (red *). (B) Immunoblots show steady-state levels of JspA-
1070 HA, LppA-HA, and ExoR-FLAG in DH10B. All strains were induced with 0.1 mM IPTG in LB
1071 medium for 4 hours. ExoR-FLAG expression is indicated above the blots: + signifies expression
1072 from pMB859, while - signifies carriage of the pSRKKm vector. Expression of different versions
1073 of JspA-HA and varying levels of LppA-HA was achieved using different plasmids, similarly
1074 indicated above the blots as in (A): lane 1, pDSW208 vector (expressing GFP); lanes 2 and 8,
1075 pJC720 (*jspA-HA* only); lanes 3 and 9, pJC733 ($jspA_{E148A}$-*HA*); lane 4, pJC730 (*jspA-HA* and
1076 *lppA-HA*, with intervening RBS); lane 5, pJC735 ($jspA_{E148A}$-*HA* and *lppA-HA*, with intervening
1077 RBS); lane 6, pJC731 (*jspA-HA* translationally coupled to *lppA-HA*); and lane 7, pJC736
1078 ($jspA_{E148A}$-*HA* translationally coupled to *lppA-HA*). Higher levels of expression of LppA-HA in
1079 lanes 6 and 7 are represented by the larger, bold + sign above the blots. Blots were first probed
1080 with anti-FLAG antibodies and then with anti-HA antibodies. Approximate molecular mass, in
1081 kDa, are shown to the left of the blots, while lane numbers are shown below. Positions of bands
1082 representing JspA-HA, LppA-HA, and ExoR-FLAG are indicated to the right of the blots. Protein
1083 band designated by a red asterisk is presumed to be a fusion of JspA-HA and LppA-HA that

1084 resulted from translational read-through. *E. coli* anti-HA images were captured from the same
1085 representative blot (with longer exposure for LppA-HA), while the anti-FLAG image was from a
1086 duplicate blot of the same samples.
1087
1088

1089
1090 Table 1. Expression levels of select promoters in wild type and deletion mutants, as measured by
1091 transcriptional fusions to the GUS reporter (encoded by *uidA*).
1092
1093

Promoter tested / Strain genotype	**LB**					**PYE**				
***exoY* (SMb20946)**										
Rm1021	8.7	±	2.0		**100%**	6.9	±	0.8		**100%**
Δ*jspA*	4.8	±	0.8	**	**55%**	4.4	±	1.0	**	**64%**
Δ*lppA*	5.6	±	1.5	*	**64%**	5.0	±	0.5	**	**72%**
Δ*jspA* Δ*lppA*	4.6	±	0.5	**	**52%**	4.0	±	0.5	**	**58%**
***flaC* (SMc03040)**										
Rm1021	4.4	±	0.5		**100%**	10.3	±	1.1		**100%**
Δ*jspA*	6.0	±	1.2	**	**136%**	11.8	±	0.9	*	**115%**
Δ*lppA*	5.9	±	1.0	**	**134%**	11.8	±	0.7	*	**114%**
Δ*jspA* Δ*lppA*	6.1	±	0.6	**	**140%**	12.2	±	1.4	*	**118%**
***mcpU* (SMc00975)**										
Rm1021	6.5	±	0.8		**100%**	52.8	±	7.7		**100%**
Δ*jspA*	10.4	±	0.9	**	**159%**	67.9	±	7.9	**	**129%**
Δ*lppA*	9.8	±	1.2	**	**149%**	61.8	±	11.2		**117%**
Δ*jspA* Δ*lppA*	10.4	±	1.4	**	**159%**	62.1	±	8.1		**118%**

1094
1095
1096 β-glucuronidase (GUS) activities (averages ± standard deviations, in Miller units) of strains grown in LB or
1097 PYE were measured as described in Materials and methods. Averages and standard deviations were
1098 calculated from values obtained with at least five biological replicates. Percentage equals the enzymatic
1099 activity, expressed from the indicated promoter-*uidA* fusion, in the mutant divided by that in wild-type
1100 Rm1021. Two-tailed, unequal variances t-test was used to determine whether differences between wild-
1101 type and mutant strains were statistically significant: *, $0.01 < p < 0.05$; **, $p < 0.01$. Nonreplicating
1102 plasmids integrated into the genome to create transcriptional fusions to *exoY*, *flaC*, and *mcpU* were
1103 pEC340, pMB694, and pMB696, respectively.
1104
1105
1106

1107
1108 Table 2. Activities of transcriptional fusion reporters when *jspA* or *lppA* ectopically expressed.
1109
1110

Condition / Strain genotype	**Promoter activity**				
PYE + 10 mM taurine, 3 hr	***flaC* (SMc03040)**				
Rm1021 / pCM130 (vector)	9.8	±	0.5		**100%**
Rm1021 / pJC535 (P_{tau}-***jspA***)	7.1	±	0.4	**	**72%**
Rm1021 / pJC532 (P_{tau}-***lppA***)	9.5	±	0.9		**98%**
	***exoY* (SMb20946)**				
Rm1021 / pCM130	7.3	±	0.6		**100%**
Rm1021 / pJC535 (P_{tau}-***jspA***)	14.6	±	0.8	**	**199%**
Rm1021 / pJC532 (P_{tau}-***lppA***)	8.2	±	0.5		**112%**
Δ*jspA* / pCM130	5.1	±	0.8	**	**69%**
Δ*jspA* / pJC535 (P_{tau}-***jspA***)	11.3	±	2.2	*	**155%**
Δ*lppA* / pCM130	5.4	±	1.3		**75%**
Δ*lppA* / pJC535 (P_{tau}-***jspA***)	6.2	±	1.7		**84%**
LB + 100 mM taurine, 6 hr	***exoY* (SMb20946)**				
Rm1021 / pCM130	9.0	±	0.5		**100%**
Rm1021 / pJC532 (P_{tau}-***lppA***)	10.6	±	0.7	*	**118%**
Δ*lppA* / pCM130	5.0	±	1.1	**	**56%**
Δ*lppA* / pJC532 (P_{tau}-***lppA***)	9.1	±	0.8		**102%**
Δ*jspA* / pCM130	4.7	±	0.8	**	**52%**
Δ*jspA* / pJC532 (P_{tau}-***lppA***)	4.8	±	0.6	**	**54%**

1111
1112
1113 β-glucuronidase (GUS) activities (averages ± standard deviations, in Miller units) of strains grown under
1114 the indicated conditions were measured as described in Materials and methods. Averages and standard
1115 deviations were calculated from values obtained with at least three biological replicates. Percentages
1116 equal the enzymatic activities, expressed from the indicated promoter-*uidA* fusions, of the respective
1117 strains divided by that in wild-type Rm1021 carrying the pCM130 vector. Two-tailed, unequal variances t-
1118 test was used to determine whether differences from the vector-carrying wild type were statistically
1119 significant: *, $0.01 < p < 0.05$; **, $p < 0.01$. Nonreplicating plasmids integrated into the genome to create
1120 transcriptional fusions to *exoY* and *flaC* were pEC340 and pMB694, respectively.
1121
1122
1123

1124
1125 Table 3. Expression from reporter fusion to *exoY* promoter when mutant *jspA* or *lppA* allele
1126 overexpressed.
1127
1128

Strain genotype	*exoY* (SMb20946) expression				
Overexpress *jspA* alleles	**PYE + 10 mM tau, 4.5 hrs**				
Rm1021 / pCM130 (vector)	7.5	±	1.5		**100%**
Rm1021 / pJC535 (P_{tau}-***jspA***)	17.8	±	3.7	**	**238%**
Rm1021 / pJC555 (P_{tau}-***jspA***$_{E148A}$)	8.4	±	0.4	*	**113%**
Rm1021 / pJC556 (P_{tau}-***jspA***$_{E148D}$)	8.4	±	1.0		**112%**
Rm1021 / pJC558 (P_{tau}-***jspA-HA***)	11.8	±	1.7	**	**158%**
Rm1021 / pJC559 (P_{tau}-***jspA***$_{E148A}$***-HA***)	7.1	±	1.6		**96%**
Rm1021 / pJC560 (P_{tau}-***jspA***$_{E148D}$***-HA***)	6.8	±	0.8		**90%**
Δ*jspA* / pJC558 (P_{tau}-***jspA-HA***)	10.9	±	1.4	**	**146%**
Δ*lppA* / pJC558 (P_{tau}-***jspA-HA***)	7.0	±	1.2		**93%**
Overexpress *lppA* alleles	**LB + 100 mM tau, 6 hrs**				
Δ*lppA* / pCM130	6.1	±	0.6		**100%**
Δ*lppA* / pJC532 (P_{tau}-***lppA***)	11.9	±	1.1	**	**195%**
Δ*lppA* / pJC605 (P_{tau}-***lppA***$_{C23S}$)	7.0	±	0.7		**115%**
Δ*lppA* / pJC606 (P_{tau}-***lppA-HA***)	11.0	±	1.3	**	**180%**
Δ*lppA* / pJC607 (P_{tau}-***lppA***$_{C23S}$***-HA***)	6.8	±	1.0		**111%**
Δ*lppA* / pJC608 (P_{tau}-***lppA***$_{G96W}$***-HA***)	8.8	±	0.4	**	**130%**
Δ*lppA* / pJC609 (P_{tau}-***lppA***$_{A78S}$***-HA***)	8.3	±	0.3	**	**123%**

1129
1130
1131 β-glucuronidase (GUS) activities (in Miller units) of strains grown under the indicated conditions were
1132 measured as described in Materials and methods. Averages and standard deviations were derived from
1133 values obtained with at least three biological replicates. Averages for the vector-carrying wild type and
1134 *lppA* deletion mutant (first line of each group) were set at 100% and used to calculate relative activities.
1135 Statistical significance of differences from the vector-carrying wild type or *lppA* deletion mutant was
1136 determined with t-test (two-tailed, unequal variances): *, $0.01 < p < 0.05$; **, $p < 0.01$. Nonreplicating
1137 plasmid pEC340 was integrated into the genomes of different strains to generate transcriptional fusion to
1138 *exoY*.
1139
1140
1141

1142
1143 Table 4. Select promoters confirm transcriptional changes when *jspA* overexpressed.
1144
1145

Promoter tested / Strain genotype	**GUS activity**				**% WT**
***mcpU* (SMc00975)**	**PYE + 10 mM tau, 4.5 hrs**				
Rm1021 / pCM130 (vector)	40.0	±	3.7		**100%**
Rm1021 / pJC535 (P_{tau}-***jspA***)	25.3	±	2.7	*	**63%**
Rm1021 / pJC555 (P_{tau}-***jspA***$_{E148A}$)	39.2	±	2.0		**98%**
SMc01580					
Rm1021 / pCM130	6.3	±	1.2		**100%**
Rm1021 / pJC535 (P_{tau}-***jspA***)	20.3	±	1.1	**	**321%**
Rm1021 / pJC555 (P_{tau}-***jspA***$_{E148A}$)	7.1	±	0.6		**113%**
***pckA* (SMc02562)**					
Rm1021 / pCM130	38.4	±	9.4		**100%**
Rm1021 / pJC535 (P_{tau}-***jspA***)	59.1	±	8.7	**	**154%**
Rm1021 / pJC555 (P_{tau}-***jspA***$_{E148A}$)	45.5	±	12.6		**119%**
***chvI* (SMc02560)**					
Rm1021 / pCM130	20.4	±	2.8		**100%**
Rm1021 / pJC535 (P_{tau}-***jspA***)	39.3	±	6.7	**	**193%**
Rm1021 / pJC555 (P_{tau}-***jspA***$_{E148A}$)	23.5	±	3.3		**115%**
***chvI* (SMc02560)**	**PYE + 1 mM IPTG, 4.5 hrs**				
Rm1021 / pSRKGm	27.1	±	1.5		**100%**
Rm1021 / pJC652 (P_{lac}-***jspA***)	43.2	±	7.0	**	**159%**
Rm1021 / pJC653 (P_{lac}-***jspA***$_{E148A}$)	30.8	±	4.5		**114%**
Rm1021 / pJC654 (P_{lac}-***jspA-HA***)	41.2	±	3.6	**	**152%**
Rm1021 / pJC655 (P_{lac}-***jspA***$_{E148A}$***-HA***)	31.4	±	2.8	*	**116%**

1146
1147
1148 β-glucuronidase (GUS) activities (in Miller units) of strains grown under the indicated conditions were
1149 measured as described in Materials and methods. Averages and standard deviations were derived from
1150 values obtained with at least three biological replicates. Averages for the vector-carrying wild type (first
1151 line of each group) were set at 100% and used to calculate relative activities (% WT). Statistical
1152 significance of differences from the vector-carrying wild type was determined with t-test (two-tailed,
1153 unequal variances): *, $0.01 < p < 0.05$; **, $p < 0.01$. Nonreplicating plasmids integrated into the genome
1154 to create transcriptional fusions of *uidA* to *mcpU*, SMc01580, *pckA*, and *chvI* were pMB696, pJC640,
1155 pJC639, and pJC638, respectively.
1156
1157
1158

1159 # Supporting information

1160

1161 **S1 Fig. Production of calcofluor-binding exopolysaccharides in *S. medicae* WSM419 and**
1162 **its derivatives.** Ten-fold serial dilutions of logarithmic-phase cultures were spotted onto solid
1163 media and allowed to grow for three days prior to imaging. (A) Representative images show
1164 fluorescence of wild-type WSM419, Δ*jspA* (ΔSmed_3110) mutant, Δ*lppA* (ΔSmed_0632)
1165 mutant, and derivatives marked with neomycin (Nm^R) or spectinomycin (Sp^R) resistance [*nptII* or
1166 *aadA* linked to *podJ* (Smed_0147) or replacing *jspA*] on LB plates containing calcofluor. Darker
1167 spots indicate brighter fluorescence. (B) WSM, Δ*jspA*, and Δ*lppA* strains carrying the vector
1168 (pCM130) or a plasmid with *S. meliloti jspA*, $jspA_{E148A}$, or *lppA* under the control of a taurine-
1169 inducible promoter (pJC535, pJC555, or pJC532, respectively) were grown on LB plates
1170 containing tetracycline (Tet) and calcofluor, without or with taurine (5 mM taurine for *jspA*
1171 complementation, 10 mM for *lppA*). Visible-light images of corresponding strains grown on PYE
1172 plates show mucoid colonies. Labels on the left indicate strain numbers, while labels on the
1173 right indicate genotypes. Each experiment was performed at least twice.

1174

1175 **S2 Fig. Overexpression of *jspA* alleles in *S. medicae* WSM419, *S. fredii* NGR234, and *C.***
1176 ***crescentus* NA1000.** Ten-fold serial dilutions of logarithmic-phase cultures were spotted onto
1177 PYE plates containing 0, 5, or 10 mM taurine. NA1000 strains were grown with 1 μg/mL
1178 oxytetracycline for two days, while WSM419 and NGR234 strains were grown with 5 μg/mL
1179 oxytetracycline for three days at 30°C prior to imaging. Labels on the left indicate strain
1180 numbers, while labels on the right indicate the *jspA* alleles being expressed from a plasmid.
1181 Plasmids used were pJC614 (*jspA*), pJC615 ($jspA_{E148A}$), pJC616 (*jspA-HA*), and pJC617
1182 ($jspA_{E148A}$-*HA*). Images shown represent four replicates on two different days.

1183

1184 **S3 Fig. Depletion of ChvI.** (A) Plate images show growth of ChvI depletion strain on LB
1185 medium in the presence and absence of 1 mM IPTG. The top strain (AD124) carried the
1186 pSRKKm vector and had a Δ*chvI* allelic replacement plasmid (pAD112) integrated into its
1187 chromosome but retained a copy of $chvI^+$, while the bottom strain (AD115) carried pAD101, with
1188 *chvI* under the control of the P_{lac} promoter, and had its *chvI* replaced by a hygromycin resistance
1189 gene (*hph*). (B) Plots show growth curves of ChvI depletion strains over 24 hours in LB, in the
1190 presence or absence of 0.5 mM IPTG. $chvI^+$ or Δ*chvI* strains carried pAD101, as well as a
1191 compatible vector (pCM130) or derivatives (pJC535 or pJC555) containing taurine-regulated

1192 *jspA* or *jspA*$_{E184A}$ (abbreviated as E148A), under control of the P_{tau} promoter. No taurine was
1193 added in these growth experiments. Cultures were shaken at 1000 rpm in 48-well plates, with
1194 0.4 mL medium (containing kanamycin and oxytetracycline) per well. Absorbance at 600 nm
1195 (A600) was measured every 30 minutes. Average readings for three different days are shown,
1196 with corresponding shadings indicating standard deviations. In the presence of IPTG, all strains
1197 exhibited similar growth patterns; curves for depletion strains carrying P_{tau}-*jspA* or *jspA*$_{E148A}$
1198 grown with IPTG were omitted for clarity. Strains shown here for growth curves (JOE5579,
1199 JOE5605, JOE5607, JOE5609) all contain a genomic *exoY-uidA* reporter and constitute a
1200 subset of those used for GUS assays in Figure 6C.
1201
1202 **S4 Fig. Growth curves of *exoR-V5* strains carrying the pSRKGm vector or derivatives**
1203 **(pJC652 or pJC653) with *jspA* or *jspA*$_{E184A}$ (noted as E148A) under control of the P_{lac}**
1204 **promoter.** (A) Strains JOE5242, JOE5244, and JOE5246 were grown in 48-well plates, with
1205 0.4 mL PYE per well, in the presence of absence of 1 mM IPTG. Absorbance at 600 nm (A600)
1206 was measured every 30 minutes. Average readings for three different days are depicted, with
1207 surrounding shadings indicating standard deviations. Lines without markers represent growth in
1208 the absence of IPTG (-); standard deviations for these were omitted for simplicity. Figure 7
1209 shows a portion of this graph. (B, C) Liquid cultures of the same strains were grown in flasks
1210 with 1 mM IPTG in (B) PYE or (C) LB medium, and A600 was measured every hour for 12
1211 hours. The plots were generated from single experiments.
1212
1213 **S5 Fig. Steady-state levels of ExoR-FLAG when co-expressed with different forms of**
1214 **JspA and varying levels of LppA in *C. crescentus* NA1000 or *E. coli* DH10B.** (A) Levels of
1215 ExoR-FLAG and JspA-HA were assessed in NA1000 by immunoblotting with anti-FLAG and
1216 anti-HA antibodies. ExoR-FLAG expression is indicated above the blot: + signifies that
1217 expression of ExoR-FLAG from pMB859 was induced with 0.1 mM IPTG in PYE medium for 4
1218 hours, while - signifies that the strain carried the empty vector pSRKKm under the same
1219 conditions. Expression of LppA and different versions of JspA were induced with 10 mM taurine
1220 from the following plasmids: lanes 1 and 4, pJC473 vector when neither expressed (- for both
1221 LppA and JspA); lanes 2 and 9, pJC616 for JspA-HA only (red +); lanes 3 and 10, pJC617 for
1222 JspA$_{E148A}$-HA (red *); lane 5, pJC614 for JspA (black +); lane 6, pJC615 for JspA$_{E148A}$ (black *);
1223 lane 7, pJC702 for LppA and JspA; lane 8, pJC706 for LppA and JspA$_{E148A}$; lane 11, pJC707 for
1224 LppA and JspA-HA; and lane12, pJC708 for LppA and JspA$_{E148A}$-HA. (B) Immunoblots show
1225 steady-state levels of JspA-HA, LppA-HA, and ExoR-FLAG in DH10B. All strains were induced

1226 with 0.1 mM IPTG in LB medium for 4 hours. ExoR-FLAG expression is indicated above the
1227 blots: + signifies expression from pMB859, while - signifies carriage of the pSRKKm vector.
1228 Expression of different versions of JspA-HA and varying levels of LppA-HA was achieved using
1229 different plasmids, similarly indicated above the blots as in (A): lane 1 and 14, pDSW208 vector
1230 (expressing GFP); lanes 2 and 10, pJC720 (*jspA-HA* only); lanes 3 and 11, pJC733 ($jspA_{E148A}$-
1231 *HA*); lane 4, pJC730 (*jspA-HA* and *lppA-HA*, with intervening RBS); lane 5, pJC735 ($jspA_{E148A}$-
1232 *HA* and *lppA-HA*, with intervening RBS); lane 6, pJC731 (*jspA-HA* translationally coupled to
1233 *lppA-HA*); lane 7, pJC736 ($jspA_{E148A}$-*HA* translationally coupled to *lppA-HA*); lanes 8 and12,
1234 pJC734 (*lppA-HA* followed by *jspA-HA*); and lanes 9 and 13, pJC737 (*lppA-HA* followed by
1235 $jspA_{E148A}$-*HA*). Schematics above the blots represent gene arrangements on plasmids: red *
1236 indicates plasmids that carry the $jspA_{E148A}$-*HA* mutant allele and the approximate location of the
1237 active site mutation in the gene; RBS preceding *lppA-HA* in pJC730 and pJC735 is the
1238 ribosome binding site of *E. coli araB*. Lanes 1 - 7 have the same configuration of strains as
1239 those in Figure 9B. The size of the + symbol in the LppA-HA row above the blots reflects the
1240 level of expression, with the orange, bold + indicating the highest levels. (LppA-HA is not
1241 detectable in some lanes because the signal is overwhelmed by that in lanes with high
1242 expression.) Approximate molecular mass, in kDa, are shown to the left of the blots, while lane
1243 numbers are shown below. Positions of bands representing JspA-HA, LppA-HA, and ExoR-
1244 FLAG are indicated to the right of the blots. Blots were first probed with anti-FLAG antibodies
1245 and then with anti-HA antibodies. The ExoR-FLAG image was captured first, and the JspA-HA
1246 image was obtained from the same representative blot after the second probing, while the
1247 LppA-HA image was acquired from a duplicate blot of the same samples.
1248
1249 **S1 Table. Orthologs of JspA, LppA, and ExoR in representative bacterial species.**
1250
1251 **S2 Table. Number of pink and white nodules on individual *M. sativa* or *M. truncatula***
1252 **seedlings inoculated with Rm1021 or WSM419 strains.**
1253
1254 **S3 Table. Compilations of symbiosis competitions between Rm1021 strains in *M. sativa***
1255 **or between WSM419 strains in *M. truncatula*.**
1256
1257 **S4 Table. JspA-regulated genes.**
1258

1259 **S5 Table. Hypergeometric probability tests for overlaps between JspA, ExoRS, and**
1260 **RpoH1 transcriptomes and ChvI regulon.**
1261
1262 **S6 Table. Hypergeometric probability tests for overlap of JspA transcriptome with genes**
1263 **that altered expression in NCR247-treated cells or the Δ*podJ1* mutant.**
1264
1265 **S7 Table. Overlap of JspA transcriptome with genes that changed expression upon acid**
1266 **stress.**
1267
1268 **S8 Table. *Sinorhizobium* strains used in this study.**
1269
1270 **S9 Table. Plasmids used in this study.**
1271
1272 **S1 File. Plasmid sequences.**
1273
1274

References

Alakavuklar, M.A., Fiebig, A., and Crosson, S. (2023) The *Brucella* Cell Envelope. *Annu Rev Microbiol*.

Alakavuklar, M.A., Heckel, B.C., Stoner, A.M., Stembel, J.A., and Fuqua, C. (2021) Motility control through an anti-activation mechanism in *Agrobacterium tumefaciens*. *Mol Microbiol* **116**: 1281-1297.

Alba, B.M., Leeds, J.A., Onufryk, C., Lu, C.Z., and Gross, C.A. (2002) DegS and YaeL participate sequentially in the cleavage of RseA to activate the sigma(E)-dependent extracytoplasmic stress response. *Genes Dev* **16**: 2156-2168.

Albicoro, F.J., Draghi, W.O., Martini, M.C., Salas, M.E., Torres Tejerizo, G.A., Lozano, M.J., Lopez, J.L., Vacca, C., Cafiero, J.H., Pistorio, M., Bednarz, H., Meier, D., Lagares, A., Niehaus, K., Becker, A., and Del Papa, M.F. (2021) The two-component system ActJK is involved in acid stress tolerance and symbiosis in *Sinorhizobium meliloti*. *J Biotechnol* **329**: 80-91.

Albicoro, F.J., Vacca, C., Cafiero, J.H., Draghi, W.O., Martini, M.C., Goulian, M., Lagares, A., and Del Papa, M.F. (2023) Comparative Proteomic Analysis Revealing ActJ-Regulated Proteins in *Sinorhizobium meliloti*. *J Proteome Res*.

Altamirano-Silva, P., Cordero-Serrano, M., Méndez-Montoya, J., Chacón-Díaz, C., Guzmán-Verri, C., Moreno, E., and Chaves-Olarte, E. (2021) Intracellular Passage Triggers a Molecular Response in *Brucella abortus* That Increases Its Infectiousness. *Infection and Immunity* **89**: e00004-00021.

Altamirano-Silva, P., Meza-Torres, J., Castillo-Zeledon, A., Ruiz-Villalobos, N., Zuniga-Pereira, A.M., Chacon-Diaz, C., Moreno, E., Guzman-Verri, C., and Chaves-Olarte, E. (2018) *Brucella abortus* senses the intracellular environment through the BvrR/BvrS two-component system, which allows *B. abortus* to adapt to its replicative niche. *Infect Immun* **86**.

An, F., Li, N., Zhang, L., Zheng, W., Xing, S., Tang, G., Yan, J., Yu, L., and Luo, L. (2021) Identification of *Sinorhizobium meliloti* LsrB regulon. *Acta biochimica et biophysica Sinica* **53**: 955-957.

Arnold, M.F.F., Penterman, J., Shabab, M., Chen, E.J., and Walker, G.C. (2018) Important Late-Stage Symbiotic Role of the *Sinorhizobium meliloti* Exopolysaccharide Succinoglycan. *J Bacteriol* **200**.

Arnold, M.F.F., Shabab, M., Penterman, J., Boehme, K.L., Griffitts, J.S., and Walker, G.C. (2017) Genome-Wide Sensitivity Analysis of the Microsymbiont *Sinorhizobium meliloti* to Symbiotically Important, Defensin-Like Host Peptides. *mBio* **8**.

Ausubel, F.M., Brent, R., Kingston, R.E., Moore, D.D., Seidman, J.G., Smith, J.A., and Struhl, K., (1998) *Current Protocols in Molecular Biology*. John Wiley & Sons, New York, NY.

Bahlawane, C., McIntosh, M., Krol, E., and Becker, A. (2008) *Sinorhizobium meliloti* regulator MucR couples exopolysaccharide synthesis and motility. *Mol Plant Microbe Interact* **21**: 1498-1509.

Baraquet, C., Dai, W., Mendiola, J., Pechter, K., and Harwood, C.S. (2021) Transposon sequencing analysis of *Bradyrhizobium diazoefficiens* 110*spc*4. *Scientific reports* **11**: 13211.

Barnett, M.J., Bittner, A.N., Toman, C.J., Oke, V., and Long, S.R. (2012) Dual RpoH sigma factors and transcriptional plasticity in a symbiotic bacterium. *J Bacteriol* **194**: 4983-4994.

Barnett, M.J., and Fisher, R.F. (2006) Global gene expression in the rhizobial-legume symbiosis. *Symbiosis* **42**: 1-24.

Barnett, M.J., and Long, S.R. (2015) The *Sinorhizobium meliloti* SyrM regulon: effects on global gene expression are mediated by *syrA* and *nodD3*. *J Bacteriol* **197**: 1792-1806.

Barnett, M.J., and Long, S.R. (2018) Novel Genes and Regulators That Influence Production of Cell Surface Exopolysaccharides in *Sinorhizobium meliloti*. *J Bacteriol* **200**.

Barnett, M.J., Oke, V., and Long, S.R. (2000) New genetic tools for use in the *Rhizobiaceae* and other bacteria. *Biotechniques* **29**: 240-242, 244-245.

1321 Barnett, M.J., Solow-Cordero, D.E., and Long, S.R. (2019) A high-throughput system to identify inhibitors
1322 of *Candidatus* Liberibacter asiaticus transcription regulators. *Proc Natl Acad Sci U S A* **116**:
1323 18009-18014.
1324 Barnett, M.J., Toman, C.J., Fisher, R.F., and Long, S.R. (2004) A dual-genome Symbiosis Chip for
1325 coordinate study of signal exchange and development in a prokaryote-host interaction. *Proc*
1326 *Natl Acad Sci USA* **101**: 16636-16641.
1327 Barrett, T., Wilhite, S.E., Ledoux, P., Evangelista, C., Kim, I.F., Tomashevsky, M., Marshall, K.A., Phillippy,
1328 K.H., Sherman, P.M., Holko, M., Yefanov, A., Lee, H., Zhang, N., Robertson, C.L., Serova, N.,
1329 Davis, S., and Soboleva, A. (2013) NCBI GEO: archive for functional genomics data sets--update.
1330 *Nucleic Acids Res* **41**: D991-995.
1331 Becker, A., Barnett, M.J., Capela, D., Dondrup, M., Kamp, P.B., Krol, E., Linke, B., Ruberg, S., Runte, K.,
1332 Schroeder, B.K., Weidner, S., Yurgel, S.N., Batut, J., Long, S.R., Pühler, A., and Goesmann, A.
1333 (2009) A portal for rhizobial genomes: RhizoGATE integrates a *Sinorhizobium meliloti* genome
1334 annotation update with postgenome data. *J Biotechnol* **140**: 45-50.
1335 Becker, A., Ruberg, S., Baumgarth, B., Bertram-Drogatz, P.A., Quester, I., and Puhler, A. (2002)
1336 Regulation of succinoglycan and galactoglucan biosynthesis in *Sinorhizobium meliloti*. *J Mol*
1337 *Microbiol Biotechnol* **4**: 187-190.
1338 Bélanger, L., Dimmick, K.A., Fleming, J.S., and Charles, T.C. (2009) Null mutations in *Sinorhizobium*
1339 *meliloti exoS* and *chvI* demonstrate the importance of this two-component regulatory system for
1340 symbiosis. *Mol Microbiol* **74**: 1223-1237.
1341 Benedict, A.B., Ghosh, P., Scott, S.M., and Griffitts, J.S. (2021) A conserved rhizobial peptidase that
1342 interacts with host-derived symbiotic peptides. *Scientific reports* **11**: 11779.
1343 Bensig, E.O., Valadez-Cano, C., Kuang, Z., Freire, I.R., Reyes-Prieto, A., and MacLellan, S.R. (2022) The
1344 two-component regulatory system CenK-CenR regulates expression of a previously
1345 uncharacterized protein required for salinity and oxidative stress tolerance in *Sinorhizobium*
1346 *meliloti*. *Front Microbiol* **13**: 1020932.
1347 Blum, M., Chang, H.Y., Chuguransky, S., Grego, T., Kandasaamy, S., Mitchell, A., Nuka, G., Paysan-
1348 Lafosse, T., Qureshi, M., Raj, S., Richardson, L., Salazar, G.A., Williams, L., Bork, P., Bridge, A.,
1349 Gough, J., Haft, D.H., Letunic, I., Marchler-Bauer, A., Mi, H., Natale, D.A., Necci, M., Orengo, C.A.,
1350 Pandurangan, A.P., Rivoire, C., Sigrist, C.J.A., Sillitoe, I., Thanki, N., Thomas, P.D., Tosatto, S.C.E.,
1351 Wu, C.H., Bateman, A., and Finn, R.D. (2021) The InterPro protein families and domains
1352 database: 20 years on. *Nucleic Acids Res* **49**: D344-D354.
1353 Boratyn, G.M., Camacho, C., Cooper, P.S., Coulouris, G., Fong, A., Ma, N., Madden, T.L., Matten, W.T.,
1354 McGinnis, S.D., Merezhuk, Y., Raytselis, Y., Sayers, E.W., Tao, T., Ye, J., and Zaretskaya, I. (2013)
1355 BLAST: a more efficient report with usability improvements. *Nucleic Acids Res* **41**: W29-33.
1356 Brockhurst, M.A. (2011) Sex, death, and the Red Queen. *Science* **333**: 166-167.
1357 Budnick, J.A., Sheehan, L.M., Ginder, M.J., Failor, K.C., Perkowski, J.M., Pinto, J.F., Kohl, K.A., Kang, L.,
1358 Michalak, P., Luo, L., Heindl, J.E., and Caswell, C.C. (2020) A central role for the transcriptional
1359 regulator VtlR in small RNA-mediated gene regulation in *Agrobacterium tumefaciens*. *Scientific*
1360 *reports* **10**: 14968.
1361 Burks, D., Azad, R., Wen, J., and Dickstein, R. (2018) The *Medicago truncatula* Genome: Genomic Data
1362 Availability. *Methods Mol Biol* **1822**: 39-59.
1363 Calatrava-Morales, N., Nogales, J., Ameztoy, K., van Steenbergen, B., and Soto, M.J. (2017) The
1364 NtrY/NtrX System of *Sinorhizobium meliloti* GR4 Regulates Motility, EPS I Production, and
1365 Nitrogen Metabolism but Is Dispensable for Symbiotic Nitrogen Fixation. *Mol Plant Microbe*
1366 *Interact* **30**: 566-577.
1367 Cao, P., and Wall, D. (2020) The Fluidity of the Bacterial Outer Membrane Is Species Specific: Bacterial
1368 Lifestyles and the Emergence of a Fluid Outer Membrane. *Bioessays* **42**: e1900246.

1369 Cao, Y., Halane, M.K., Gassmann, W., and Stacey, G. (2017) The Role of Plant Innate Immunity in the
1370 Legume-Rhizobium Symbiosis. *Annu Rev Plant Biol* **68**: 535-561.
1371 Carroll, L., (1900 [1872]) *Through the Looking-Glass, and What Alice Found There*. W. B. Conkey Co.,
1372 Chicago.
1373 Castillo-Zeledón, A., Ruiz-Villalobos, N., Altamirano-Silva, P., Chacón-Díaz, C., Barquero-Calvo, E., Chaves-
1374 Olarte, E., and Guzmán-Verri, C. (2021) A *Sinorhizobium meliloti* and *Agrobacterium tumefaciens*
1375 ExoR ortholog is not crucial for *Brucella abortus* virulence. *PLoS One* **16**: e0254568.
1376 Charles, T.C., and Nester, E.W. (1993) A chromosomally encoded two-component sensory transduction
1377 system is required for virulence of *Agrobacterium tumefaciens*. *J Bacteriol* **175**: 6614-6625.
1378 Chen, E.J., Fisher, R.F., Perovich, V.M., Sabio, E.A., and Long, S.R. (2009) Identification of direct
1379 transcriptional target genes of ExoS/ChvI two-component signaling in *Sinorhizobium meliloti*. *J*
1380 *Bacteriol* **191**: 6833-6842.
1381 Chen, E.J., Sabio, E.A., and Long, S.R. (2008) The periplasmic regulator ExoR inhibits ExoS/ChvI two-
1382 component signalling in *Sinorhizobium meliloti*. *Mol Microbiol* **69**: 1290-1303.
1383 Cheng, H.P., and Walker, G.C. (1998a) Succinoglycan is required for initiation and elongation of infection
1384 threads during nodulation of alfalfa by Rhizobium meliloti. *J Bacteriol* **180**: 5183-5191.
1385 Cheng, H.P., and Walker, G.C. (1998b) Succinoglycan production by *Rhizobium meliloti* is regulated
1386 through the ExoS-ChvI two-component regulatory system. *J Bacteriol* **180**: 20-26.
1387 Crook, M.B., Lindsay, D.P., Biggs, M.B., Bentley, J.S., Price, J.C., Clement, S.C., Clement, M.J., Long, S.R.,
1388 and Griffitts, J.S. (2012) Rhizobial plasmids that cause impaired symbiotic nitrogen fixation and
1389 enhanced host invasion. *Mol Plant Microbe Interact* **25**: 1026-1033.
1390 Davies, B.W., and Walker, G.C. (2007) Identification of novel *Sinorhizobium meliloti* mutants
1391 compromised for oxidative stress protection and symbiosis. *J Bacteriol* **189**: 2110-2113.
1392 De Las Peñas, A., Connolly, L., and Gross, C.A. (1997) SigmaE is an essential sigma factor in *Escherichia*
1393 *coli*. *J Bacteriol* **179**: 6862-6864.
1394 de Lucena, D.K., Pühler, A., and Weidner, S. (2010) The role of sigma factor RpoH1 in the pH stress
1395 response of *Sinorhizobium meliloti*. *BMC Microbiol* **10**: 265.
1396 diCenzo, G.C., Benedict, A.B., Fondi, M., Walker, G.C., Finan, T.M., Mengoni, A., and Griffitts, J.S. (2018)
1397 Robustness encoded across essential and accessory replicons of the ecologically versatile
1398 bacterium *Sinorhizobium meliloti*. *PLoS Genet* **14**: e1007357.
1399 Doherty, D., Leigh, J.A., Glazebrook, J., and Walker, G.C. (1988) Rhizobium meliloti mutants that
1400 overproduce the *R. meliloti* acidic calcofluor-binding exopolysaccharide. *J Bacteriol* **170**: 4249-
1401 4256.
1402 Draghi, W.O., Del Papa, M.F., Hellweg, C., Watt, S.A., Watt, T.F., Barsch, A., Lozano, M.J., Lagares, A., Jr.,
1403 Salas, M.E., López, J.L., Albicoro, F.J., Nilsson, J.F., Torres Tejerizo, G.A., Luna, M.F., Pistorio, M.,
1404 Boiardi, J.L., Pühler, A., Weidner, S., Niehaus, K., and Lagares, A. (2016) A consolidated analysis
1405 of the physiologic and molecular responses induced under acid stress in the legume-symbiont
1406 model-soil bacterium *Sinorhizobium meliloti*. *Scientific reports* **6**: 29278.
1407 Eisfeld, J., Kraus, A., Ronge, C., Jagst, M., Brandenburg, V.B., and Narberhaus, F. (2021) A LysR-type
1408 transcriptional regulator controls the expression of numerous small RNAs in *Agrobacterium*
1409 *tumefaciens*. *Mol Microbiol* **116**: 126-139.
1410 Evinger, M., and Agabian, N. (1977) Envelope-associated nucleoid from *Caulobacter crescentus* stalked
1411 and swarmer cells. *J Bacteriol* **132**: 294-301.
1412 Fang, F.C., Frawley, E.R., Tapscott, T., and Vázquez-Torres, A. (2016) Bacterial Stress Responses during
1413 Host Infection. *Cell Host Microbe* **20**: 133-143.
1414 Farkas, A., Maroti, G., Durgo, H., Gyorgypal, Z., Lima, R.M., Medzihradszky, K.F., Kereszt, A., Mergaert, P.,
1415 and Kondorosi, E. (2014) *Medicago truncatula* symbiotic peptide NCR247 contributes to

1416 bacteroid differentiation through multiple mechanisms. *Proc Natl Acad Sci U S A* **111**: 5183-
1417 5188.
1418 Ferguson, B.J., Indrasumunar, A., Hayashi, S., Lin, M.H., Lin, Y.H., Reid, D.E., and Gresshoff, P.M. (2010)
1419 Molecular analysis of legume nodule development and autoregulation. *J Integr Plant Biol* **52**: 61-
1420 76.
1421 Fields, A.T., Navarrete, C.S., Zare, A.Z., Huang, Z., Mostafavi, M., Lewis, J.C., Rezaeihaghighi, Y., Brezler,
1422 B.J., Ray, S., Rizzacasa, A.L., Barnett, M.J., Long, S.R., Chen, E.J., and Chen, J.C. (2012) The
1423 conserved polarity factor *podJ1* impacts multiple cell envelope-associated functions in
1424 *Sinorhizobium meliloti*. *Mol Microbiol* **84**: 892-920.
1425 Finan, T.M., Hirsch, A.M., Leigh, J.A., Johansen, E., Kuldau, G.A., Deegan, S., Walker, G.C., and Signer, E.R.
1426 (1985) Symbiotic mutants of *Rhizobium meliloti* that uncouple plant from bacterial
1427 differentiation. *Cell* **40**: 869-877.
1428 Finan, T.M., Kunkel, B., De Vos, G.F., and Signer, E.R. (1986) Second symbiotic megaplasmid in *Rhizobium*
1429 *meliloti* carrying exopolysaccharide and thiamine synthesis genes. *J Bacteriol* **167**: 66-72.
1430 Flores-Tinoco, C.E., Tschan, F., Fuhrer, T., Margot, C., Sauer, U., Christen, M., and Christen, B. (2020) Co-
1431 catabolism of arginine and succinate drives symbiotic nitrogen fixation. *Molecular systems*
1432 *biology* **16**: e9419.
1433 Frohlich, K.S., Forstner, K.U., and Gitai, Z. (2018) Post-transcriptional gene regulation by an Hfq-
1434 independent small RNA in *Caulobacter crescentus*. *Nucleic Acids Res* **46**: 10969-10982.
1435 Fujimura-Kamada, K., Nouvet, F.J., and Michaelis, S. (1997) A novel membrane-associated
1436 metalloprotease, Ste24p, is required for the first step of NH2-terminal processing of the yeast a-
1437 factor precursor. *J Cell Biol* **136**: 271-285.
1438 Gage, D.J. (2002) Analysis of infection thread development using Gfp- and DsRed-expressing
1439 *Sinorhizobium meliloti*. *J Bacteriol* **184**: 7042-7046.
1440 Galibert, F., Finan, T.M., Long, S.R., Pühler, A., Abola, P., Ampe, F., Barloy-Hubler, F., Barnett, M.J.,
1441 Becker, A., Boistard, P., Bothe, G., Boutry, M., Bowser, L., Buhrmester, J., Cadieu, E., Capela, D.,
1442 Chain, P., Cowie, A., Davis, R.W., Dreano, S., Federspiel, N.A., Fisher, R.F., Gloux, S., Godrie, T.,
1443 Goffeau, A., Golding, B., Gouzy, J., Gurjal, M., Hernandez-Lucas, I., Hong, A., Huizar, L., Hyman,
1444 R.W., Jones, T., Kahn, D., Kahn, M.L., Kalman, S., Keating, D.H., Kiss, E., Komp, C., Lelaure, V.,
1445 Masuy, D., Palm, C., Peck, M.C., Pohl, T.M., Portetelle, D., Purnelle, B., Ramsperger, U., Surzycki,
1446 R., Thebault, P., Vandenbol, M., Vorholter, F.J., Weidner, S., Wells, D.H., Wong, K., Yeh, K.C., and
1447 Batut, J. (2001) The composite genome of the legume symbiont *Sinorhizobium meliloti*. *Science*
1448 **293**: 668-672.
1449 Geddes, B.A., Gonzalez, J.E., and Oresnik, I.J. (2014) Exopolysaccharide production in response to
1450 medium acidification is correlated with an increase in competition for nodule occupancy. *Mol*
1451 *Plant Microbe Interact* **27**: 1307-1317.
1452 Geiger, O., Sohlenkamp, C., Vera-Cruz, D., Medeot, D.B., Martínez-Aguilar, L., Sahonero-Canavesi, D.X.,
1453 Weidner, S., Pühler, A., and López-Lara, I.M. (2021) ExoS/ChvI Two-Component Signal-
1454 Transduction System Activated in the Absence of Bacterial Phosphatidylcholine. *Frontiers in*
1455 *Plant Science* **12**: 678976.
1456 Ghosh, P., Adolphsen, K.N., Yurgel, S.N., and Kahn, M.L. (2021) *Sinorhizobium medicae* WSM419 Genes
1457 That Improve Symbiosis between *Sinorhizobium meliloti* Rm1021 and *Medicago truncatula*
1458 Jemalong A17 and in Other Symbiosis Systems. *Appl Environ Microbiol* **87**: e0300420.
1459 Gibson, K.E., Barnett, M.J., Toman, C.J., Long, S.R., and Walker, G.C. (2007) The symbiosis regulator CbrA
1460 modulates a complex regulatory network affecting the flagellar apparatus and cell envelope
1461 proteins. *J Bacteriol* **189**: 3591-3602.
1462 Gibson, K.E., Kobayashi, H., and Walker, G.C. (2008) Molecular determinants of a symbiotic chronic
1463 infection. *Annu Rev Genet* **42**: 413-441.

1464 Godessart, P., Lannoy, A., Dieu, M., Van der Verren, S.E., Soumillion, P., Collet, J.F., Remaut, H., Renard,
1465 P., and De Bolle, X. (2021) beta-Barrels covalently link peptidoglycan and the outer membrane in
1466 the alpha-proteobacterium *Brucella abortus*. *Nat Microbiol* **6**: 27-33.
1467 Graham, P.H., and Vance, C.P. (2003) Legumes: Importance and Constraints to Greater Use. *Plant*
1468 *Physiology* **131**: 872-877.
1469 Greenwich, J.L., Heckel, B.C., Alakavuklar, M.A., and Fuqua, C. (2023) The ChvG-ChvI Regulatory
1470 Network: A Conserved Global Regulatory Circuit Among the Alphaproteobacteria with Pervasive
1471 Impacts on Host Interactions and Diverse Cellular Processes. *Annu Rev Microbiol*.
1472 Griffitts, J.S., Carlyon, R.E., Erickson, J.H., Moulton, J.L., Barnett, M.J., Toman, C.J., and Long, S.R. (2008)
1473 A Sinorhizobium meliloti osmosensory two-component system required for cyclic glucan export
1474 and symbiosis. *Mol Microbiol* **69**: 479-490.
1475 Griffitts, J.S., and Long, S.R. (2008) A symbiotic mutant of *Sinorhizobium meliloti* reveals a novel genetic
1476 pathway involving succinoglycan biosynthetic functions. *Mol Microbiol* **67**: 1292-1306.
1477 Guzman-Verri, C., Manterola, L., Sola-Landa, A., Parra, A., Cloeckaert, A., Garin, J., Gorvel, J.P., Moriyon,
1478 I., Moreno, E., and Lopez-Goni, I. (2002) The two-component system BvrR/BvrS essential for
1479 *Brucella abortus* virulence regulates the expression of outer membrane proteins with
1480 counterparts in members of the Rhizobiaceae. *Proc Natl Acad Sci U S A* **99**: 12375-12380.
1481 Guzman, L.M., Belin, D., Carson, M.J., and Beckwith, J. (1995) Tight regulation, modulation, and high-
1482 level expression by vectors containing the arabinose PBAD promoter. *J Bacteriol* **177**: 4121-
1483 4130.
1484 Haag, A.F., Baloban, M., Sani, M., Kerscher, B., Pierre, O., Farkas, A., Longhi, R., Boncompagni, E.,
1485 Herouart, D., Dall'angelo, S., Kondorosi, E., Zanda, M., Mergaert, P., and Ferguson, G.P. (2011)
1486 Protection of *Sinorhizobium* against host cysteine-rich antimicrobial peptides is critical for
1487 symbiosis. *PLoS Biol* **9**: e1001169.
1488 Hawkins, J.P., Geddes, B.A., and Oresnik, I.J. (2017) Succinoglycan Production Contributes to Acidic pH
1489 Tolerance in *Sinorhizobium meliloti* Rm1021. *Mol Plant Microbe Interact* **30**: 1009-1019.
1490 Hawkins, J.P., and Oresnik, I.J. (2021) The Rhizobium-Legume Symbiosis: Co-opting Successful Stress
1491 Management. *Front Plant Sci* **12**: 796045.
1492 Heavner, M.E., Qiu, W.G., and Cheng, H.P. (2015) Phylogenetic Co-Occurrence of ExoR, ExoS, and ChvI,
1493 Components of the RSI Bacterial Invasion Switch, Suggests a Key Adaptive Mechanism
1494 Regulating the Transition between Free-Living and Host-Invading Phases in Rhizobiales. *PLoS*
1495 *One* **10**: e0135655.
1496 Heckel, B.C., Tomlinson, A.D., Morton, E.R., Choi, J.H., and Fuqua, C. (2014) *Agrobacterium tumefaciens*
1497 ExoR controls acid response genes and impacts exopolysaccharide synthesis, horizontal gene
1498 transfer, and virulence gene expression. *J Bacteriol* **196**: 3221-3233.
1499 Hellweg, C., Pühler, A., and Weidner, S. (2009) The time course of the transcriptomic response of
1500 *Sinorhizobium meliloti* 1021 following a shift to acidic pH. *BMC Microbiol* **9**: 37.
1501 Herridge, D.F., Peoples, M.B., and Boddey, R.M. (2008) Global inputs of biological nitrogen fixation in
1502 agricultural systems. *PLANT AND SOIL* **311**: 1-18.
1503 Hews, C.L., Cho, T., Rowley, G., and Raivio, T.L. (2019) Maintaining Integrity Under Stress: Envelope
1504 Stress Response Regulation of Pathogenesis in Gram-Negative Bacteria. *Front Cell Infect*
1505 *Microbiol* **9**: 313.
1506 Hoang, H.H., Gurich, N., and Gonzalez, J.E. (2008) Regulation of motility by the ExpR/Sin quorum-sensing
1507 system in *Sinorhizobium meliloti*. *J Bacteriol* **190**: 861-871.
1508 Horváth, B., Domonkos, A., Kereszt, A., Szucs, A., Abraham, E., Ayaydin, F., Boka, K., Chen, Y., Chen, R.,
1509 Murray, J.D., Udvardi, M.K., Kondorosi, E., and Kalo, P. (2015) Loss of the nodule-specific
1510 cysteine rich peptide, NCR169, abolishes symbiotic nitrogen fixation in the *Medicago truncatula*
1511 *dnf7* mutant. *Proc Natl Acad Sci U S A* **112**: 15232-15237.

1512 House, B.L., Mortimer, M.W., and Kahn, M.L. (2004) New recombination methods for *Sinorhizobium*
1513 *meliloti* genetics. *Appl Environ Microbiol* **70**: 2806-2815.
1514 Humphreys, S., Stevenson, A., Bacon, A., Weinhardt, A.B., and Roberts, M. (1999) The alternative sigma
1515 factor, sigmaE, is critically important for the virulence of *Salmonella typhimurium*. *Infect Immun*
1516 **67**: 1560-1568.
1517 Isaac, D.D., Pinkner, J.S., Hultgren, S.J., and Silhavy, T.J. (2005) The extracytoplasmic adaptor protein
1518 CpxP is degraded with substrate by DegP. *Proc Natl Acad Sci U S A* **102**: 17775-17779.
1519 Jones, K.M. (2012) Increased production of the exopolysaccharide succinoglycan enhances
1520 *Sinorhizobium meliloti* 1021 symbiosis with the host plant *Medicago truncatula*. *J Bacteriol* **194**:
1521 4322-4331.
1522 Jones, K.M., Kobayashi, H., Davies, B.W., Taga, M.E., and Walker, G.C. (2007) How rhizobial symbionts
1523 invade plants: the *Sinorhizobium-Medicago* model. *Nat Rev Microbiol* **5**: 619-633.
1524 Jones, K.M., Sharopova, N., Lohar, D.P., Zhang, J.Q., VandenBosch, K.A., and Walker, G.C. (2008)
1525 Differential response of the plant *Medicago truncatula* to its symbiont *Sinorhizobium meliloti* or
1526 an exopolysaccharide-deficient mutant. *Proc Natl Acad Sci U S A* **105**: 704-709.
1527 Juncker, A.S., Willenbrock, H., Von Heijne, G., Brunak, S., Nielsen, H., and Krogh, A. (2003) Prediction of
1528 lipoprotein signal peptides in Gram-negative bacteria. *Protein Sci* **12**: 1652-1662.
1529 Kawaharada, Y., Kelly, S., Nielsen, M.W., Hjuler, C.T., Gysel, K., Muszynski, A., Carlson, R.W., Thygesen,
1530 M.B., Sandal, N., Asmussen, M.H., Vinther, M., Andersen, S.U., Krusell, L., Thirup, S., Jensen, K.J.,
1531 Ronson, C.W., Blaise, M., Radutoiu, S., and Stougaard, J. (2015) Receptor-mediated
1532 exopolysaccharide perception controls bacterial infection. *Nature* **523**: 308-312.
1533 Kawaharada, Y., Nielsen, M.W., Kelly, S., James, E.K., Andersen, K.R., Rasmussen, S.R., Fuchtbauer, W.,
1534 Madsen, L.H., Heckmann, A.B., Radutoiu, S., and Stougaard, J. (2017) Differential regulation of
1535 the Epr3 receptor coordinates membrane-restricted rhizobial colonization of root nodule
1536 primordia. *Nat Commun* **8**: 14534.
1537 Keating, D.H. (2007) The *Sinorhizobium meliloti* ExoR protein is required for the downregulation of *lpsS*
1538 transcription and succinoglycan biosynthesis in response to divalent cations. *FEMS Microbiol*
1539 *Lett* **267**: 23-29.
1540 Kelly, S.J., Muszynski, A., Kawaharada, Y., Hubber, A.M., Sullivan, J.T., Sandal, N., Carlson, R.W.,
1541 Stougaard, J., and Ronson, C.W. (2013) Conditional requirement for exopolysaccharide in the
1542 *Mesorhizobium-Lotus* symbiosis. *Mol Plant Microbe Interact* **26**: 319-329.
1543 Khan, S.R., Gaines, J., Roop, R.M., 2nd, and Farrand, S.K. (2008) Broad-host-range expression vectors
1544 with tightly regulated promoters and their use to examine the influence of TraR and TraM
1545 expression on Ti plasmid quorum sensing. *Appl Environ Microbiol* **74**: 5053-5062.
1546 Kim, M., Chen, Y., Xi, J., Waters, C., Chen, R., and Wang, D. (2015) An antimicrobial peptide essential for
1547 bacterial survival in the nitrogen-fixing symbiosis. *Proc Natl Acad Sci U S A* **112**: 15238-15243.
1548 Kovacs-Simon, A., Titball, R.W., and Michell, S.L. (2011) Lipoproteins of bacterial pathogens. *Infect*
1549 *Immun* **79**: 548-561.
1550 Krol, E., and Becker, A. (2004) Global transcriptional analysis of the phosphate starvation response in
1551 *Sinorhizobium meliloti* strains 1021 and 2011. *Mol Genet Genomics* **272**: 1-17.
1552 Krol, E., Klaner, C., Gnau, P., Kaever, V., Essen, L.O., and Becker, A. (2016) Cyclic mononucleotide- and
1553 Clr-dependent gene regulation in *Sinorhizobium meliloti*. *Microbiology* **162**: 1840-1856.
1554 Lai, K.K., Davis-Richardson, A.G., Dias, R., and Triplett, E.W. (2016) Identification of the Genes Required
1555 for the Culture of *Liberibacter crescens*, the Closest Cultured Relative of the *Liberibacter* Plant
1556 Pathogens. *Front Microbiol* **7**: 547.
1557 Lakey, B.D., Myers, K.S., Alberge, F., Mettert, E.L., Kiley, P.J., Noguera, D.R., and Donohue, T.J. (2022) The
1558 essential *Rhodobacter sphaeroides* CenKR two-component system regulates cell division and
1559 envelope biosynthesis. *PLoS Genet* **18**: e1010270.

1560 Lamontagne, J., Butler, H., Chaves-Olarte, E., Hunter, J., Schirm, M., Paquet, C., Tian, M., Kearney, P.,
1561 Hamaidi, L., Chelsky, D., Moriyon, I., Moreno, E., and Paramithiotis, E. (2007) Extensive cell
1562 envelope modulation is associated with virulence in *Brucella abortus*. *J Proteome Res* **6**: 1519-
1563 1529.
1564 Larrainzar, E., Gil-Quintana, E., Seminario, A., Arrese-Igor, C., and Gonzalez, E.M. (2014) Nodule
1565 carbohydrate catabolism is enhanced in the *Medicago truncatula* A17-*Sinorhizobium medicae*
1566 WSM419 symbiosis. *Front Microbiol* **5**: 447.
1567 Ledermann, R., Schulte, C.C.M., and Poole, P.S. (2021) How Rhizobia Adapt to the Nodule Environment. *J*
1568 *Bacteriol* **203**: e0053920.
1569 Lehman, A.P., and Long, S.R. (2013) Exopolysaccharides from *Sinorhizobium meliloti* can protect against
1570 H2O2-dependent damage. *J Bacteriol* **195**: 5362-5369.
1571 LeVier, K., Phillips, R.W., Grippe, V.K., Roop, R.M., 2nd, and Walker, G.C. (2000) Similar requirements of a
1572 plant symbiont and a mammalian pathogen for prolonged intracellular survival. *Science* **287**:
1573 2492-2493.
1574 Li, L., Jia, Y., Hou, Q., Charles, T.C., Nester, E.W., and Pan, S.Q. (2002) A global pH sensor: *Agrobacterium*
1575 sensor protein ChvG regulates acid-inducible genes on its two chromosomes and Ti plasmid.
1576 *Proc Natl Acad Sci U S A* **99**: 12369-12374.
1577 Li, S. (2018). *Role of a bacterial polar adhesion factor during legume-microbe symbiosis* [Master's thesis].
1578 San Francisco State University, San Francisco, CA. http://hdl.handle.net/10211.3/199775
1579 Long, S., Reed, J.W., Himawan, J., and Walker, G.C. (1988) Genetic analysis of a cluster of genes required
1580 for synthesis of the calcofluor-binding exopolysaccharide of *Rhizobium meliloti*. *J Bacteriol* **170**:
1581 4239-4248.
1582 Long, S.R. (2016) SnapShot: Signaling in Symbiosis. *Cell* **167**: 582-582 e581.
1583 Lu, H.Y., and Cheng, H.P. (2010) Autoregulation of *Sinorhizobium meliloti exoR* gene expression.
1584 *Microbiology (Reading, England)* **156**: 2092-2101.
1585 Lu, H.Y., Luo, L., Yang, M.H., and Cheng, H.P. (2012) *Sinorhizobium meliloti* ExoR is the target of
1586 periplasmic proteolysis. *J Bacteriol* **194**: 4029-4040.
1587 Lund, J., Tedesco, P., Duke, K., Wang, J., Kim, S.K., and Johnson, T.E. (2002) Transcriptional profile of
1588 aging in *C. elegans*. *Curr Biol* **12**: 1566-1573.
1589 Luo, L., Yao, S.Y., Becker, A., Rüberg, S., Yu, G.Q., Zhu, J.B., and Cheng, H.P. (2005) Two new
1590 *Sinorhizobium meliloti* LysR-type transcriptional regulators required for nodulation. *J Bacteriol*
1591 **187**: 4562-4572.
1592 Maillet, F., Fournier, J., Mendis, H.C., Tadege, M., Wen, J., Ratet, P., Mysore, K.S., Gough, C., and Jones,
1593 K.M. (2020) *Sinorhizobium meliloti* succinylated high-molecular-weight succinoglycan and the
1594 *Medicago truncatula* LysM receptor-like kinase MtLYK10 participate independently in symbiotic
1595 infection. *Plant J* **102**: 311-326.
1596 Manterola, L., Guzman-Verri, C., Chaves-Olarte, E., Barquero-Calvo, E., de Miguel, M.J., Moriyon, I.,
1597 Grillo, M.J., Lopez-Goni, I., and Moreno, E. (2007) BvrR/BvrS-controlled outer membrane
1598 proteins Omp3a and Omp3b are not essential for *Brucella abortus* virulence. *Infect Immun* **75**:
1599 4867-4874.
1600 Manterola, L., Moriyon, I., Moreno, E., Sola-Landa, A., Weiss, D.S., Koch, M.H., Howe, J., Brandenburg,
1601 K., and Lopez-Goni, I. (2005) The lipopolysaccharide of *Brucella abortus* BvrS/BvrR mutants
1602 contains lipid A modifications and has higher affinity for bactericidal cationic peptides. *J*
1603 *Bacteriol* **187**: 5631-5639.
1604 Mantis, N.J., and Winans, S.C. (1993) The chromosomal response regulatory gene *chvI* of *Agrobacterium*
1605 *tumefaciens* complements an *Escherichia coli phoB* mutation and is required for virulence. *J*
1606 *Bacteriol* **175**: 6626-6636.

1607 Maroti, G., Downie, J.A., and Kondorosi, E. (2015) Plant cysteine-rich peptides that inhibit pathogen
1608 growth and control rhizobial differentiation in legume nodules. *Curr Opin Plant Biol* **26**: 57-63.
1609 Martin, M.O., and Long, S.R. (1984) Generalized transduction in *Rhizobium meliloti*. *J Bacteriol* **159**: 125-
1610 129.
1611 Martinez-Nunez, C., Altamirano-Silva, P., Alvarado-Guillen, F., Moreno, E., Guzman-Verri, C., and Chaves-
1612 Olarte, E. (2010) The two-component system BvrR/BvrS regulates the expression of the type IV
1613 secretion system VirB in *Brucella abortus*. *J Bacteriol* **192**: 5603-5608.
1614 Masson-Boivin, C., and Sachs, J.L. (2018) Symbiotic nitrogen fixation by rhizobia-the roots of a success
1615 story. *Curr Opin Plant Biol* **44**: 7-15.
1616 Meade, H.M., Long, S.R., Ruvkun, G.B., Brown, S.E., and Ausubel, F.M. (1982) Physical and genetic
1617 characterization of symbiotic and auxotrophic mutants of *Rhizobium meliloti* induced by
1618 transposon Tn5 mutagenesis. *J Bacteriol* **149**: 114-122.
1619 Mendis, H.C., Madzima, T.F., Queiroux, C., and Jones, K.M. (2016) Function of Succinoglycan
1620 Polysaccharide in *Sinorhizobium meliloti* Host Plant Invasion Depends on Succinylation, Not
1621 Molecular Weight. *mBio* **7**.
1622 Mergaert, P., Nikovics, K., Kelemen, Z., Maunoury, N., Vaubert, D., Kondorosi, A., and Kondorosi, E.
1623 (2003) A novel family in *Medicago truncatula* consisting of more than 300 nodule-specific genes
1624 coding for small, secreted polypeptides with conserved cysteine motifs. *Plant Physiol* **132**: 161-
1625 173.
1626 Miller-Williams, M., Loewen, P.C., and Oresnik, I.J. (2006) Isolation of salt-sensitive mutants of
1627 *Sinorhizobium meliloti* strain Rm1021. *Microbiology (Reading, England)* **152**: 2049-2059.
1628 Mistry, J., Chuguransky, S., Williams, L., Qureshi, M., Salazar, G.A., Sonnhammer, E.L.L., Tosatto, S.C.E.,
1629 Paladin, L., Raj, S., Richardson, L.J., Finn, R.D., and Bateman, A. (2021) Pfam: The protein families
1630 database in 2021. *Nucleic Acids Res* **49**: D412-d419.
1631 Mitchell, A.M., and Silhavy, T.J. (2019) Envelope stress responses: balancing damage repair and toxicity.
1632 *Nat Rev Microbiol* **17**: 417-428.
1633 Morris, J., and Gonzalez, J.E. (2009) The novel genes *emmABC* are associated with exopolysaccharide
1634 production, motility, stress adaptation, and symbiosis in *Sinorhizobium meliloti*. *J Bacteriol* **191**:
1635 5890-5900.
1636 Mostafavi, M., Lewis, J.C., Saini, T., Bustamante, J.A., Gao, I.T., Tran, T.T., King, S.N., Huang, Z., and Chen,
1637 J.C. (2014) Analysis of a taurine-dependent promoter in *Sinorhizobium meliloti* that offers tight
1638 modulation of gene expression. *BMC Microbiol* **14**: 295.
1639 Motulsky, H.J., "Interpreting results: Mann-Whitney test", GraphPad Statistics Guide. Accessed April 20,
1640 2023. https://www.graphpad.com/guides/prism/latest/statistics/how_the_mann-
1641 whitney_test_works.htm
1642 Nicoloff, H., Gopalkrishnan, S., and Ades, S.E. (2017) Appropriate Regulation of the σ(E)-Dependent
1643 Envelope Stress Response Is Necessary To Maintain Cell Envelope Integrity and Stationary-Phase
1644 Survival in *Escherichia coli*. *J Bacteriol* **199**.
1645 Oke, V., and Long, S.R. (1999) Bacterial genes induced within the nodule during the Rhizobium-legume
1646 symbiosis. *Mol Microbiol* **32**: 837-849.
1647 Olivares, J., Bedmar, E.J., and Sanjuán, J. (2013) Biological nitrogen fixation in the context of global
1648 change. *Mol Plant Microbe Interact* **26**: 486-494.
1649 Ozga, D.A., Lara, J.C., and Leig, J.A. (1994) The regulation of exopolysaccharide production is important
1650 at two levels of nodule development in *Rhizobium meliloti*. *Mol Plant Microbe Interact* **7**: 758-
1651 765.
1652 Pagliai, F.A., Gardner, C.L., Bojilova, L., Sarnegrim, A., Tamayo, C., Potts, A.H., Teplitski, M., Folimonova,
1653 S.Y., Gonzalez, C.F., and Lorca, G.L. (2014) The transcriptional activator LdtR from 'Candidatus
1654 *Liberibacter asiaticus*' mediates osmotic stress tolerance. *PLoS Pathog* **10**: e1004101.

1655 Pellock, B.J., Cheng, H.P., and Walker, G.C. (2000) Alfalfa root nodule invasion efficiency is dependent on
1656 *Sinorhizobium meliloti* polysaccharides. *J Bacteriol* **182**: 4310-4318.
1657 Penterman, J., Abo, R.P., De Nisco, N.J., Arnold, M.F., Longhi, R., Zanda, M., and Walker, G.C. (2014) Host
1658 plant peptides elicit a transcriptional response to control the *Sinorhizobium meliloti* cell cycle
1659 during symbiosis. *Proceedings of the National Academy of Sciences of the United States of*
1660 *America* **111**: 3561-3566.
1661 Perry, B.J., Akter, M.S., and Yost, C.K. (2016) The Use of Transposon Insertion Sequencing to Interrogate
1662 the Core Functional Genome of the Legume Symbiont *Rhizobium leguminosarum*. *Front*
1663 *Microbiol* **7**: 1873.
1664 Poole, P., Ramachandran, V., and Terpolilli, J. (2018) Rhizobia: from saprophytes to endosymbionts. *Nat*
1665 *Rev Microbiol* **16**: 291-303.
1666 Price, M.N., Wetmore, K.M., Waters, R.J., Callaghan, M., Ray, J., Liu, H., Kuehl, J.V., Melnyk, R.A.,
1667 Lamson, J.S., Suh, Y., Carlson, H.K., Esquivel, Z., Sadeeshkumar, H., Chakraborty, R., Zane, G.M.,
1668 Rubin, B.E., Wall, J.D., Visel, A., Bristow, J., Blow, M.J., Arkin, A.P., and Deutschbauer, A.M.
1669 (2018) Mutant phenotypes for thousands of bacterial genes of unknown function. *Nature* **557**:
1670 503-509.
1671 Price, P.A., Tanner, H.R., Dillon, B.A., Shabab, M., Walker, G.C., and Griffitts, J.S. (2015) Rhizobial
1672 peptidase HrrP cleaves host-encoded signaling peptides and mediates symbiotic compatibility.
1673 *Proc Natl Acad Sci U S A* **112**: 15244-15249.
1674 Quandt, J., and Hynes, M.F. (1993) Versatile suicide vectors which allow direct selection for gene
1675 replacement in gram-negative bacteria. *Gene* **127**: 15-21.
1676 Quebatte, M., Dehio, M., Tropel, D., Basler, A., Toller, I., Raddatz, G., Engel, P., Huser, S., Schein, H.,
1677 Lindroos, H.L., Andersson, S.G., and Dehio, C. (2010) The BatR/BatS two-component regulatory
1678 system controls the adaptive response of *Bartonella henselae* during human endothelial cell
1679 infection. *J Bacteriol* **192**: 3352-3367.
1680 Quintero-Yanes, A., Mayard, A., and Hallez, R. (2022) The two-component system ChvGI maintains cell
1681 envelope homeostasis in *Caulobacter crescentus*. *PLoS Genet* **18**: e1010465.
1682 Raivio, T.L. (2005) Envelope stress responses and Gram-negative bacterial pathogenesis. *Mol Microbiol*
1683 **56**: 1119-1128.
1684 Ratib, N.R., Sabio, E.Y., Mendoza, C., Barnett, M.J., Clover, S.B., Ortega, J.A., Dela Cruz, F.M., Balderas, D.,
1685 White, H., Long, S.R., and Chen, E.J. (2018) Genome-wide identification of genes directly
1686 regulated by ChvI and a consensus sequence for ChvI binding in *Sinorhizobium meliloti*. *Mol*
1687 *Microbiol* **110**: 596-615.
1688 Reeve, W., Chain, P., O'Hara, G., Ardley, J., Nandesena, K., Brau, L., Tiwari, R., Malfatti, S., Kiss, H.,
1689 Lapidus, A., Copeland, A., Nolan, M., Land, M., Hauser, L., Chang, Y.J., Ivanova, N., Mavromatis,
1690 K., Markowitz, V., Kyrpides, N., Gollagher, M., Yates, R., Dilworth, M., and Howieson, J. (2010)
1691 Complete genome sequence of the *Medicago* microsymbiont *Ensifer* (*Sinorhizobium*) *medicae*
1692 strain WSM419. *Stand Genomic Sci* **2**: 77-86.
1693 Reuber, T.L., and Walker, G.C. (1993) Biosynthesis of succinoglycan, a symbiotically important
1694 exopolysaccharide of Rhizobium meliloti. *Cell* **74**: 269-280.
1695 Rivas-Solano, O., Van der Henst, M., Castillo-Zeledon, A., Suarez-Esquivel, M., Munoz-Vargas, L., Capitan-
1696 Barrios, Z., Thomson, N.R., Chaves-Olarte, E., Moreno, E., De Bolle, X., and Guzman-Verri, C.
1697 (2022) The regulon of *Brucella abortus* two-component system BvrR/BvrS reveals the
1698 coordination of metabolic pathways required for intracellular life. *PLoS One* **17**: e0274397.
1699 Ryoji, M., Hsia, K., and Kaji, A. (1983) Read-through translation. *Trends in Biochemical Sciences* **8**: 88-90.
1700 Sambrook, J., Fritsch, E.F., and Maniatis, T., (1989) *Molecular cloning: a laboratory manual*. Cold Spring
1701 Harbor Laboratory Press, Cold Spring Harbor, N.Y.

1702 Sankari, S., Babu, V.M.P., Bian, K., Alhhazmi, A., Andorfer, M.C., Avalos, D.M., Smith, T.A., Yoon, K.,
1703 Drennan, C.L., Yaffe, M.B., Lourido, S., and Walker, G.C. (2022) A haem-sequestering plant
1704 peptide promotes iron uptake in symbiotic bacteria. *Nat Microbiol* **7**: 1453-1465.
1705 Santos, M.R., Cosme, A.M., Becker, J.D., Medeiros, J.M., Mata, M.F., and Moreira, L.M. (2010) Absence
1706 of functional TolC protein causes increased stress response gene expression in *Sinorhizobium*
1707 *meliloti*. *BMC Microbiol* **10**: 180.
1708 Santos, M.R., Marques, A.T., Becker, J.D., and Moreira, L.M. (2014) The *Sinorhizobium meliloti* EmrR
1709 regulator is required for efficient colonization of *Medicago sativa* root nodules. *Mol Plant*
1710 *Microbe Interact* **27**: 388-399.
1711 Sayers, E.W., Bolton, E.E., Brister, J.R., Canese, K., Chan, J., Comeau, D.C., Connor, R., Funk, K., Kelly, C.,
1712 Kim, S., Madej, T., Marchler-Bauer, A., Lanczycki, C., Lathrop, S., Lu, Z., Thibaud-Nissen, F.,
1713 Murphy, T., Phan, L., Skripchenko, Y., Tse, T., Wang, J., Williams, R., Trawick, B.W., Pruitt, K.D.,
1714 and Sherry, S.T. (2022) Database resources of the national center for biotechnology information.
1715 *Nucleic Acids Res* **50**: D20-D26.
1716 Scharf, B., and Schmitt, R. (2002) Sensory transduction to the flagellar motor of *Sinorhizobium meliloti*. *J*
1717 *Mol Microbiol Biotechnol* **4**: 183-186.
1718 Sheehan, L.M., Budnick, J.A., Blanchard, C., Dunman, P.M., and Caswell, C.C. (2015) A LysR-family
1719 transcriptional regulator required for virulence in *Brucella abortus* is highly conserved among
1720 the alpha-proteobacteria. *Mol Microbiol* **98**: 318-328.
1721 Sola-Landa, A., Pizarro-Cerdá, J., Grilló, M.J., Moreno, E., Moriyón, I., Blasco, J.M., Gorvel, J.P., and
1722 López-Goñi, I. (1998) A two-component regulatory system playing a critical role in plant
1723 pathogens and endosymbionts is present in *Brucella abortus* and controls cell invasion and
1724 virulence. *Mol Microbiol* **29**: 125-138.
1725 Stanley, J., and Cervantes, E. (1991) Biology and genetics of the broad host range *Rhizobium* sp. NGR234.
1726 *Journal of Applied Bacteriology* **70**: 9-19.
1727 Stein, B.J., Fiebig, A., and Crosson, S. (2021) The ChvG-ChvI and NtrY-NtrX Two-Component Systems
1728 Coordinately Regulate Growth of *Caulobacter crescentus*. *J Bacteriol* **203**: e0019921.
1729 Sun, J., Rutherford, S.T., Silhavy, T.J., and Huang, K.C. (2022) Physical properties of the bacterial outer
1730 membrane. *Nat Rev Microbiol* **20**: 236-248.
1731 Swanson, J.A., Mulligan, J.T., and Long, S.R. (1993) Regulation of syrM and nodD3 in Rhizobium meliloti.
1732 *Genetics* **134**: 435-444.
1733 Tang, G., Li, Q., Xing, S., Li, N., Tang, Z., Yu, L., Yan, J., Li, X., and Luo, L. (2018) The LsrB Protein Is
1734 Required for *Agrobacterium tumefaciens* Interaction with Host Plants. *Mol Plant Microbe*
1735 *Interact* **31**: 951-961.
1736 Tata, M., Kumar, S., Lach, S.R., Saha, S., Hart, E.M., and Konovalova, A. (2021) High-throughput
1737 suppressor screen demonstrates that RcsF monitors outer membrane integrity and not Bam
1738 complex function. *Proc Natl Acad Sci U S A* **118**.
1739 Taylor, D.L., Bina, X.R., Slamti, L., Waldor, M.K., and Bina, J.E. (2014) Reciprocal regulation of resistance-
1740 nodulation-division efflux systems and the Cpx two-component system in *Vibrio cholerae*. *Infect*
1741 *Immun* **82**: 2980-2991.
1742 Terpolilli, J.J., O'Hara, G.W., Tiwari, R.P., Dilworth, M.J., and Howieson, J.G. (2008) The model legume
1743 *Medicago truncatula* A17 is poorly matched for N2 fixation with the sequenced microsymbiont
1744 *Sinorhizobium meliloti* 1021. *New Phytol* **179**: 62-66.
1745 Testerman, T.L., Vazquez-Torres, A., Xu, Y., Jones-Carson, J., Libby, S.J., and Fang, F.C. (2002) The
1746 alternative sigma factor sigmaE controls antioxidant defences required for *Salmonella* virulence
1747 and stationary-phase survival. *Mol Microbiol* **43**: 771-782.

1748 Tomlinson, A.D., Ramey-Hartung, B., Day, T.W., Merritt, P.M., and Fuqua, C. (2010) *Agrobacterium*
1749 *tumefaciens* ExoR represses succinoglycan biosynthesis and is required for biofilm formation and
1750 motility. *Microbiology (Reading, England)* **156**: 2670-2681.
1751 Trinick, M.J. (1980) Relationships Amongst the Fast-growing Rhizobia of *Lablab purpureus*, *Leucaena*
1752 *leucocephala*, *Mimosa* spp., *Acacia farnesiana* and *Sesbania grandiflora* and their Affinities with
1753 Other Rhizobial Groups. *Journal of Applied Bacteriology* **49**: 39-53.
1754 Van de Velde, W., Zehirov, G., Szatmari, A., Debreczeny, M., Ishihara, H., Kevei, Z., Farkas, A., Mikulass,
1755 K., Nagy, A., Tiricz, H., Satiat-Jeunemaitre, B., Alunni, B., Bourge, M., Kucho, K., Abe, M., Kereszt,
1756 A., Maroti, G., Uchiumi, T., Kondorosi, E., and Mergaert, P. (2010) Plant peptides govern terminal
1757 differentiation of bacteria in symbiosis. *Science* **327**: 1122-1126.
1758 Van Valen, L. (1973) A new evolutionary law. *Evol. Theory* **1**: 1-30.
1759 Vanderlinde, E.M., and Yost, C.K. (2012) Mutation of the sensor kinase *chvG* in *Rhizobium*
1760 *leguminosarum* negatively impacts cellular metabolism, outer membrane stability, and
1761 symbiosis. *J Bacteriol* **194**: 768-777.
1762 VanYperen, R.D., Orton, T.S., and Griffitts, J.S. (2015) Genetic analysis of signal integration by the
1763 *Sinorhizobium meliloti* sensor kinase FeuQ. *Microbiology (Reading, England)* **161**: 244-253.
1764 Viadas, C., Rodriguez, M.C., Sangari, F.J., Gorvel, J.P., Garcia-Lobo, J.M., and Lopez-Goni, I. (2010)
1765 Transcriptome analysis of the *Brucella abortus* BvrR/BvrS two-component regulatory system.
1766 *PLoS One* **5**: e10216.
1767 Vriezen, J.A., de Bruijn, F.J., and Nusslein, K. (2007) Responses of rhizobia to desiccation in relation to
1768 osmotic stress, oxygen, and temperature. *Appl Environ Microbiol* **73**: 3451-3459.
1769 Walsh, N.P., Alba, B.M., Bose, B., Gross, C.A., and Sauer, R.T. (2003) OMP peptide signals initiate the
1770 envelope-stress response by activating DegS protease via relief of inhibition mediated by its PDZ
1771 domain. *Cell* **113**: 61-71.
1772 Wang, C., Kemp, J., Da Fonseca, I.O., Equi, R.C., Sheng, X., Charles, T.C., and Sobral, B.W. (2010a)
1773 *Sinorhizobium meliloti* 1021 loss-of-function deletion mutation in *chvI* and its phenotypic
1774 characteristics. *Mol Plant Microbe Interact* **23**: 153-160.
1775 Wang, D., Griffitts, J., Starker, C., Fedorova, E., Limpens, E., Ivanov, S., Bisseling, T., and Long, S. (2010b)
1776 A nodule-specific protein secretory pathway required for nitrogen-fixing symbiosis. *Science* **327**:
1777 1126-1129.
1778 Wang, D., Xue, H., Wang, Y., Yin, R., Xie, F., and Luo, L. (2013) The *Sinorhizobium meliloti ntrX* gene is
1779 involved in succinoglycan production, motility, and symbiotic nodulation on alfalfa. *Appl Environ*
1780 *Microbiol* **79**: 7150-7159.
1781 Weiss, D.S., Chen, J.C., Ghigo, J.M., Boyd, D., and Beckwith, J. (1999) Localization of FtsI (PBP3) to the
1782 septal ring requires its membrane anchor, the Z ring, FtsA, FtsQ, and FtsL. *J Bacteriol* **181**: 508-
1783 520.
1784 Wells, D.H., Chen, E.J., Fisher, R.F., and Long, S.R. (2007) ExoR is genetically coupled to the ExoS-ChvI
1785 two-component system and located in the periplasm of *Sinorhizobium meliloti*. *Mol Microbiol*
1786 **64**: 647-664.
1787 Wiech, E.M., Cheng, H.P., and Singh, S.M. (2015) Molecular modeling and computational analyses
1788 suggests that the *Sinorhizobium meliloti* periplasmic regulator protein ExoR adopts a
1789 superhelical fold and is controlled by a unique mechanism of proteolysis. *Protein Sci* **24**: 319-
1790 327.
1791 Williams, M.A., Bouchier, J.M., Mason, A.K., and Brown, P.J.B. (2022) Activation of ChvG-ChvI regulon by
1792 cell wall stress confers resistance to beta-lactam antibiotics and initiates surface spreading in
1793 *Agrobacterium tumefaciens*. *PLoS Genet* **18**: e1010274.
1794 Wu, C.F., Lin, J.S., Shaw, G.C., and Lai, E.M. (2012) Acid-induced type VI secretion system is regulated by
1795 ExoR-ChvG/ChvI signaling cascade in *Agrobacterium tumefaciens*. *PLoS Pathog* **8**: e1002938.

1796 Xing, S., Zheng, W., An, F., Huang, L., Yang, X., Zeng, S., Li, N., Ouenzar, K., Yu, L., and Luo, L. (2022)
1797 Transcription Regulation of Cell Cycle Regulatory Genes Mediated by NtrX to Affect
1798 *Sinorhizobium meliloti* Cell Division. *Genes (Basel)* **13**.
1799 Yao, S.Y., Luo, L., Har, K.J., Becker, A., Rüberg, S., Yu, G.Q., Zhu, J.B., and Cheng, H.P. (2004)
1800 *Sinorhizobium meliloti* ExoR and ExoS proteins regulate both succinoglycan and flagellum
1801 production. *J Bacteriol* **186**: 6042-6049.
1802 Yuan, Z.C., Liu, P., Saenkham, P., Kerr, K., and Nester, E.W. (2008) Transcriptome profiling and functional
1803 analysis of *Agrobacterium tumefaciens* reveals a general conserved response to acidic conditions
1804 (pH 5.5) and a complex acid-mediated signaling involved in *Agrobacterium*-plant interactions. *J*
1805 *Bacteriol* **190**: 494-507.
1806

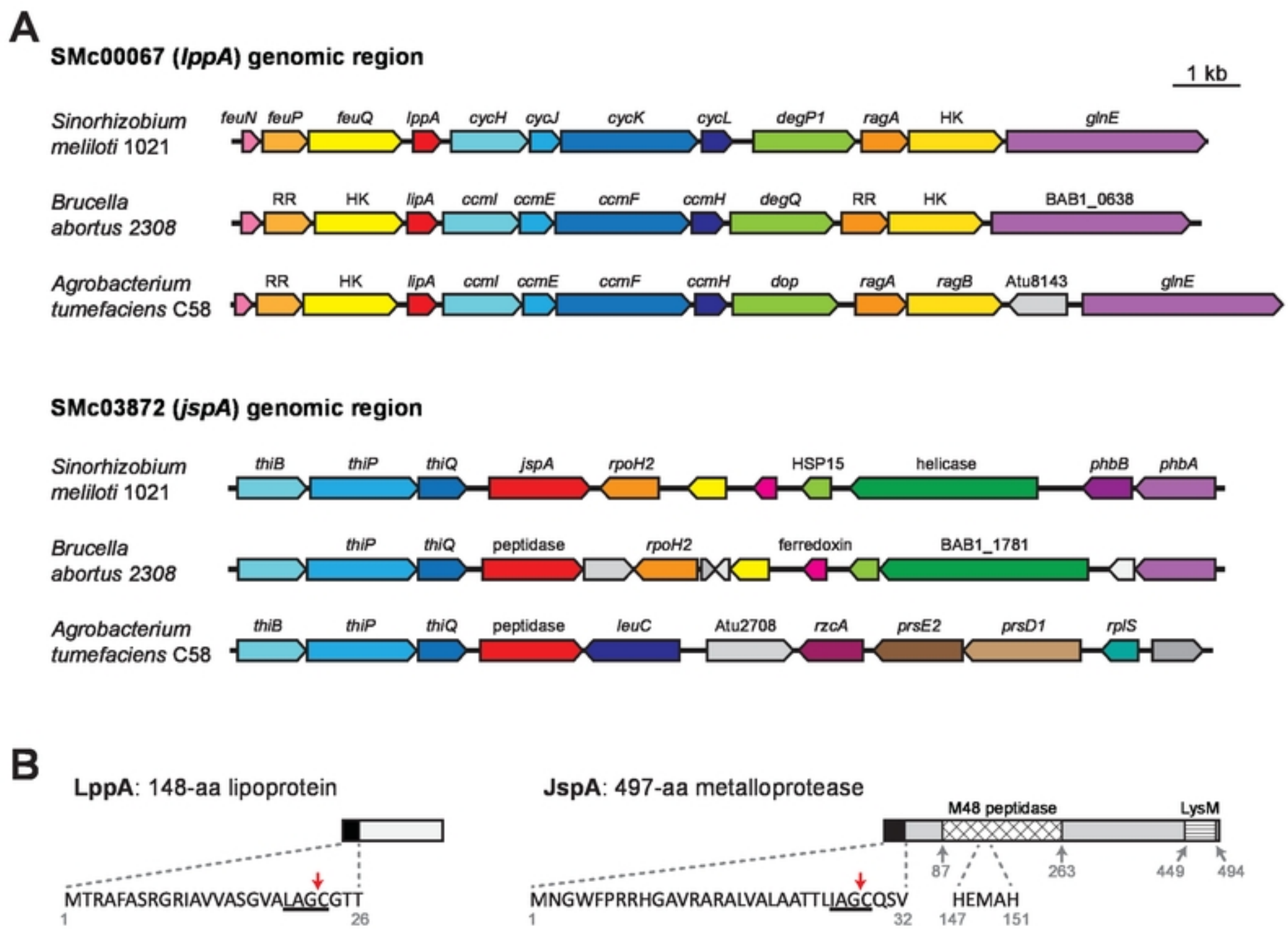
A
SMc00067 (lppA) genomic region
1 kb
Sinorhizobium meliloti 1021
feuN feuP feuQ lppA cycH cycJ cycK cycL degP1 ragA HK glnE
Brucella abortus 2308
RR HK lipA ccmI ccmE ccmF ccmH degQ RR HK BAB1_0638
Agrobacterium tumefaciens C58
RR HK lipA ccmI ccmE ccmF ccmH dop ragA ragB Atu8143 glnE
SMc03872 (jspA) genomic region
Sinorhizobium meliloti 1021
thiB thiP thiQ jspA rpoH2 HSP15 helicase phbB phbA
Brucella abortus 2308
thiP thiQ peptidase rpoH2 ferredoxin BAB1_1781
Agrobacterium tumefaciens C58
thiB thiP thiQ peptidase leuC Atu2708 rzcA prsE2 prsD1 rplS
B
LppA: 148-aa lipoprotein
MTRAFASRGRIAVVASGVALAGCGTT
1
26
JspA: 497-aa metalloprotease
M48 peptidase
LysM
87
263
449
494
MNGWFPRRHGAVRARALVALAATTLIAGCQSV
HEMAH
1
32
147
151

FIG. 1

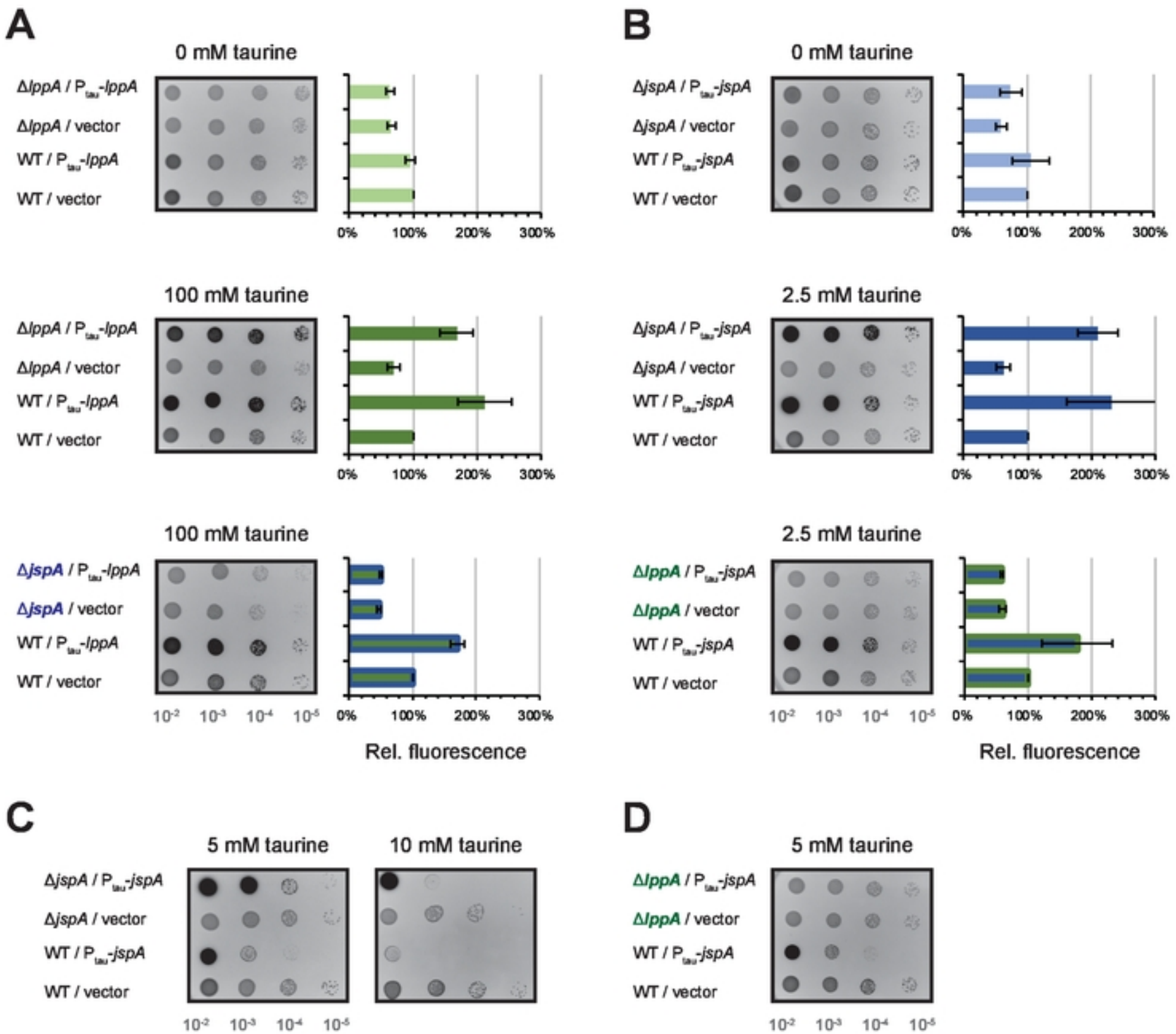
A
0 mM taurine
ΔlppA / P_tau-lppA
ΔlppA / vector
WT / P_tau-lppA
WT / vector
0%
100%
200%
300%
100 mM taurine
ΔlppA / P_tau-lppA
ΔlppA / vector
WT / P_tau-lppA
WT / vector
0%
100%
200%
300%
100 mM taurine
ΔjspA / P_tau-lppA
ΔjspA / vector
WT / P_tau-lppA
WT / vector
10^-2
10^-3
10^-4
10^-5
0%
100%
200%
300%
Rel. fluorescence
B
0 mM taurine
ΔjspA / P_tau-jspA
ΔjspA / vector
WT / P_tau-jspA
WT / vector
0%
100%
200%
300%
2.5 mM taurine
ΔjspA / P_tau-jspA
ΔjspA / vector
WT / P_tau-jspA
WT / vector
0%
100%
200%
300%
2.5 mM taurine
ΔlppA / P_tau-jspA
ΔlppA / vector
WT / P_tau-jspA
WT / vector
10^-2
10^-3
10^-4
10^-5
0%
100%
200%
300%
Rel. fluorescence
C
5 mM taurine
10 mM taurine
ΔjspA / P_tau-jspA
ΔjspA / vector
WT / P_tau-jspA
WT / vector
10^-2
10^-3
10^-4
10^-5
D
5 mM taurine
ΔlppA / P_tau-jspA
ΔlppA / vector
WT / P_tau-jspA
WT / vector
10^-2
10^-3
10^-4
10^-5

FIG. 2

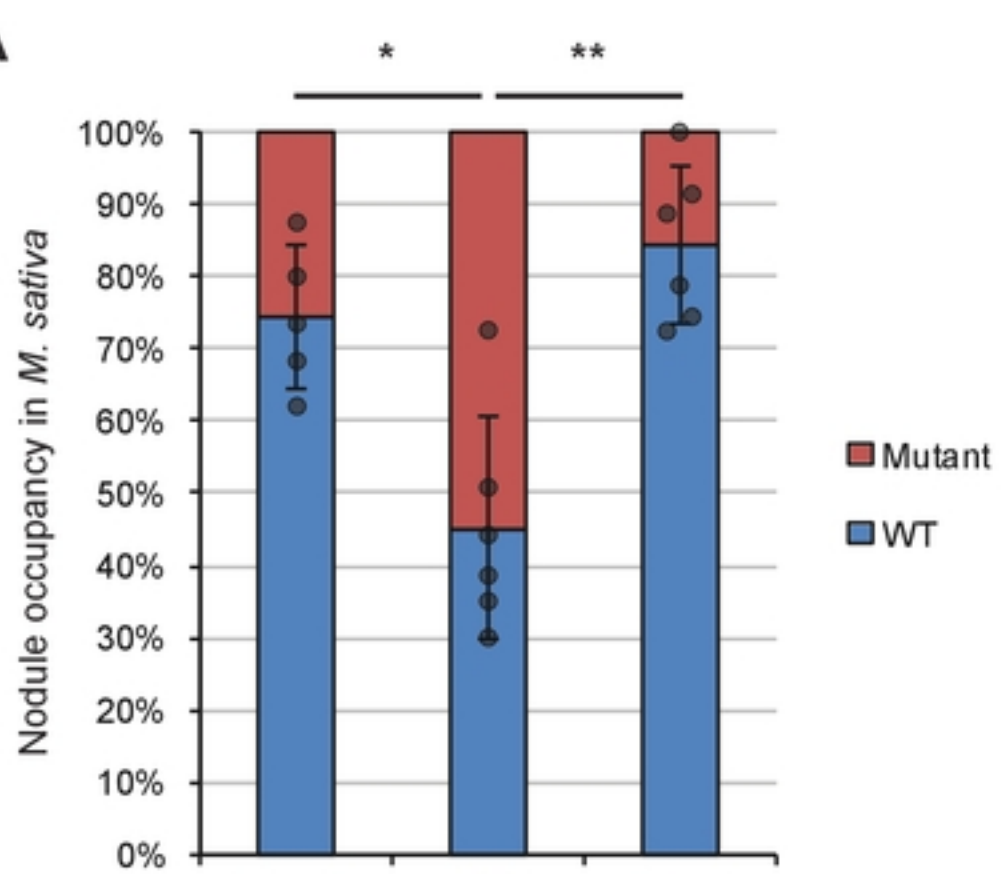

	lppA vs. Rm1021	Rm1021 (Ω) vs. Rm1021	jspA vs. Rm1021
Mutant	21% ± 8%	47% ± 14%	15% ± 10%
WT	63% ± 14%	38% ± 13%	82% ± 13%
Mixed	15% ± 8%	15% ± 4%	3% ± 4%
Trials (nodules)	5 (253)	6 (403)	6 (265)

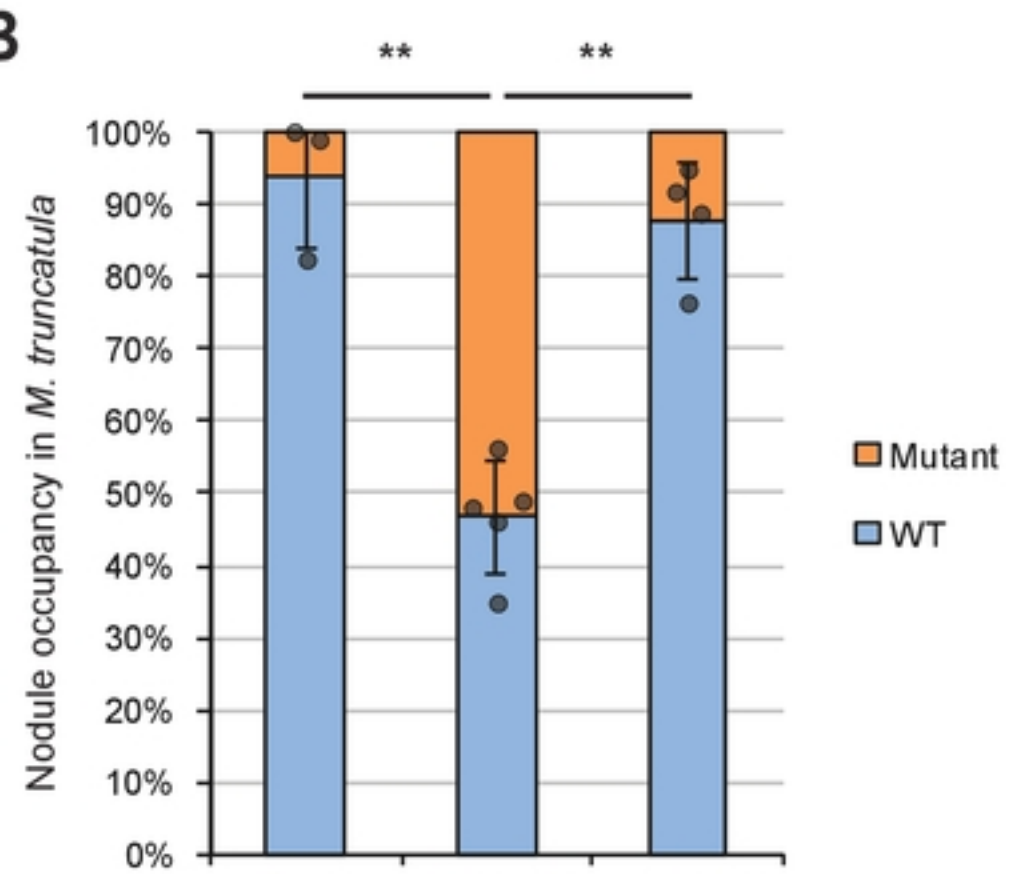

	ΔlppA vs. WSM419	WSM419R vs. WSM419	ΔjspA vs. WSM419
Mutant	6% ± 9%	45% ± 5%	12% ± 8%
WT	90% ± 10%	40% ± 8%	82% ± 5%
Mixed	4% ± 2%	14% ± 6%	6% ± 4%
Trials (nodules)	3 (288)	5 (450)	4 (312)

FIG. 3

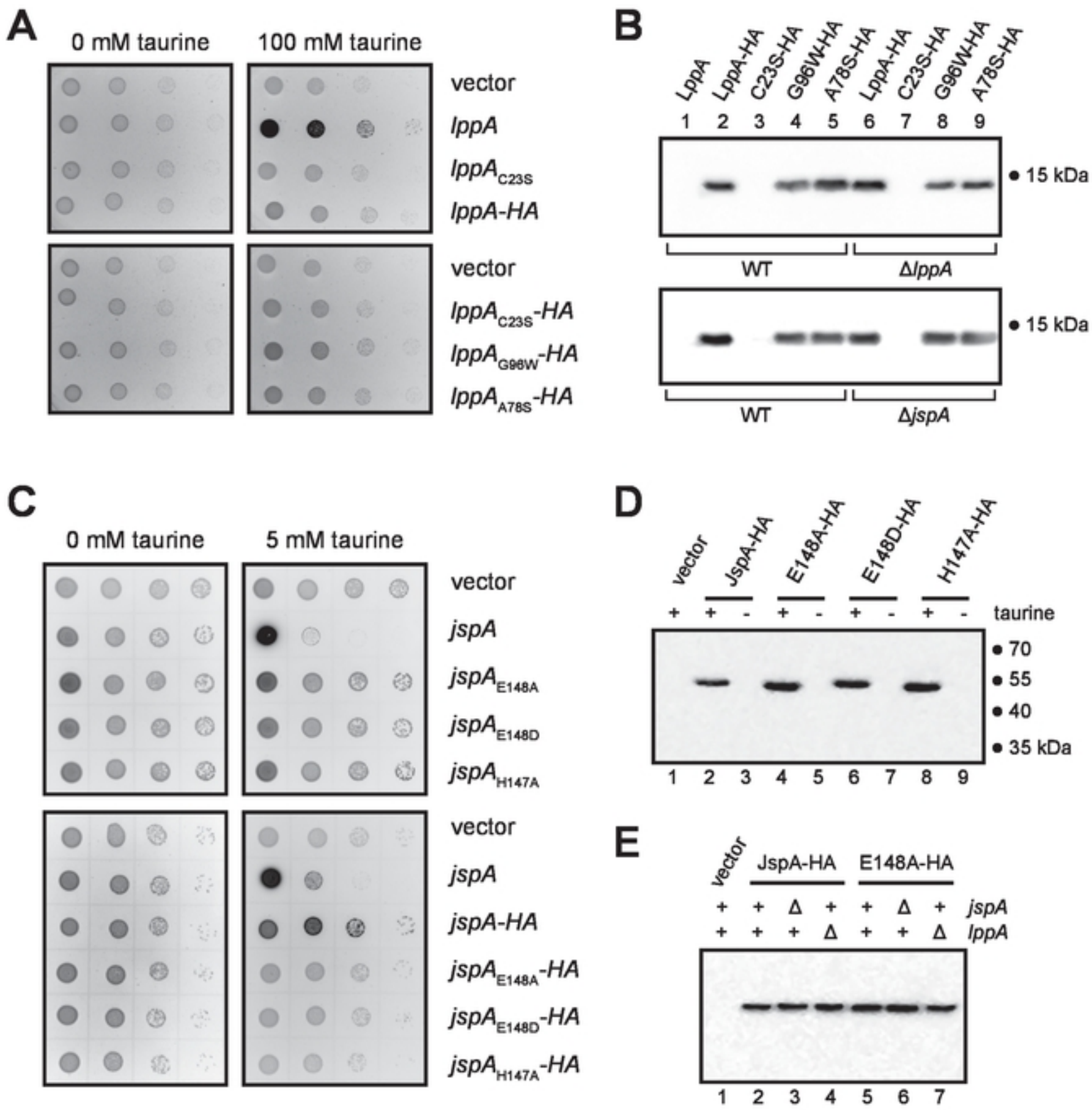
A
0 mM taurine
100 mM taurine
vector
lppA
lppA C23S
lppA-HA
vector
lppA C23S-HA
lppA G96W-HA
lppA A78S-HA
B
LppA
LppA-HA
C23S-HA
G96W-HA
A78S-HA
LppA-HA
C23S-HA
G96W-HA
A78S-HA
1 2 3 4 5 6 7 8 9
15 kDa
WT
ΔlppA
15 kDa
WT
ΔjspA
C
0 mM taurine
5 mM taurine
vector
jspA
jspA E148A
jspA E148D
jspA H147A
vector
jspA
jspA-HA
jspA E148A-HA
jspA E148D-HA
jspA H147A-HA
D
vector
JspA-HA
E148A-HA
E148D-HA
H147A-HA
taurine
70
55
40
35 kDa
1 2 3 4 5 6 7 8 9
E
vector
JspA-HA
E148A-HA
jspA
lppA
1 2 3 4 5 6 7

FIG. 4

A **Altered gene expression when JspA overexpressed > 1.5-fold change**

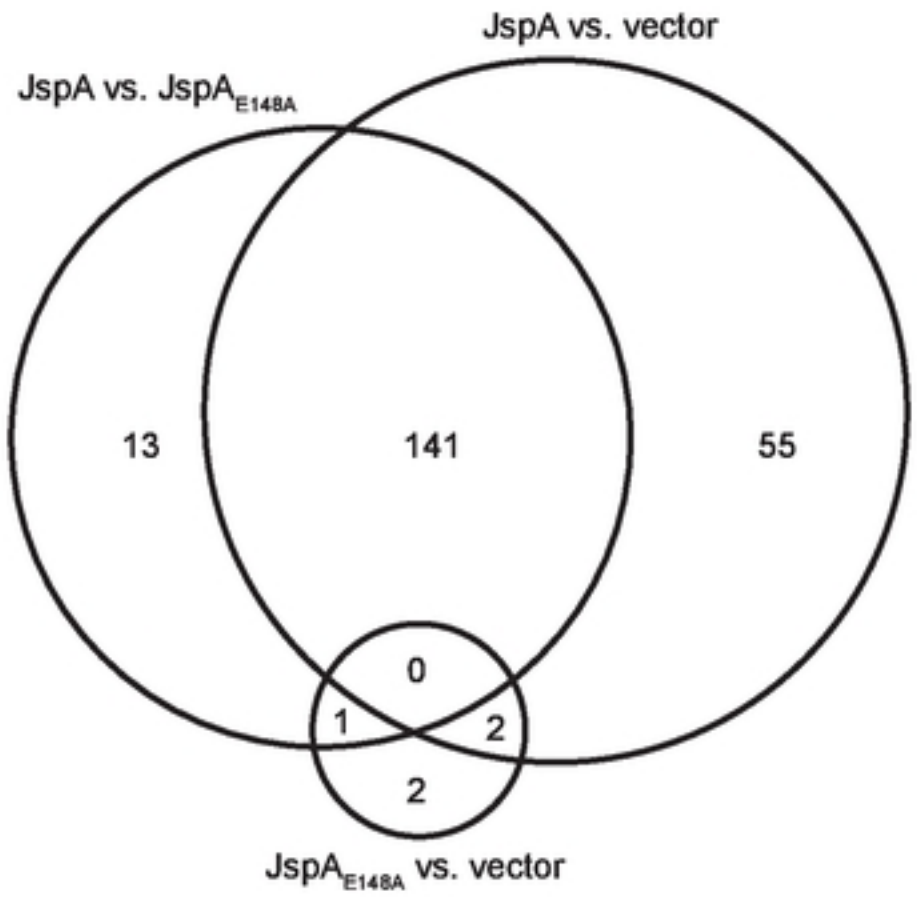

80 genes UP-regulated

Exopolysaccharide biosynthesis:	23
Regulators (including ChvI):	6
Metabolism:	6
Miscellaneous:	10
Hypothetical proteins:	35

61 genes DOWN-regulated

Flagellar biosynthesis and motility:	40
Pili biogenesis:	2
Metabolism and biosynthesis:	9
Regulators:	3
Miscellaneous:	1
Hypothetical proteins:	6

B **Comparisons of JspA and ExoR/ExoS transcriptomes and ChvI regulon**

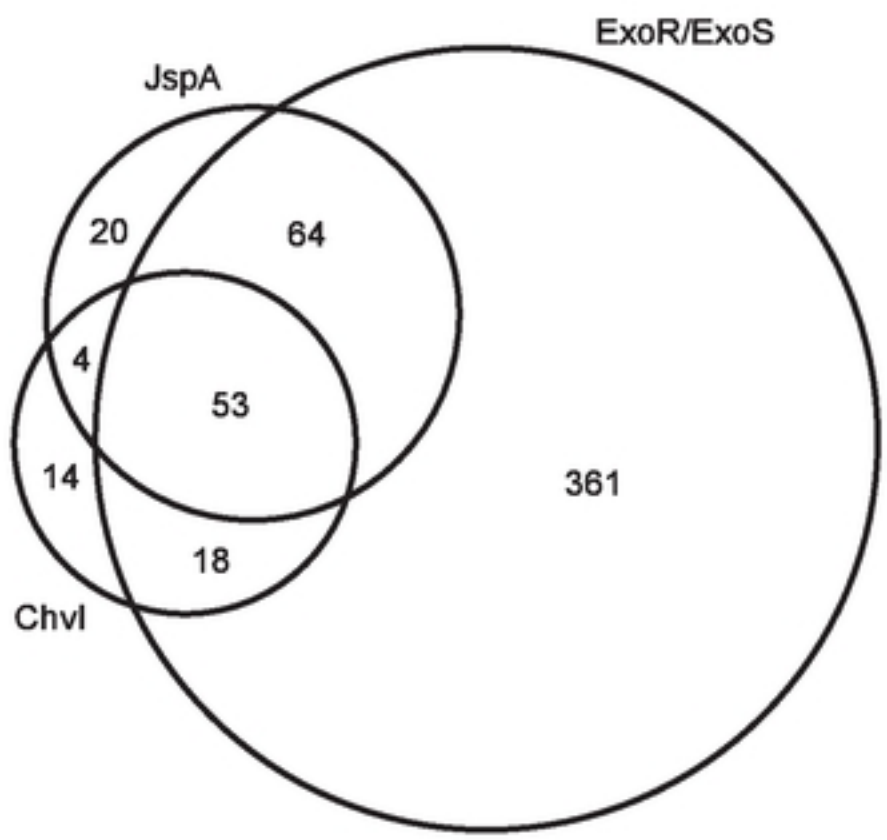

C **Comparisons of JspA and RpoH1 transcriptomes**

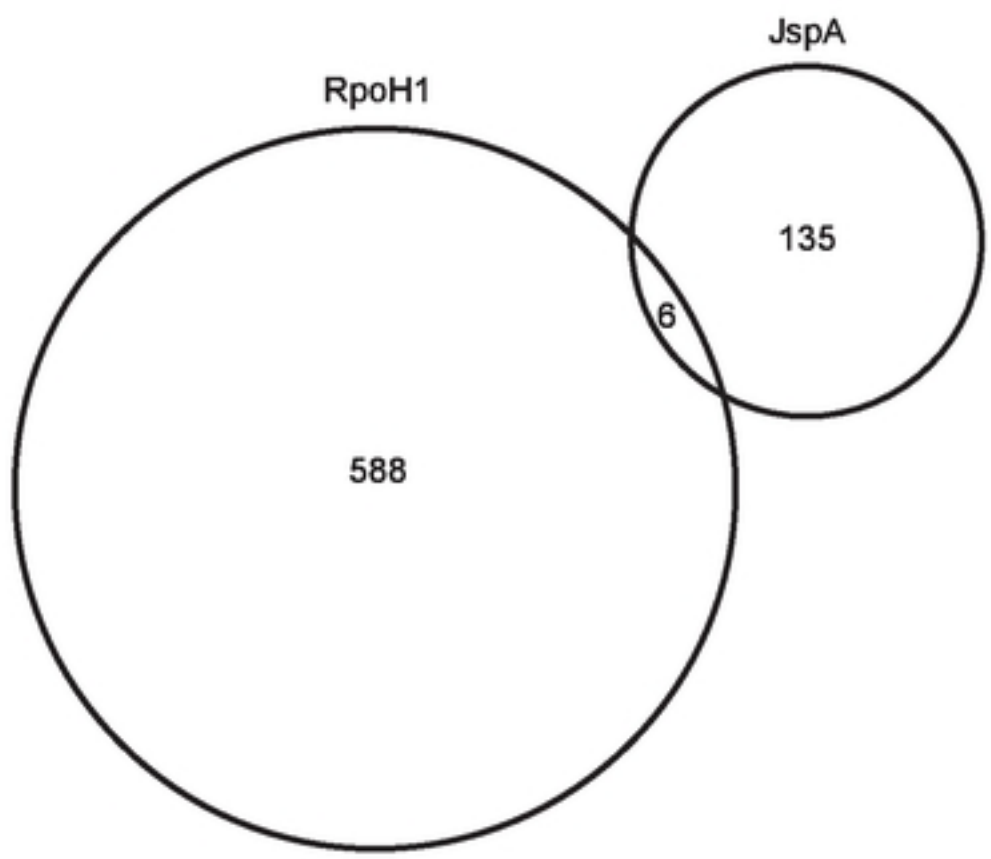

FIG. 5

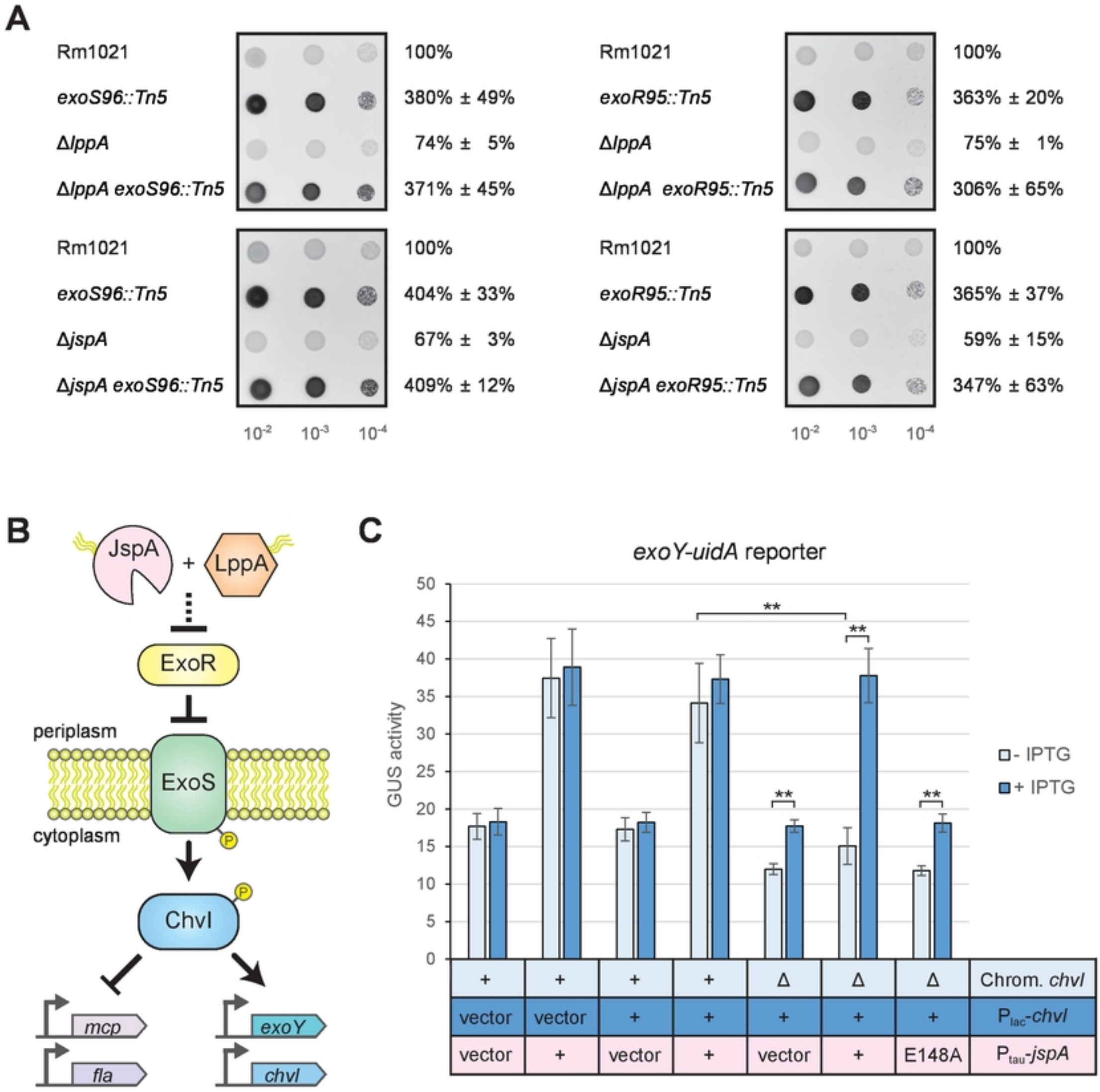
A
Rm1021
exoS96::Tn5
ΔlppA
ΔlppA exoS96::Tn5
100%
380% ± 49%
74% ± 5%
371% ± 45%
Rm1021
exoR95::Tn5
ΔlppA
ΔlppA exoR95::Tn5
100%
363% ± 20%
75% ± 1%
306% ± 65%
Rm1021
exoS96::Tn5
ΔjspA
ΔjspA exoS96::Tn5
100%
404% ± 33%
67% ± 3%
409% ± 12%
Rm1021
exoR95::Tn5
ΔjspA
ΔjspA exoR95::Tn5
100%
365% ± 37%
59% ± 15%
347% ± 63%
10-2 10-3 10-4
B
JspA
LppA
ExoR
periplasm
ExoS
cytoplasm
P
ChvI
mcp
fla
exoY
chvI
C
exoY-uidA reporter
GUS activity
50
45
40
35
30
25
20
15
10
5
0
**
- IPTG
+ IPTG
Chrom. chvI
Plac-chvI
Ptau-jspA
vector
E148A

FIG. 6

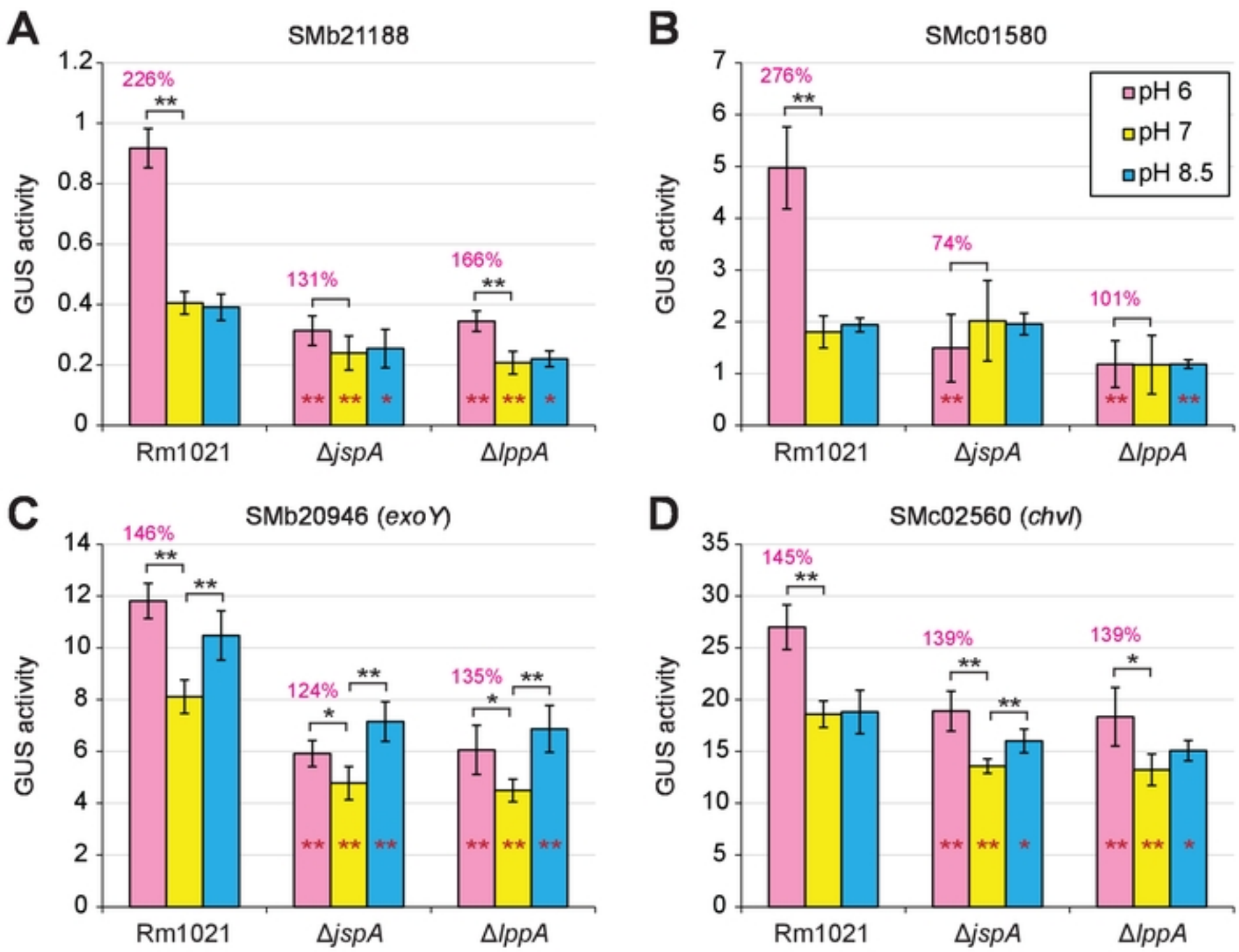
A
SMb21188
GUS activity
226%
131%
166%
Rm1021
ΔjspA
ΔlppA
B
SMc01580
pH 6
pH 7
pH 8.5
276%
74%
101%
C
SMb20946 (exoY)
146%
124%
135%
D
SMc02560 (chvI)
145%
139%
139%

FIG. 7

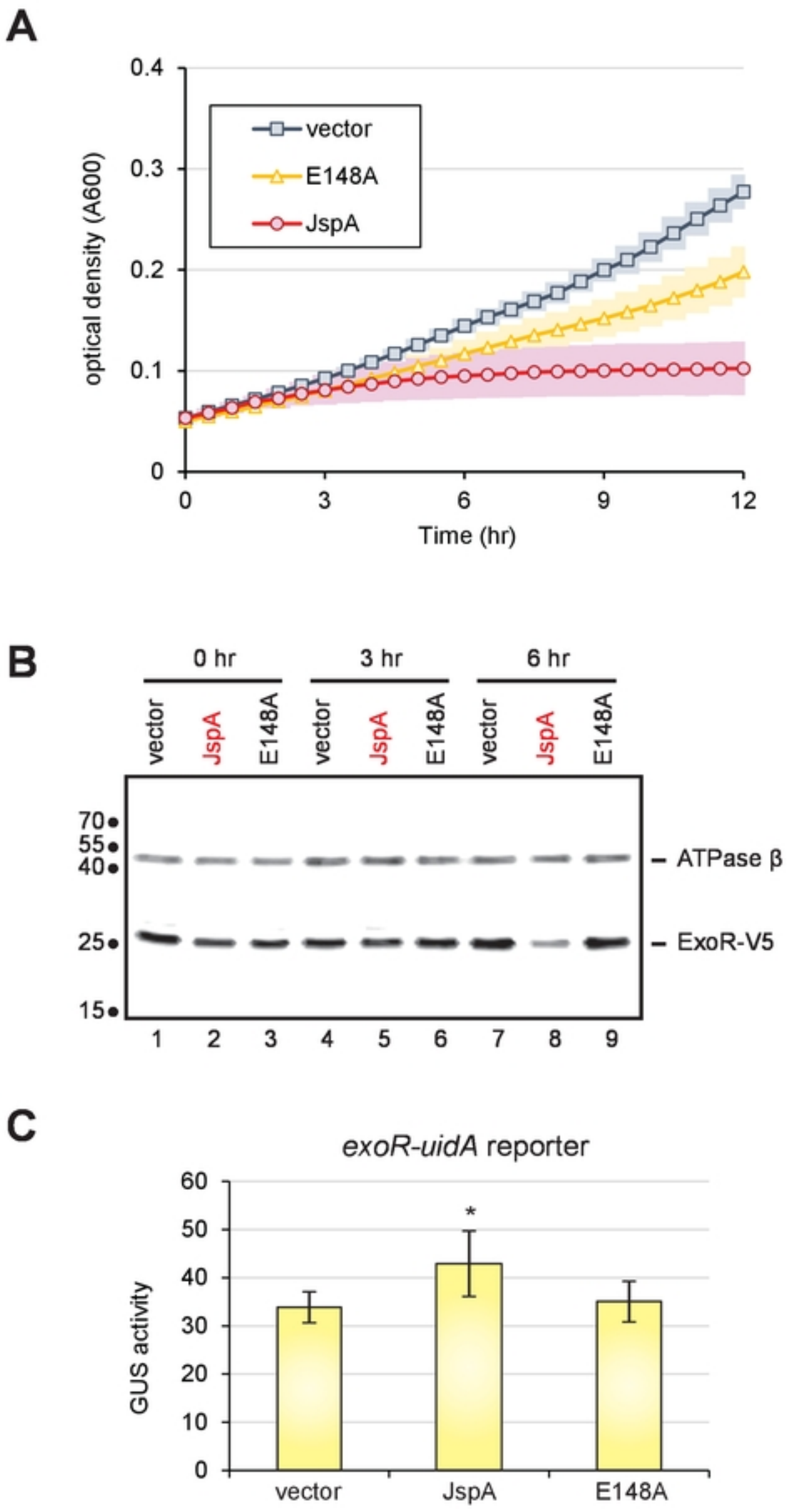
A
0.4
0.3
0.2
0.1
0
optical density (A600)
vector
E148A
JspA
0
3
6
9
12
Time (hr)
B
0 hr
3 hr
6 hr
vector
JspA
E148A
vector
JspA
E148A
vector
JspA
E148A
70
55
40
25
15
ATPase β
ExoR-V5
1
2
3
4
5
6
7
8
9
C
exoR-uidA reporter
60
50
40
30
20
10
0
GUS activity
*
vector
JspA
E148A

FIG. 8

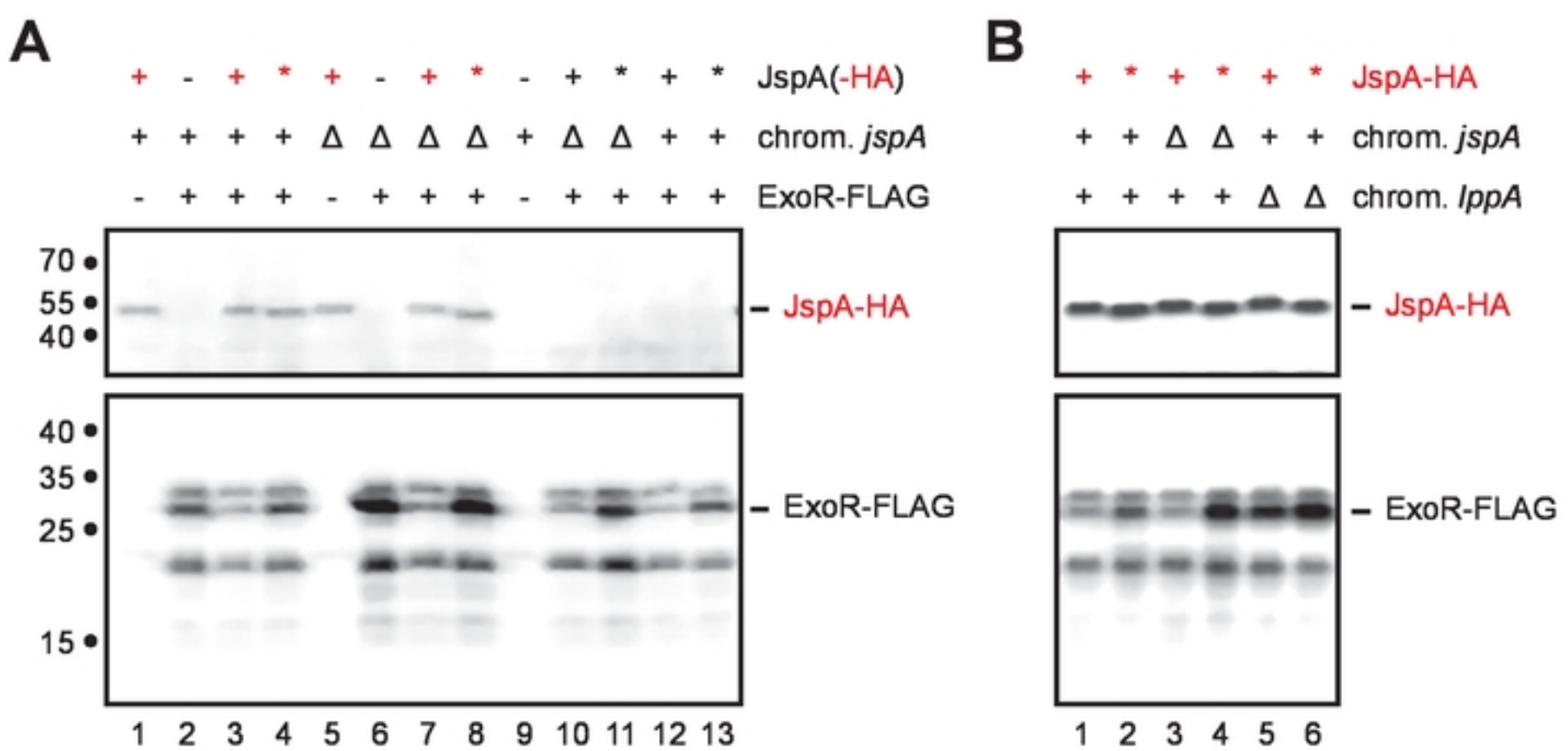
A
+ - + * + - + * - + * + * JspA(-HA)
+ + + + Δ Δ Δ Δ + Δ Δ + + chrom. jspA
- + + + - + + + - + + + + ExoR-FLAG
70
55
40
JspA-HA
40
35
25
15
ExoR-FLAG
1 2 3 4 5 6 7 8 9 10 11 12 13
B
+ * + * + * JspA-HA
+ + Δ Δ + + chrom. jspA
+ + + + Δ Δ chrom. lppA
JspA-HA
ExoR-FLAG
1 2 3 4 5 6

FIG. 9

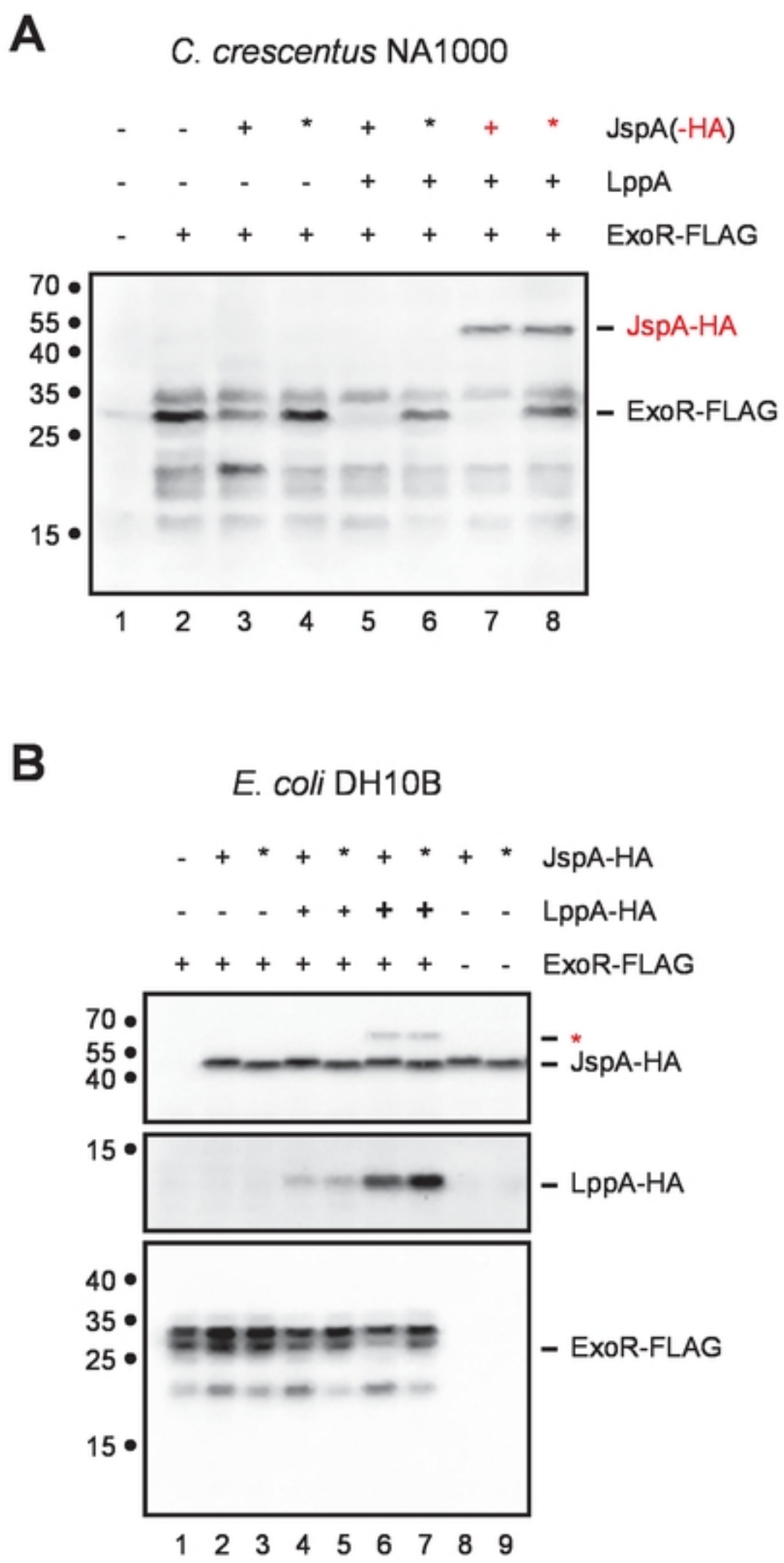
A
C. crescentus NA1000
JspA(-HA)
LppA
ExoR-FLAG
70
55
40
35
25
15
JspA-HA
ExoR-FLAG
1 2 3 4 5 6 7 8
B
E. coli DH10B
JspA-HA
LppA-HA
ExoR-FLAG
70
55
40
JspA-HA
15
LppA-HA
40
35
25
ExoR-FLAG
15
1 2 3 4 5 6 7 8 9

FIG. 10